ADDIS ABABA UNIVERSITY

SCHOOL OF GRADUATE STUDIES

Deformation Characteristics of Deep Excavation Supported by Contiguous pile wall

On

Soils Commonly Found in Addis Ababa

By:

Anteneh Geremew

November, 2017

Deformation Characteristics of Deep Excavation Supported by Contiguous pile wall On Soils Commonly Found in Addis Ababa

A thesis submitted to the school of graduate studies of Addis Ababa University in partial fulfillment of the requirements for the Degree of

Masters of Science

in

Civil and Environmental Engineering

By:

Anteneh Geremew

Advisor:

Dr. Henok Fikre

Addis Ababa University School of Graduate Studies

Department of Civil Engineering

DEFORMATION CHARACTERISTICS OF DEEP EXCAVATION SUPPORTED BY CONTIGUOUS PILEWALL ON SOILS COMMONLY FOUND IN ADDIS ABABA

By:

Anteneh Geremew

A Thesis Submitted to School of Graduate Studies in Partial Fulfillment of the Requirement for Degree of

Master of Science

in

Geotechnical Engineering

Approved by Board of Examiners:

Dr. Henok Fikre		
Advisor	*Signature*	*Date*
Dr.-Ing. Asrat Worku		
Internal Examiner	*Signature*	*Date*
Dr.-Ing. Mesele Haile		
External Examiner	*Signature*	*Date*
Ato Ermias		
Chair Person	*Signature*	*Date*

DECLARATION

I, the undersigned, declare that this thesis is my original work performed under the supervision of my research advisor Dr. Henok Fikre and has not been presented as a thesis for a degree in any other university. All sources of materials used for this thesis have also been duly acknowledged.

Name: Anteneh Geremew

Signature: _____

Place: Institute of Technology
Addis Ababa University
Addis Ababa

Date: November, 2017

Acknowledgement

First, I would like to thank the LORD JESUS for all the blessings I have received during course of my studies. I thank HIM because HE never moved the mountain, but gave me strength to climb it.

I would like to express my deepest gratitude to my advisor, Dr. Henok Fikre in Addis Ababa University, Department of Civil and Environmental Engineering, for his continued support during my studies, for his mentoring, for being a great source of inspiration and for his guidance and encouragement throughout this endeavor.

I am grateful to Ato Yohannes Abbay, Managing Director in Yohannes Abbay Consulting Architects and Engineers Plc. for his valuable understanding and assistance during the course of my studies.

Lastly but most importantly, many thanks also go to my colleagues and friends in the University.

Abstract

A two dimensional Finite Element (2D FE) study is carried out in this thesis, considering soil-structure interaction. This thesis presents a study of the effects of deep excavations supported by tie-back anchored contiguous pile wall, which is constructed at the center of Addis Ababa and analyzed on three types of soil.

The objectives of this study is to investigate a deformation characteristic of deep excavation to study the effect of the stiffness of the supporting system and stiffness of the supported soils, with different drainage conditions, and to understand the performance of deep excavations from the point of view of the effects on the already existing neighboring structures load types. This analysis monitors the following parameters: maximum lateral wall deflection, maximum settlement, angular deformation of the neighboring structures, lateral movements of the structure corner and maximum bending moment in the retaining wall. Moreover, following the normalization of lateral wall deflection and settlement with the excavation depth, the relationship between the lateral wall deflection (δ_{hm}) & settlement (δ_{vm}) and the distance excavation-neighboring structures are observed in graph and expressed by exponential decay function equation in order to get preliminary contiguous pile wall and soil parameters for design. Furthermore, this research also analyzes the influence of structures load and soil types on its admissible deformation compared with previous studies.

Parametric studies have been carried out to identify important variables controlling the mechanisms and design of soil-structure interaction. The parameters considered in the study include; soil type, diameter of contiguous pile wall (wall stiffness), strut (tie-back anchor) spacing and strut (tie-back anchor) pre-stress force. Results of these analyses have recorded in terms of lateral wall deflection, ground settlement and bending moments induced in contiguous pile wall. Finally, the main accomplishments of the thesis and the corresponding conclusions are summarized & recommendations are also made for further design of deep excavation support systems.

Keywords: Deep excavation, excavation support system, contiguous pile wall, Finite Element Method, ground deformation.

Table of Contents

List of Tables

List of Figures

List of abbreviations

BEF	Beam on Elastic Foundation Method
CP	Contiguous pile
FE	Finite Element
FEM	Finite Element Method
FS	Factor of safety
MC	Mohr-Coulomb

CHAPTER 1
INTRODUCTION

1.1 General

It is very important and should be a legal necessity with any construction to provide protection to the adjacent structures when excavating to any appreciable depth. Without adequate lateral support, the new excavation will almost certainly cause loss of bearing capacity, settlements, or lateral movements to existing property and these can damage buildings, streets, and utilities. Therefore, identifying and understanding the factors that affect the performance of deep excavation is an important issue for geotechnical engineers.

1.2 Soil types in Addis Ababa

Regarding soil types in Addis Ababa, residual soils ranging from red to dark grey (black cotton soils) are found covering extensive areas in the city. Red clays are mainly found around kolfe keranyo and Asko Areas. The black cotton soils cover relatively flat areas starting from Bole Medhanealem through Megenagna to the entire CMC and kality in the east and southeastern part. In the western and southwestern Addis Ababa, Black cotton soils cover the entire Mekanisa and Lebu areas. On the other hand, the collovial and alluvial deposit in the city and its surroundings are commonly observed at the foot of hills and river Banks. Further, in between rock layers at variable depths, over consolidated brown soils (Paleosols) are not uncommon.

1.3 Synopsis of the problem

Addis Ababa, the capital city of Ethiopia facing high density urban growth, leads to the need to build tall buildings with deep foundations, positioning the car parks and other facilities in their basements.

Limiting movements that result from constructing deep excavations is becoming a significant design issue, especially in urban environments. Failure to control deformations can cause significant damage to adjacent structures and utilities. Consequences such as the following can become very costly:

- Collapse of excavation support system with major damage and delays.
- Loss of bearing capacity of shallow foundations for an adjacent building.
- Cracking of adjacent buildings that cost time and money to resolve.
- Shut down of the project and withdrawal of permits by government officials until a resolution can be found.
- Loss of factor of safety for basal heave, global instability or bearing capacity such that work must be stopped until remedial measures are implemented.
- Abandonment of the project, leaving an open hole in the ground.
- Poor relations with neighbors which take management time.
- Lawyers and litigation.

Construction of a deep excavation involves unloading of the soil. For unloading, the movements of soil are small until the factor of safety for any soil failure mechanism drops below 1.1 to 1.2. Then the movements increase rapidly and the factor of safety decreases quickly as well. This condition can worsen rapidly as the excavation becomes deeper, a fact that catches many people by surprise and leaves little time to take preventative actions.

1.4 Proposed Concept

Deep excavations are supported by systems like conventional retaining walls, sheet pile walls, braced walls, diaphragm walls and pile walls. This study aims at presenting constructional and preliminary design elements (diameter of pile, spacing of struts, strut pre-stressing force…etc.) of the retaining systems very commonly adopted in Addis Ababa city, namely contiguous piles. In this specific study, tie-back anchored contiguous pile walls retaining system for supporting a deep excavation implemented at a city center (Lideta area) analyzed on three types of soil commonly found in Addis Ababa. These three types of soil have different shear strength parameters and investigated with three drainage conditions. In this work, numerical modeling of pile walls using PLAXIS is conducted in order to carry out deformation characteristics of deep excavation on, effect of stage wise excavation on ground and pile wall deformation. Moreover, parametric studies were carried out to identify important variables controlling the mechanisms and design of soil-structure interaction. The parameters considered in the study include soil type, diameter of contiguous pile wall (wall stiffness), strut (tie-back anchor) spacing and strut (tie-back anchor) pre-stress force.

1.5 Objectives of the Research

The main objective of this study is to develop a deformation-based design methodology by providing preliminary design elements of the retaining systems based on the permissible ground deformation that will protect adjacent infrastructure from excavation-related ground movements.

The specific objectives of this work include:

- Develop a new deformation- based design methodology, based on finite element analysis that shows the effects of the commonly used excavation support system (Contiguous pile wall) stiffness on the resulting excavation-related ground movements on three types of soil commonly found in Addis Ababa.
- To guide the Engineer through the entire process of deformation-based design.
    - This will allow the designer to size the wall and predict the ground movements, given the allowable soil distortion, the soil and support system.

It is important to note that this study may be particularly used for most Addis Ababa areas which have different unconfined compressive strength (Expansive and Red clay stratum) due to similarity in soil strata and design of sub-surface excavation support systems.

1.6 Methodology

The methodology used to achieve the above objectives are described as follows;

1.6.1 Data collection:

- The available literature in the area is examined to establish the factors that influence the proper functioning of a pile wall.
- Soils shear strength parameters, which are commonly found in Addis Ababa are selected. Following this, three types of soils, which have different shear strength parameters in three different drainage conditions, are selected.
- Contiguous pile wall used as deep excavation supporting system which is implemented for Commercial Bank of Ethiopia, lideta office building project found in Addis Ababa, Lideta sub-city.

1.6.2 Data analysis

Deformation characteristics of deep excavation supported by contiguous pile wall is investigated on three types of soils, which have different shear strength parameters (Total and Effective shear strength parameters) and different drainage conditions (Drained and Undrained). In addition, parametric studies, on change in soil type, diameter of contiguous pile wall (wall stiffness), strut (tie-back anchor) spacing and strut (tie-back anchor) pre-stress force, have carried out to identify important variables controlling the mechanisms and design of soil-structure interaction.

1.6.3 Numerical modeling using PLAXIS

Finite Element Analysis is one of the most accurate numerical methods to find an approximate solution for engineering problems. In short, Finite Element Analysis creates partial differential equations to be solved numerically. With the aid of Finite Element software which can perform high number of iterations and the accuracy of finite element analysis approximately matches the actual condition of Pile wall problems.

In this work, non-linear Finite Element Methods numerical modeling using PLAXIS with linearly-elastic, Mohr-Coulomb (MC) models to represent the soil behavior in order to carry out *deformation characteristics and parametric study of deep excavation*.

The variable parameters used in the analysis are the neighboring structures load, neighboring structures distance from face of excavation (D), diameter of pile wall (D), strut (tie-back anchor) horizontal spacing (L_s) and strut pre-stress force (F_S).

1.6.4 Deformation characteristics of deep excavation

The stage wise excavation is done in phases to simulate actual site conditions on field. Deformation characteristic of deep excavation is performed to study the effect of the stiffness of the supporting system and stiffness of the supported soils with different drainage conditions, to understand the performance of deep excavations from the point of view of the effects on the already existing neighboring structures load types have monitored the following parameters:

- Maximum lateral wall deflection,
- Maximum settlement,
- Angular deformation of the neighboring structures,
- Lateral movements of the structure corner and
- Maximum bending moment in the retaining wall.

Moreover, following the normalization of lateral wall deflection and settlement with the excavation depth, the relationship between the lateral wall deflection (δ_{hm}) & settlement (δ_{vm}) and the distance excavation-neighboring structures are observed in graph and expressed by exponential decay function equation in order to get preliminary contiguous pile wall and soil parameters for design.

1.6.5 Parametric study

The models used for the parametric study are identical to the original models, except for certain parameters being changed in order to determine the impact of these specific parameters. Soil type, diameter of contiguous pile wall, neighboring structures load, neighboring structure distance from face of excavation, anchor spacing and anchor pre-stress force are the variables considered in the parametric study. When one of the above parameters is varied, the rest are kept constant and lateral wall deflection, ground settlement and bending moment verses the varied parameters graphs are obtained.

1.7 Relevance of Thesis

The most important factor for the successful implementation of deep excavation is the application of geotechnical research without defect. After obtaining information about the soil, the selection of excavation system becomes significant. The basis for the deep excavation is reaching the acceptable displacement level, according to the provisions of the excavation, and selecting the most economical, as well as feasible, support system for enabling the stability. Every excavation should be approached and analyzed according to the specific site conditions. The optimum support system should be selected by evaluating all the criteria.

Design techniques that involve sophisticated soil-structure-interaction models combined with local data and experience give a high level of confidence for predicting wall performance on projects surrounded by other structures, where control of building movement and damage are paramount to a successful project delivery.

This study will investigate the possible collapsing parameters of the retaining projects in order to provide valuable preliminary information for future design purposes. Moreover, the use of this deformation characteristics of deep excavation, parametric study and the reporting of the results are important to benefit the overall knowledge base of different areas of Addis Ababa, which have almost the same soil shear strength parameters, analyzed on this study where deep basements are popular choice for building owners and developers.

1.8 Outline of Thesis

The work presented in this thesis is divided into the following chapters:

This thesis contains four chapters.

In Chapter one, Introduction part, describes synopsis of the problem, proposed concept, objective of the research, methodology and relevance of thesis.

In Chapter Two, a literature review of past research work is carried out on field studies, analytical solutions and numerical solutions are carried out with a main focus to show on prediction of ground deformations influencing the behavior of excavations and their effects on the neighboring built environment. Moreover, approaches to design and analysis of excavation support walls, observations from field studies, results from numerical analysis, empirical methods and analytical studies on performance of deep excavation are summarized.

In Chapter Three, two-dimensional effects that the support system stiffness has on the behavior and performance of deep excavations incrementally for stage construction study by means of FEM analysis.

In the first part, using contiguous pile wall parameters on three types of soil with different drainage conditions are investigated to understand the effects of the existing structures. This study monitors the following parameters: maximum lateral wall deflection, maximum settlement, angular deformation of the neighboring structures, lateral movements of the structure corner and maximum bending moment in the retaining wall. Moreover, following the normalization of lateral wall deflection and settlement with the excavation depth, the relationship between the maximum lateral wall deflection (δ_{hm}) & the distance excavation-neighboring structures and the relationship between maximum settlement (δ_{vm}) & the distance excavation-neighboring structures are observed in graph and expressed by exponential decay function equation in order to get preliminary contiguous pile wall and soil parameters for design. Accordingly, important findings from FEM analyses output are discussed.

In the second part, the description and results of parametric study on the same base model & soils and with selected parameters; change in diameter of contiguous pile wall, change in anchor spacing and change in anchor pre-stress force are presented. Results of these analyses

were recorded in terms lateral wall deflection, ground settlement behind the contiguous pile wall, and bending moments induced in contiguous pile wall due to an adjacent deep excavation and structures.

In Chapter Four, conclusions are summarized & recommendations are also made for further design of deep excavation support systems.

CHAPTER 2
LITERATURE REVEIW

2.1 Introduction

The excavation of soil from a deep excavation has two main effects. The first is that the removal of the weight of the excavated soil results in a decrease in the vertical stress in the soil beneath the excavation. The second is that the removal of the soil in the excavation results in a loss of lateral support for the soil around the excavation. The purpose of a deep excavation support system is to provide lateral support for the soil around an excavation and to limit movement of the surrounding soil.

Support systems for deep excavations consist of two main components. The first is a retaining wall. The second component is the support provided to the retaining wall. Many types of walls and supports have been used in deep excavations. The principal types of walls are conventional retaining wall, diaphragm (structural slurry), sheet pile, soldier piles with wood lagging walls, Pile walls: secant, tangent, contiguous piles, and deep soil mixed walls. Apart from retaining walls to resist lateral earth pressure a supplementary strutting systems are also required. A strut is made of wood, reinforced concrete or steel. Based on function of a strut, it may classify as an earth berm, a horizontal strut, tie-back anchor or as a top-down floor slab.

2.2 Contiguous Piles – Merits and Demerits

Contiguous piles are considered more economical than diaphragm wall in small to medium scale excavations due to reduction in cost of site operations. Common pile diameters adopted are 0.6, 0.8 and 1.0 m. These piles are connected with a capping beam at the top, which assists equitable pressure distributions in piles. These retaining piles are suitable in areas where water table is deep or where soil permeability is low. However, some acceptable amount of water can be collected at the base and pumped out.

Contiguous piles are suitable in crowded urban areas, where traditional retaining methods would otherwise congest the adjoining land, leaving less space for working. Provision of contiguous piles restricts ground movements on the backfill side, and thus protects the neighboring structures, foundations and boundary walls from the detrimental effects of excavation. Contiguous piles facilitate deployment of several independent sets of

equipment and gangs along its alignment which can speed up its execution. They can be constructed using even the conventional piling equipment's and also can be constructed in hard and rocky sub-soil conditions, where diaphragm wall construction is difficult. Such retaining systems has advantage of employing varying diameter of piles in lieu of change in sub-surface conditions, or on encountering competent stratum at a depth which is different than that anticipated during design. Further, unlike the diaphragm wall which relies on the orthogonal geometry of the excavated area. Contiguous pile retaining system can construct to form any shape in the excavated area.

2.3 Evaluation of foundations of adjacent properties and their tolerances

Major concern during the planning and execution of deep excavation is the impact of construction related to ground movements on the adjacent properties and utilities. During excavation, the state of stresses in the ground mass around the excavation change. The most common changes in stresses in the retained side are the stress relieve on the excavation face resulting in horizontal ground movement and follows by vertical movement for equilibrium and increase in vertical stress due to lowering of water table resulting in both immediate and consolidation settlement of the ground. These ground movements that vary away from the excavation can cause building, especially those on shallow foundation, to translate, rotate, deform, distort and finally sustain damage if the magnitude exceeded the tolerable limits as shown in figure 1.

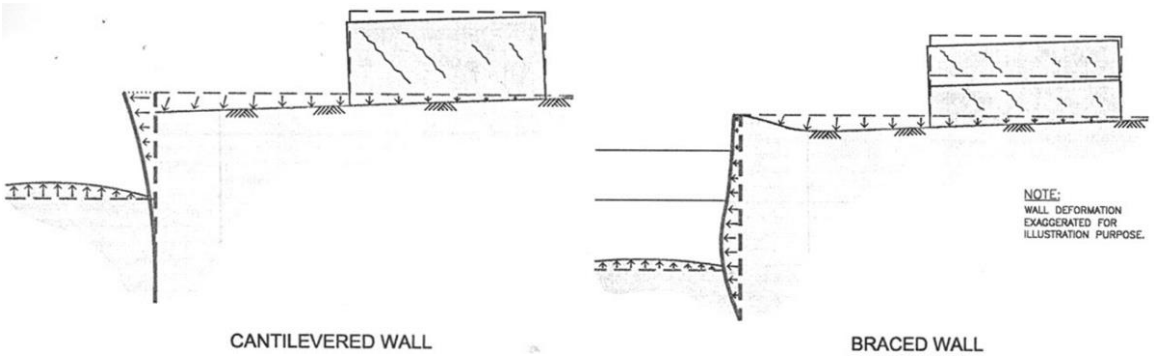

Figure 1: Effect of Deformation of retained ground on adjacent properties

2.3.1 Ground movement associated with excavation

Structural damage affecting the stability structure is usually related to cracks or distortions in primary support elements such as beam, columns, and load bearing walls. Table 1

presents the classification system that provides a defined frame work for the evaluation of the damages.

Table 1: Classification of visible damage *(Modified after Burland et al. (1977)*

Damage Category	Description of Typical damage *	Approximate width of cracks**, mm
Negligible	Hairline cracks	< 0.1
Very slight	Very slight damage includes fine cracks which can be easily treated during normal decoration, perhaps an isolated slight fracture in building, and cracks in external brickwork visible on close inspection	< 1
Slight	Slight damage includes cracks which can be easily filled and redecoration would probably be required, several slight fractures may appear showing the inside of the building, cracks which are visible externally and some repointing may be required, and doors and windows may stick.	< 5
Moderate	Moderate damage includes cracks that require some opening up and can be masked by suitable linings, repointing of external brickwork and possibly a small amount of brickwork replacement may be required, doors and windows stick, service pipes may fracture, and water tightness is often impaired.	5to15 or several cracks > 3mm
Severe	Severe damage includes large cracks requiring extensive repair work involving breaking out and replacing sections of walls (especially over doors and windows),distorted windows and door frames, noticeably sloping floors, leaning or bulging walls, some loss of baring in beams, and disrupted service pipes.	5to25 also depends on number of cracks
Very severe	Very severe damage often requires a major repair job involving partial or complete rebuilding, beams lose bearing, and walls lean and require shoring. Windows are broken with distortion, and there is danger of structural instability.	Usually >25 depends on number of cracks
* Location of damage in the building or structure must be considered when classifying degree of damage **crack width is only one aspect of damage and should not be used on alone as a direct measure of it. **Note:** Modified after Burland et al. (1977)		

In the design of deep excavation works, the designer should be aware that ground movements related to open excavation can include a substantial component of horizontal strain. This is addition to settlements of buildings caused by their own weight. The traditional criteria based on differential settlement or angular distortion alone is therefore inadequate for assessment of building response due to deep excavation works.

There are many approaches to address the subject of building damage due to ground movements. Usually, a simple and conservative method, which is the empirical approach, is needed in the preliminary assessment. Figure 2 shows the symbols and definitions of foundation movement normally used.

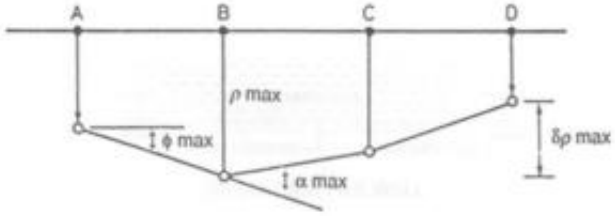

(a) Definition of settlement,ρ, relative settlement,δρ, rotation,θ and angular strain, α

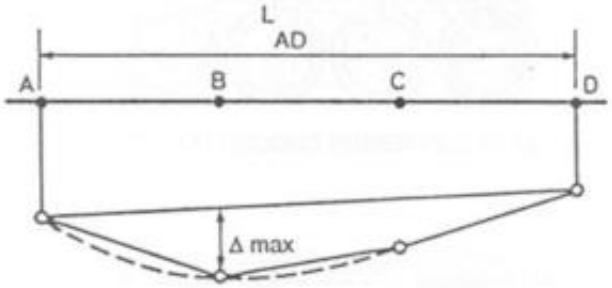

(b) Definitions of relative deflection Δ and deflection ratio Δ/L

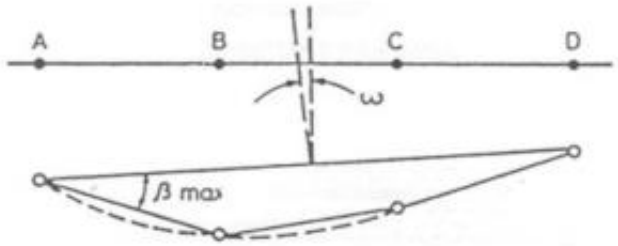

(C) Definitions of tilt and relative rotation (angular distortion) β

Figure 2: Symbols and Definitions of Foundation Movement (After Institution of Structural Engineers, 1989)

Various damage category criteria have been proposed such as the methods of Rankin (1988), Boscardin & Cording (1989) and Boone (1996). The method of Boscardin & Cording (1989) appears to produce reasonably accurate predictions as shown in Figure 3. As such, the damage criteria as proposed by Boscardin & Cording (1989) are recommended and the limiting values are summarized in Table 2.

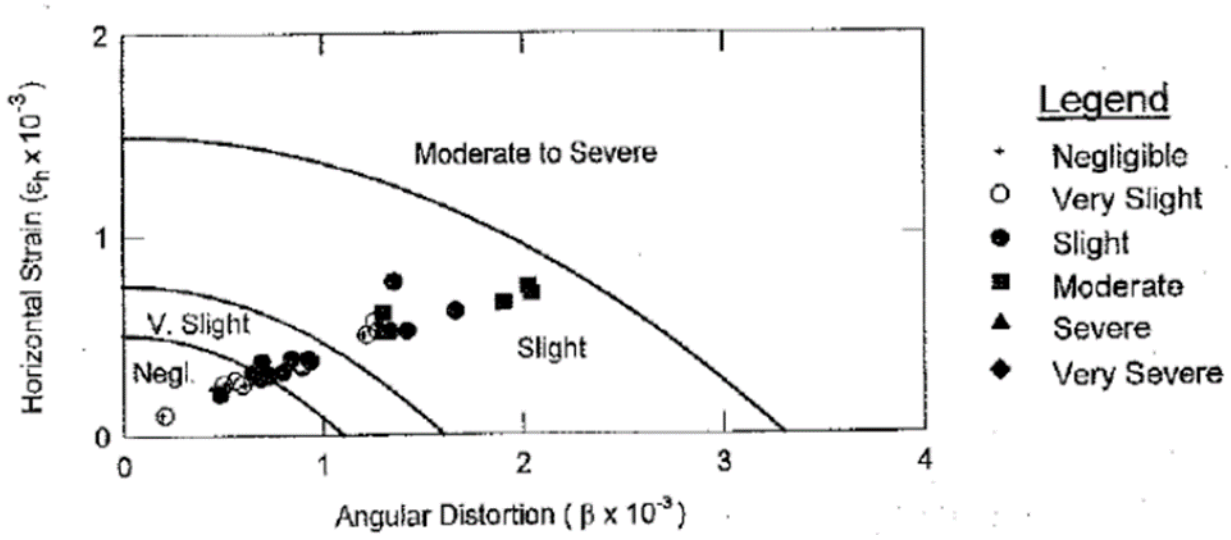

Figure 3: Summary of plots of damage estimation using the method of Boscardin & Cording (1989) and assessed ground movement behavior (Boone, 1999)

Table 2: Damage category criteria (Boscardin & Cording, 1989)

Category	Angular Distortion, β ($x10^{-3}$)	Horizontal Strain, ε_h ($x10^{-3}$)
Negligible	< ~1.1	< 0.5
Very slight	~1.1 < β < ~1.6	0.5 < ε_h < 0.75
Slight	**~1.6 < β < ~3.3**	**0.75 < ε_h < 1.5**
Moderate	~3.3 < β < ~6.7	1.5 < ε_h < 3.0
Severe	> ~6.7	> 3

For design purpose, the designer should normally limit the angular distortion and horizontal strain such that the damage category does not exceed "slight" in Table 2. Therefore, the limiting value of angular distortion (β) and horizontal strain (ε_h) for the slight category is 3.3 x 10^{-3} and 1.5 x 10^{-3} respectively. Figure 4 illustrates a simple example of the limiting values of angular distortion and horizontal strain.

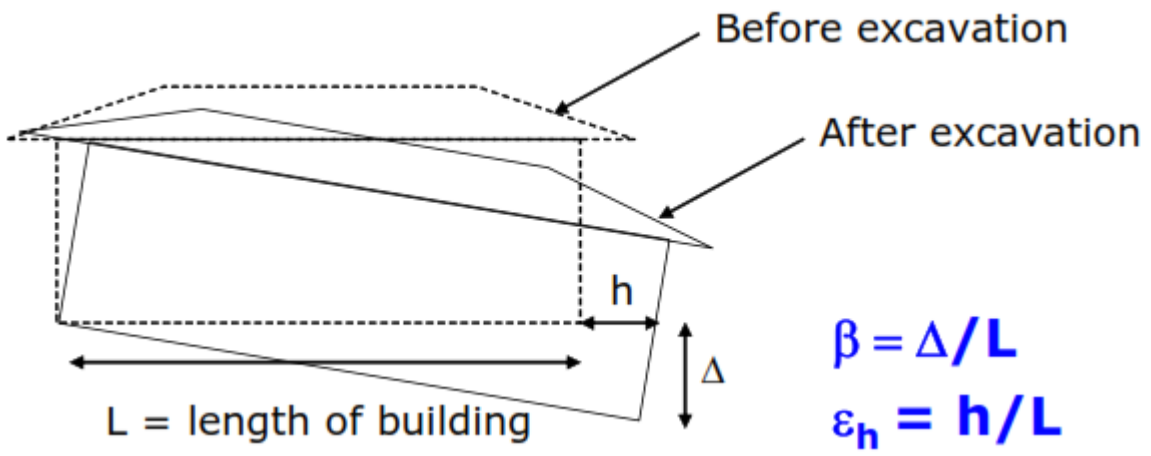

Figure 4: Example of limiting values of angular distortion and horizontal strain.

2.3.2 Empirical Method

Skempton and macdonald (1956) identify a basis on which to determine allowable total and differential foundation settlement. Guidance for design has been largely based on their work and shown in Table 3. There are three important points to be noted in their studies:

a) Confined to traditional mill-type steel-framed industrial buildings, reinforced-concrete framed buildings with traditional cladding, and some load bearing masonry wall buildings.
b) The criterion for limiting deformation was the 'angular distortion' or relative rotation as shown in Figure 3.
c) No classification of degree of architectural or visible damage was used.

Meyerhof (1956) and Polshin & Tokar (1957) recognize that reinforced load bearing walls have a different mode of deformation from that of framed structures and recommended that the deflection ration Δ/L to be used as stated in Table 3.

Table 3: Summary of limiting deformation

(a) Framed buildings and reinforced load bearing walls
Limiting values of relative rotation (angular distortion)β

	Skempton 7 macDonald (1956)	Meyerhof (1956)	Polshin & Tokar (1957)	Bjerrum (1963)
Structural damage cracking in walls and partitions	1/150 1/300 (but 1/150 recommended)	1/250 1/500	1/200 1/500 (0.7/1000 to 1/1000 for end bays)	1/150 1/500

(a) Unreinforced load bearing walls
Limiting values of deflection ratio Δ/L for the onset of visible cracking

	Meyerhof (1956)	Polshin & Tokar (1957)	Burland and wroth (1975)
Sagging	1/2500	L/H < 3: 1/3500 to 2/2500 L/H < 5: 1/2000 to 2/1500	1/2500 at L/H = 1 1/1250 at L/H = 5
Hogging (Unreinforced)	-	-	1/5000 at L/H = 1 1/2500 at L/H = 5

2.4 Approaches to design and analysis of excavation support walls

The design analyses for excavation support systems can range from relatively simple empirical analyses to more complex computer analyses, where typically all stages of the excavation sequence are evaluated. The design considerations should include not only the stresses and loads on the support system, but also the effect of construction movements on the response of adjacent structures. The level of effort for the evaluation often depends on the stage of the project, proximity of structures, contractor's methods of construction, and known local practice.

For deep excavation, usually the multi-level supported walls are used instead of cantilever or singly supported walls. The design requirements and analyses for multi-level supported walls are different from cantilever or singly supported wall. The earth pressures that act on multi-level strutted walls or multi-level tied-back walls depend on the wall stiffness relative to the soil, the support spacing and the pre-stress load. The method of construction of these walls is usually sequential, installing the wall and excavation in stages followed by installation of support like anchor or prop at each installation stage. The available method

for analysis and design of multi-level supported walls can be categorized as follows;

- Empirical methods
- Full soil-structure interaction analysis (staged excavation analysis)

2.4.1 Empirical methods

2.4.1.1 Stress analysis

Traditionally, apparent pressure envelope methods have been used successfully to design flexible wall systems such as soldier pile and lagging and steel sheet-pile systems. The approach was developed based on data from flexible wall systems, and typically assumes that the wall acts as a simple beam spanning between the brace levels (Terzaghi et al., 1996). For the more rigid slurry wall system, the pattern of wall displacement that develops during the actual excavation and bracing sequence can have a major effect on the bending moments in the wall and the distribution of load to the bracing/anchors. Hence, use of apparent pressure envelopes for design of stiffer systems can be misleading. In general, apparent pressure envelope loadings are most appropriate as upper bounds for cases that match the bases of the empirical data, which include cases with relatively flexible walls and a stable subgrade.

The pressure envelope design approach is for a temporary support system and does not necessarily provide the long-term loading corresponding to the permanent condition after the end of excavation. When the temporary support system, such as a slurry wall system, is incorporated into the permanent building foundation, a staged analysis that includes loading at each stage is required to evaluate the built-in stresses and strains that are locked into the final structure at the end of construction.

The strut load envelopes developed by Terzaghi and Peck (1967) are presented in Figure 5. These diagrams do not represent the actual earth pressure or its distribution with depth, but load envelopes from which strut loads can be evaluated. Clay is assumed “Undrained” and only considers total stresses. Sands are assumed “drained”. If non-permeable wall is used, hydrostatically distributed water pressure should be added to strut loads. Wall can be designed using the coulomb earth pressure distribution with hydrostatic water pressure except full drainage occurs through the wall.

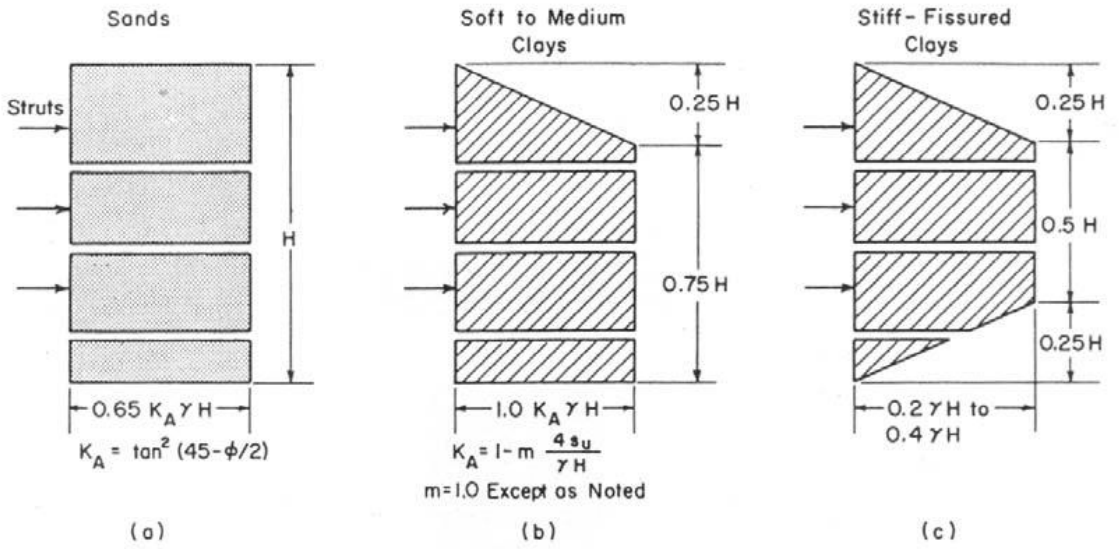

Figure 5: Apparent pressure diagram for strut loads (After Terzaghi and Peck, 1967)

Gue and Tan (1998) observe that for anchored diagram walls in Kenny Hill residual soils, the apparent lateral earth pressures that were obtained from the load cells indicated that for anchors at depths greater than 60% of the maximum excavation depth of more than 20m, the apparent earth pressure obtained is larger than the values suggested by Terzaghi and Peck (1967).

2.4.1.2 Movement analysis

The use of empirical data for the evaluations of movements is a useful tool in evaluating potential effects of a proposed excavation on adjacent buildings. Empirical data also allow the designer to validate the general magnitudes and patterns of the results of more sophisticated analyses. The empirical data can be used to estimate the zone of influence of the excavation as well as typical magnitudes of ground movements for various wall stiffness and subgrade stability conditions (e.g., Clough and O'Rourke, 1990).

2.4.2 Full soil-structure interaction analysis (staged excavation analysis)

This method will be able to model wall and soil deformation and stress in a realistic stages of operations that follow actual construction sequence. Pre-judged failure modes are not required in the analysis. This method can be carried out in two or three-dimensional depending on the computer codes used. Usually two-dimensional is sufficient.

This method is particularly useful in predicting deformations of wall and soil for serviceability checks especially there are deformation sensitive structures around the excavation. Use of soil stiffness at low strain value is essential in this approach.

Staged excavation analyses use numerical approaches to model the actual sequence of excavation and brace installation by considering each stage of the excavation as it is constructed, and the excavation support is installed and then removed. The soil and water pressures applied to the wall are representative of the actual pressures (not apparent pressure envelopes) expected in the system at each stage, and calculated loads are representative of the actual loads (not upper bound loads). The models can incorporate interaction of the soil and the structure as the earth pressures vary with displacement. The overall reliability of the structural requirements and displacement performance estimates determined from a staged excavation analysis is directly related to and very sensitive to the quality of the input parameters, particularly soil stiffness parameters.

Three general methods have been used for staged construction analyses:

- Equivalent Beam Method
- Beam on Elastic Foundation Method
- Finite Element Method

The equivalent beam method is outdated and rarely used in current practice. Our discussion will focus on the beam on elastic foundation and finite element methods. Both approaches can be used to predict stresses, loads, and system movements.

2.4.2.1 Beam on Elastic Foundation Method (BEF)

The earth pressures are modeled with a series of independent spring supports (Winkler elastic foundation model). At the start of the model, the springs are compressed to create an initial load equal to represent a state of at-rest pressure. At each stage of excavation or support system, the spring loads change as soil, water, and support system loads are applied or removed and lateral wall displacement occurs. The soil springs load-displacement relationship (modulus of subgrade reaction) is determined by the input soil stiffness and governs the spring displacement until the limiting value of active or passive pressure is reached.

The Winkler elastic foundation model approximates the wall-soil interaction with a one-dimensional model instead of a two-dimensional model that includes the soil mass, and hence does not include the effects of arching within the soil mass.

Typically, the required soil parameters include: unit weight; at-rest, active, and passive earth pressure coefficients; and values for the modulus of subgrade reaction for the various soils that may affect the system. The modulus of subgrade reaction is not a true soil property, but rather depends on both the soil conditions and the geometry of the excavation being modeled. To be representative, the modulus of subgrade reaction needs to be adjusted based on the effective influence zone, which varies with the size of the loaded area.

The BEF method does not directly estimate ground movements behind the wall. Ground movements behind the wall are evaluated using the calculated wall displacement from the model. An empirical relationship between wall movement and ground movements must then be used. There are several computer programs that automate the analysis. Some use Young's modulus as input for the soil stiffness. The program then automatically converts the Young's modulus values for the various soils to adjusted values of subgrade reaction modulus using closed-form elastic solutions.

The BEF analytical model can provide useful insights into the behavior of the wall and the wall-soil boundary, and the automated computer programs make it easy to perform multiple analyses for optimizing the design and evaluating sensitivity to input parameters.

2.4.2.2 Finite Element Methods (FEM)

Finite element models are typically two-dimensional models that include the soil mass surrounding the excavation. The stress-strain response of the soil is represented by a mathematical soil model that can vary from a simple linear- elastic model to a complex nonlinear Elasto-plastic model. The stress-strain response can be defined in terms of effective stresses or total stresses. The required input parameters depend on the soil model used.

Finite Element Method (FEM) is most well suited to this type of deformation analysis, however, FEM is too cumbersome and costly for general application and furthermore accurate determination of the required soil parameters is also difficult. In view of this, the magnitude and distribution of ground movements is generally considered based on empirical

method such as recorded case histories and often using collations such as Clough and O'Rourke (1990) in Table 4.

Table 4: Methods for predicting settlement of Adjacent ground for braced excavations *(S.S Gue & Y.C. Tan (1998))*

Proposers	Outline of prediction method	Ground	Conceptual diagram of the method
Naito, *et al.* (1958) (Empirical)	Solve for volume A_d (amount of deformed soil) and A_s (amount of settlement of ground surface) due to deformations of walls, which are the same. In recent years, amount of deformations of walls is computed by the "Elasto-plastic method" and amount of settlement is predicted from the relationship shown in the conceptual diagram.	Plastic Cohesive soil	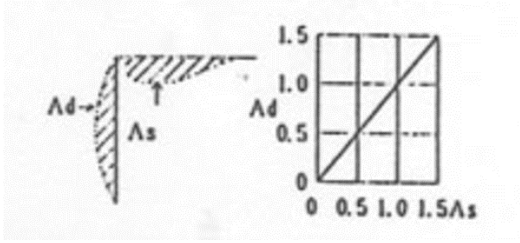
Maruoka, Ikuta, Aoki, Sato, *et al.* (1978) (1991) (Theoretical)	Determination of the relationship between the maximum amounts of settlement, $S_{max.}$ (Calculated as the following condition: a sliding surface is assumed according to the stress characteristic curve defined by Bransby (1975), and the wall displaces along with the sliding surface and appears on the ground surface.), and the heaving stability number N_b, proposed by Peck. After that, sliding surfaces are assumed by various methods, and the sliding surfaces are patterned for computing settlement of surface ground. The settlements are compared with measured data. D is the depth of excavation.	Soft Cohesive soil	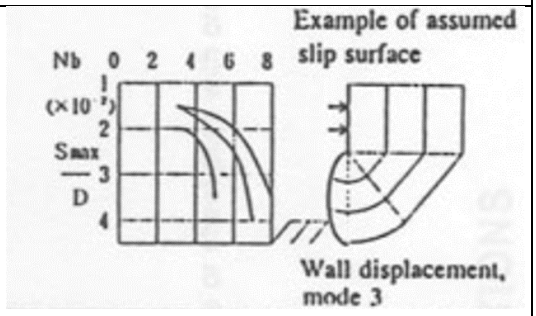
Japanese National Railways (1979) (Empirical)	Relationship between N value measured near the bottom of excavation and the maximum displacement of wall,δ_h divided by the final excavation depth H are examined. And if N-value become smaller than 5, the maximum displacement of wall becomes larger. This relationship is very similar to the relationship between Smax and Fsmin that was defined by Matuso and Kawamura (as shown below) and the relationship defined by Mana and Clough. (1981)	Cohesive to sandy soils	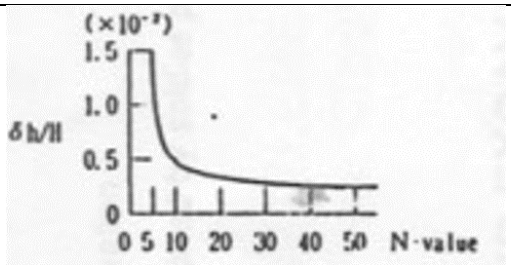
Matsuo and Kawamura (1981) (Empirical)	Showing that when the minimum safety factor Fsmin in a circular sliding surface becomes less than 1.15, the maximum amount of settlement, Smax suddenly increases (based on construction in soft cohesive soil). The relational expression for Smax and Fsmin are; Smax = 1/(0.654Fsmin - 0.719) (where Fsmin ≥ 1.10)	Soft or medium cohesive soil	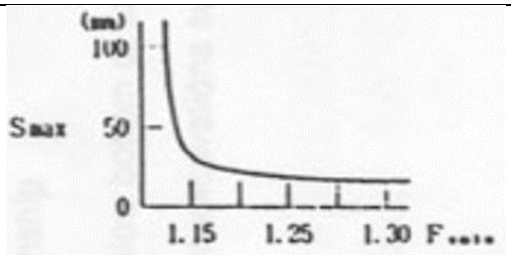

Proposers	Outline of prediction method	Ground	Conceptual diagram of the method
Marouka and Ikuta (1986) (Empirical)	Data collected from soft cohesive soil alluvial soil or sandy alluvial soil with N-value less than 10 are summarized for relationship between displacement of wall and adjacent ground.	Soft cohesive and alluvial sandy soil with SPT N less than 10	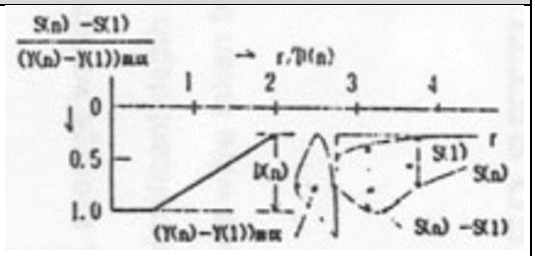
Sugimoto and Sasaki (1987) (Empirical)	The maximum amount settlement of surface ground, δ_{vmax}, will be 0.5 to 1.0 times the maximum horizontal displacement of wall, δ_{hmax}, and is confirmed based on measured data and proved by the FEM analyzing method. These results are similar to results obtained by Mana and Clough (1981).	Cohesive to Sandy soils	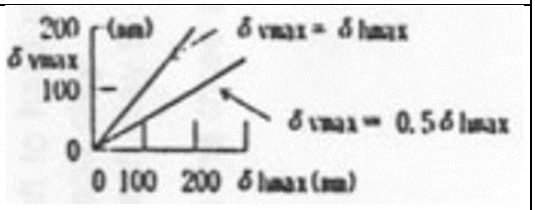
Sugimoto (1986) (Empirical)	Factors affecting the maximum amount of ground surface settlement, dz_{max} are extracted by using the many measured quantification theory, and these factors are combined to find the excavation coefficient αc. Then the relationship between αc and the maximum amount of ground settlement is determined. This relationship is verified by the FE analyzing method. Excavation coefficient $\alpha c = BH.\beta_D.D$ Embedment coefficient $\beta_D = (Es/EI)^{1/4}$		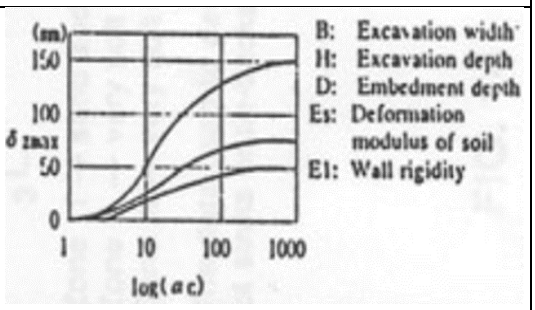

Note: The content in the parenthesis under the proposers' column are the category of the prediction method, either Theoretical or Empirical.

In contrast to the BEF analysis, the FE analysis can provide direct information on the ground movements outside of and inside the excavation. It can also be used to model the soil-structure interaction response of nearby structures to the excavation-induced ground movements. In the past, performing FE analyses have been complex and time consuming to perform, but new, user-friendly programs (e.g., PLAXIS) are making their use more common. Another difference between the FE and BEF methods is that variations in the soil stiffness (modulus) can have a greater effect on predicted loadings and movements due to the inclusion of soil arching in the FE model.

2.5 Empirical observations

2.5.1 Predicting ground movement

Ground movements behind a supported wall occur as a result of unbalanced pressure due to removal of soil mass inside the excavation site. The magnitude and distribution of the settlement are related to many factors such as construction quality, soil and ground water condition, excavation geometry, excavation sequences, duration of excavation, surcharge condition, existence of adjacent buildings, method of retaining wall construction, penetration depth, wall stiffness, type and installation of lateral support, spacing and stiffness of struts. A method derived purely from theoretical basis would be very complex.

Most of the existing predictive methods were obtained based on field measurements and local experiences. Several commonly used empirical methods in engineering practice are presented as follows:

2.5.1.1 Peck's Method

Peck (1969) summarized the field observations of ground surface settlement around excavations in a graphical form as shown in Figure 6. This method may be suitable for the spandrel-type settlement profile. As shown in the figure, the settlement curve is classified into three zones, I, II and III, depending on the type of soil and workmanship.

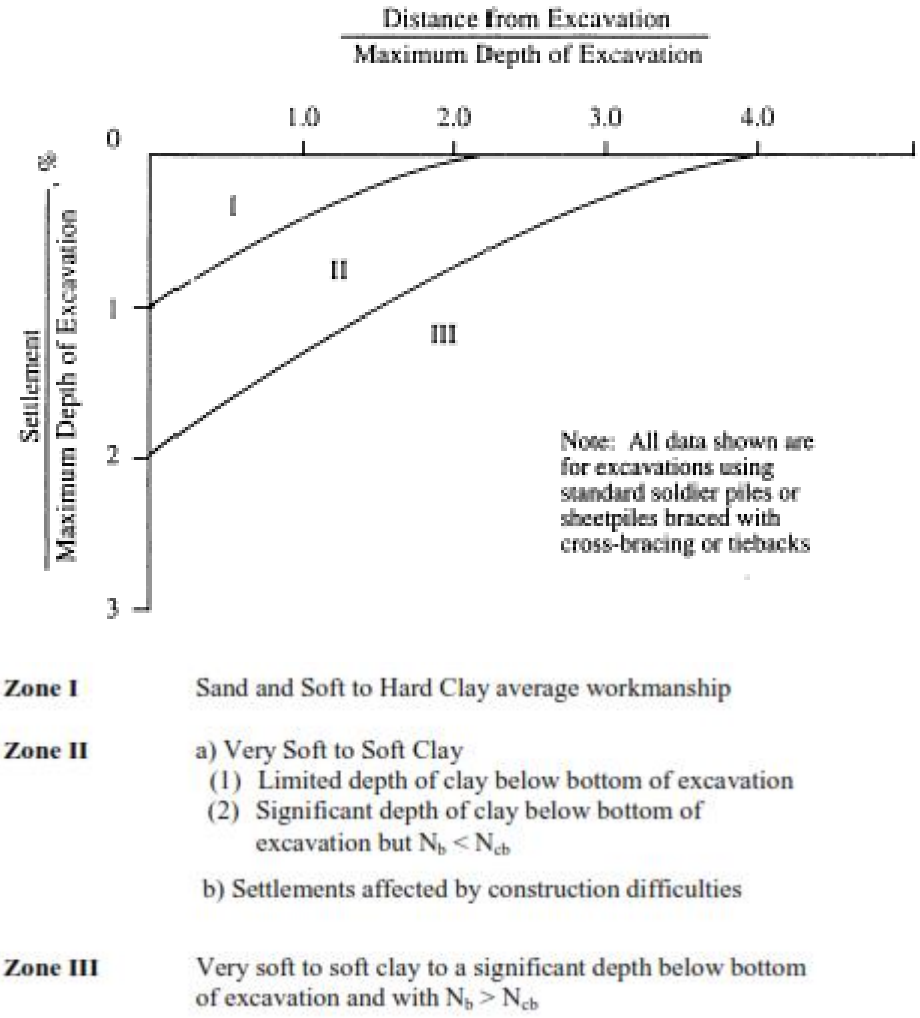

Figure 6: Summary of settlements adjacent to open cuts in various soils, as function of distance from edge of excavation (from Peck, 1969).

Figure 6 gives the settlements, divided by the maximum excavation depth H, and plotted against the distance from the walls also divided by the depth H. Three categories of behavior were defined according to soil types:

1. Sand and soft to hard clay, (zone I),
2. Very soft to soft clay (zone II)
    a. Limited depth of clay below the bottom of excavation.
    b. Significant depth of clay below the bottom of excavation but $N_b<N_{cb}$ and
3. Very soft to soft clay to a significant depth below the bottom of excavation and with $N_b > N_{cb}$ (zone III).

The stability number N_b is defined as $\gamma H / S$, where γ is the unit weight of the soil above the base of excavation, S_{ub} is the undrained shear strength below the base of excavation and N_{cb}

is the critical stability number for basal heave. The factor of safety against basal heave was defined by Terzaghi (1943) as follows in Figure 7.

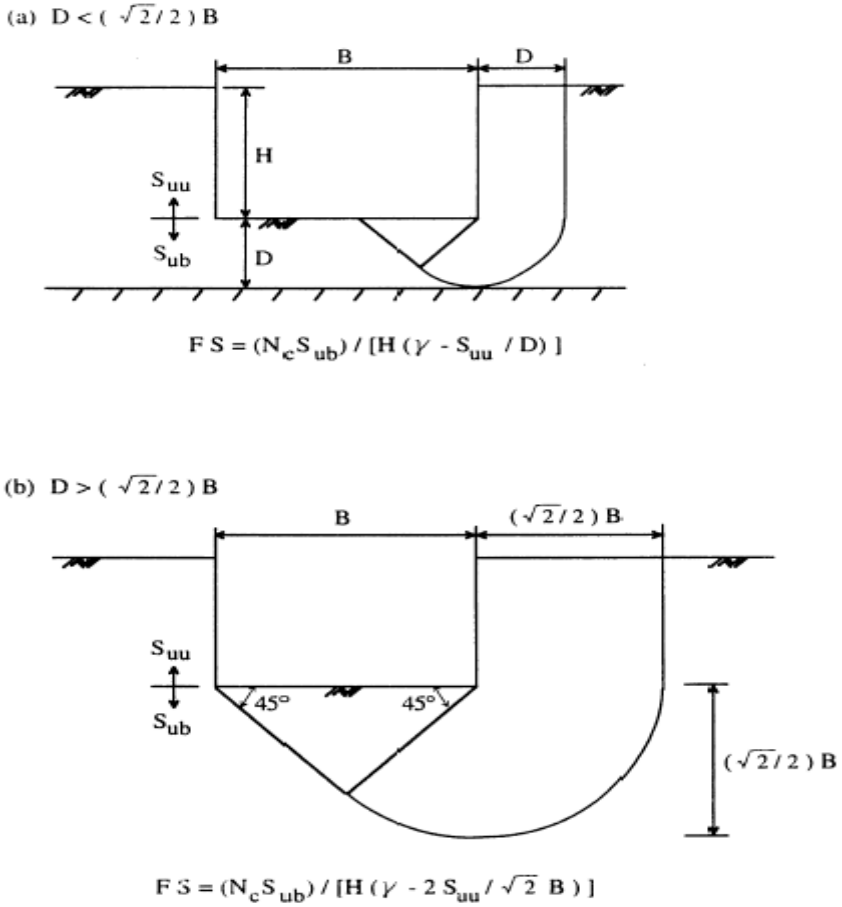

Where:
D = distance between the base of excavation and hard stratum
B = width of excavation
N_c= bearing capacity coefficient
S_{ub}= undrained shear strength below the base of excavation
S_{uu}= undrained shear strength above the base of excavation
γ = unit weight of soil

Figure 7: Excavation Geometry and Soil Strength Parameters for Factor Safety against basal Heave [Terzaghi, 1943]

2.5.1.2 Bowles' Method

Bowles (1988) proposed a method for estimating the spandrel-type settlement profile Induced by excavation. The steps are given as follows;

1. Lateral wall displacement is estimated.
2. Volume of lateral movement of soil mass is calculated.
3. The influence zone (*D*) using the method suggested by Caspe (1966) is adopted.

$$D = (H_e + H_d)\tan(45 - \frac{\phi'}{2})$$

Where;

H_e is the final excavation depth, ϕ ' is the internal frictional angle of soil.

For cohesive soil, $H_d = B$, where B = width of excavation;

For cohesion less soil, $H_d = 0.5\ B\ tan\ (45 + \phi'/2)$

4. By assuming that maximum ground settlement occurs at the wall, maximum ground settlement can be estimated by.

   $\delta_{vm} = 4Vs/D$

5. The settlement curve is assumed to be parabolic. The settlement (δ_v) at a distance from the supported wall (x) can be calculated as,

   $\delta_v = \delta_{vm}\ (x/D)^2$

   Where; x is the distance from the wall.

2.5.1.3 Clough and O'Rourke's Method

Clough and O'Rourke (1990) present the settlement profile of retained soil for properly designed and constructed excavation works using different retaining wall types & support system. In different soil types as follows:

a) Excavation in sand

Figure 8 summarizes settlements for excavation in predominantly sand and granular soils. The maximum settlements are typically less than 0.3% and extended with decreasing values up to a distance of 2 times the maximum excavation depth.

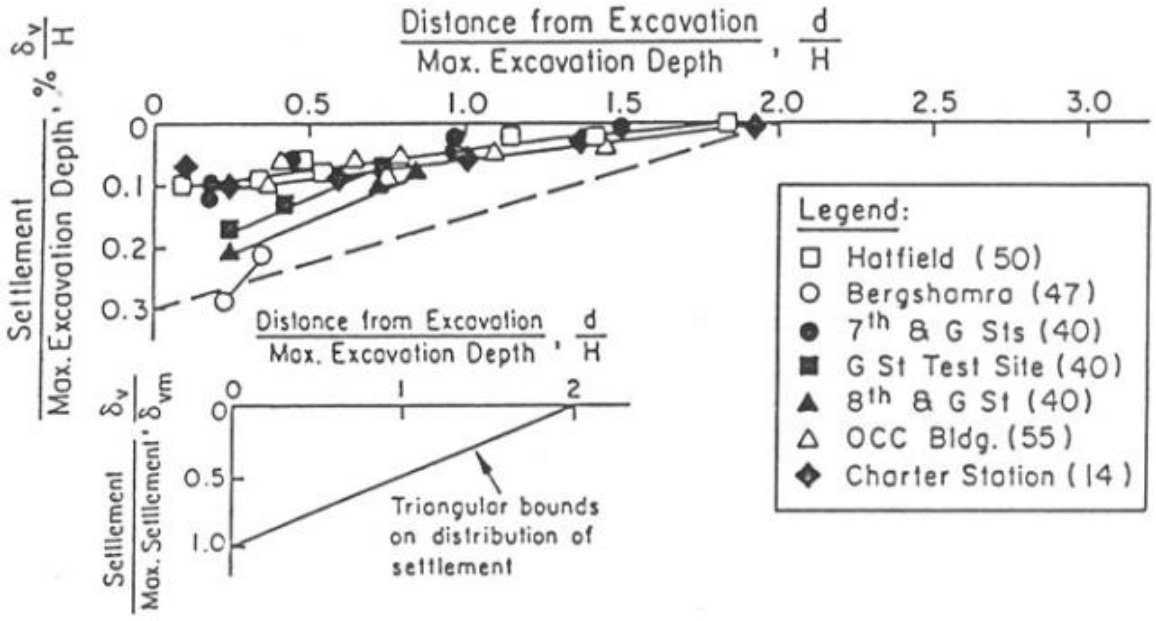

Figure 8: Summary of measured settlement adjacent to excavations in sand (From Clough & O'Rourke, 1990)

b) Excavation in stiff to very hard clays

Settlements and horizontal movements for excavation sites in stiff and very hard clays are summarized in Figure 9. The settlements are only a small percentage of excavation depth, with maximum settlement usually less than 0.3%, but are distributed over 3 times the excavation depth from the edge of excavation. Generally, the average horizontal and vertical settlements is about 0.2% and 0.15% of the depth of excavation respectively.

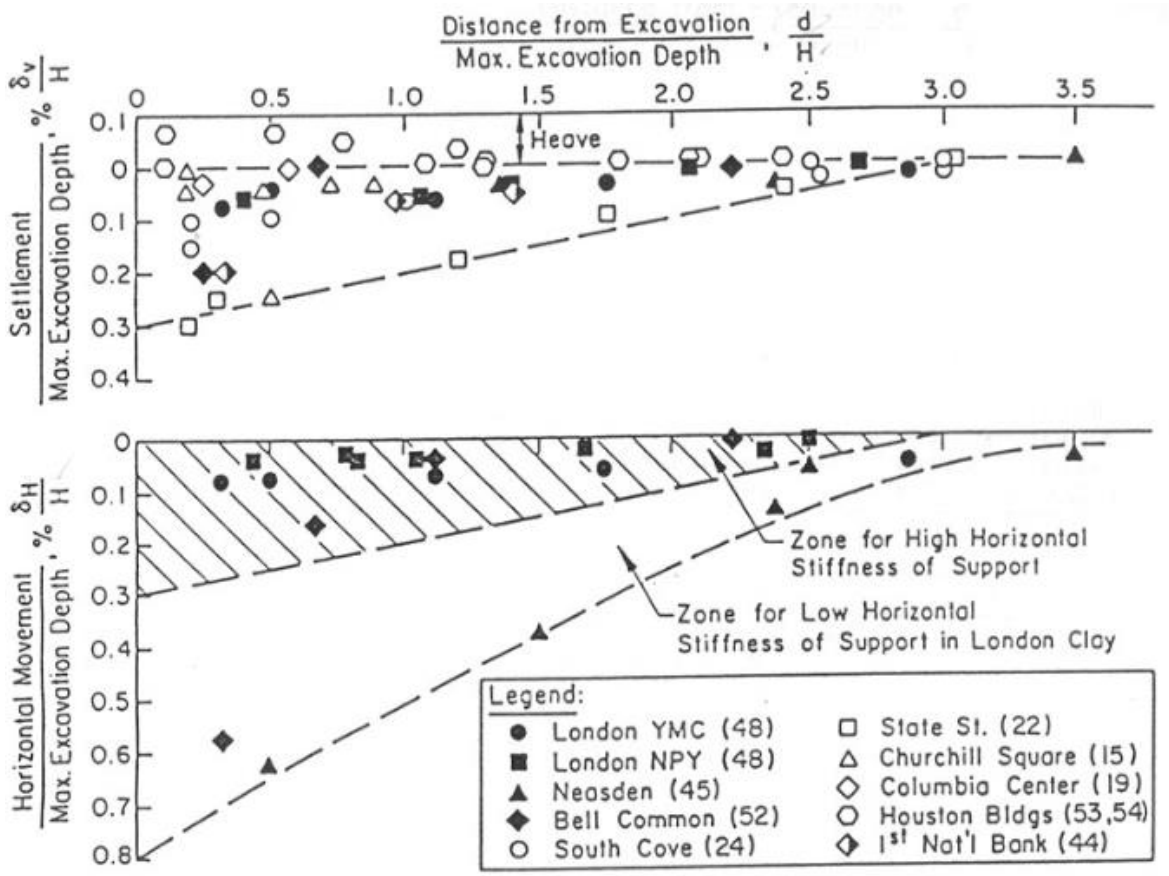

Figure 9: Summary of measured settlement to excavations in stiff to very hard clay (From Clough & O'Rourke, 1990)

c) Excavation in soft to medium stiff clays

Figure 10 shows the settlements for excavation in soft to medium clays. Zones pertaining to various levels of workmanship and soil conditions as described by Peck (1969) are also shown in this figure. Different from stiffer soils, basal stability dominates deflections of the excavation in soft to medium clays.

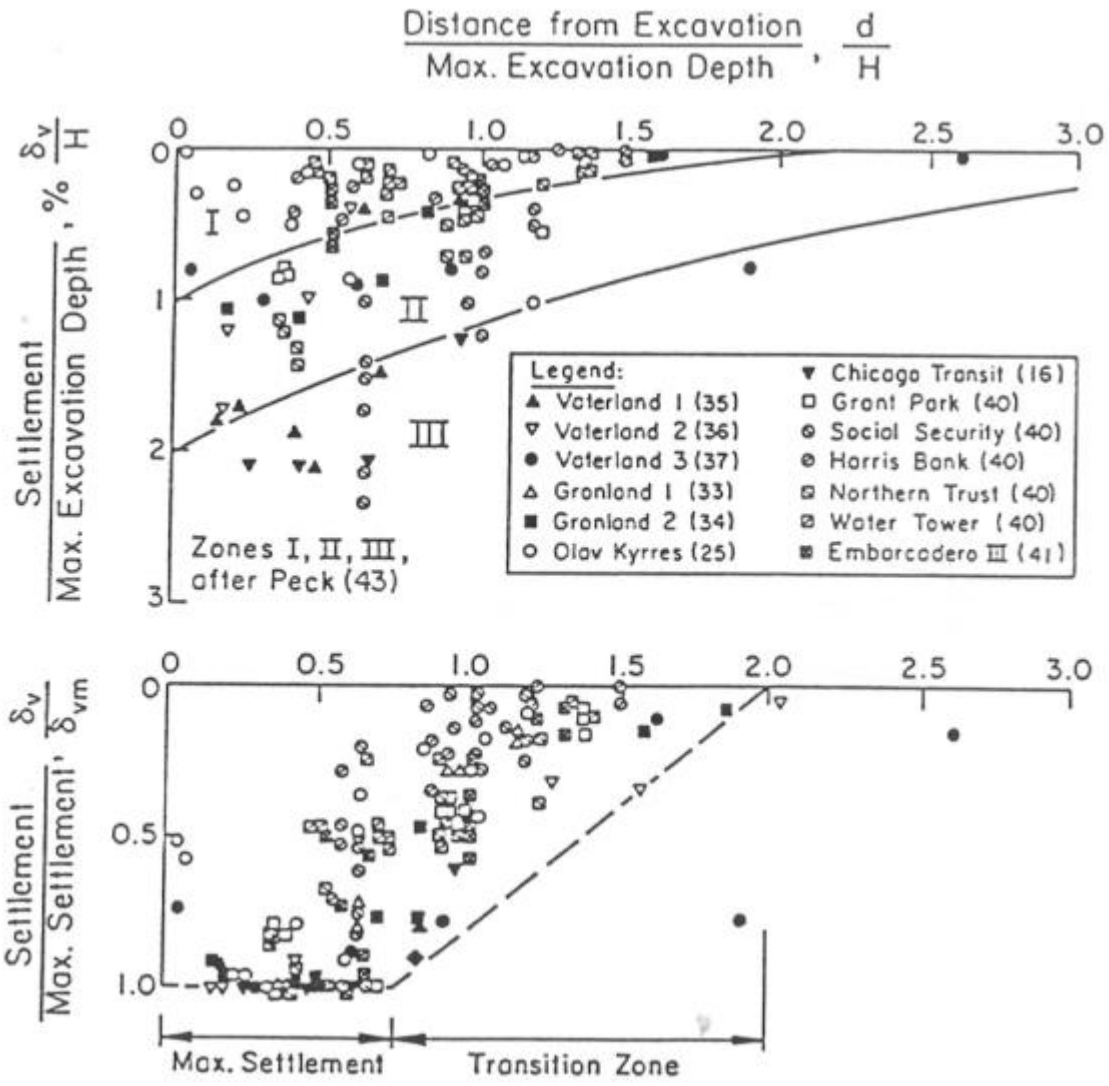

Figure 10: Summary of measured settlement to excavations in soft to medium clays (From Clough & O'Rourke, 1990)

Based on several case histories, Clough and O'Rourke (1990) suggested that the settlement profile is triangular for an excavation in sandy soil or stiff clay. The maximum ground surface settlement will occur at the wall. The non-dimensional profiles are given in Figure 11(a) and 11(b), which shows that the corresponding settlement extends to about $2H_e$ and $3H_e$ for sandy soil and stiff to very hard clays, respectively. For an excavation in soft to medium clay, the maximum settlement usually occurs at some distance away from the wall. The trapezoidal shape of the settlement tough is proposed as indicated in Figure 11(c). The influence zone extends up to 2 times the maximum excavation depth. If the δ_{vm} is known, the settlement at various locations can be estimated.

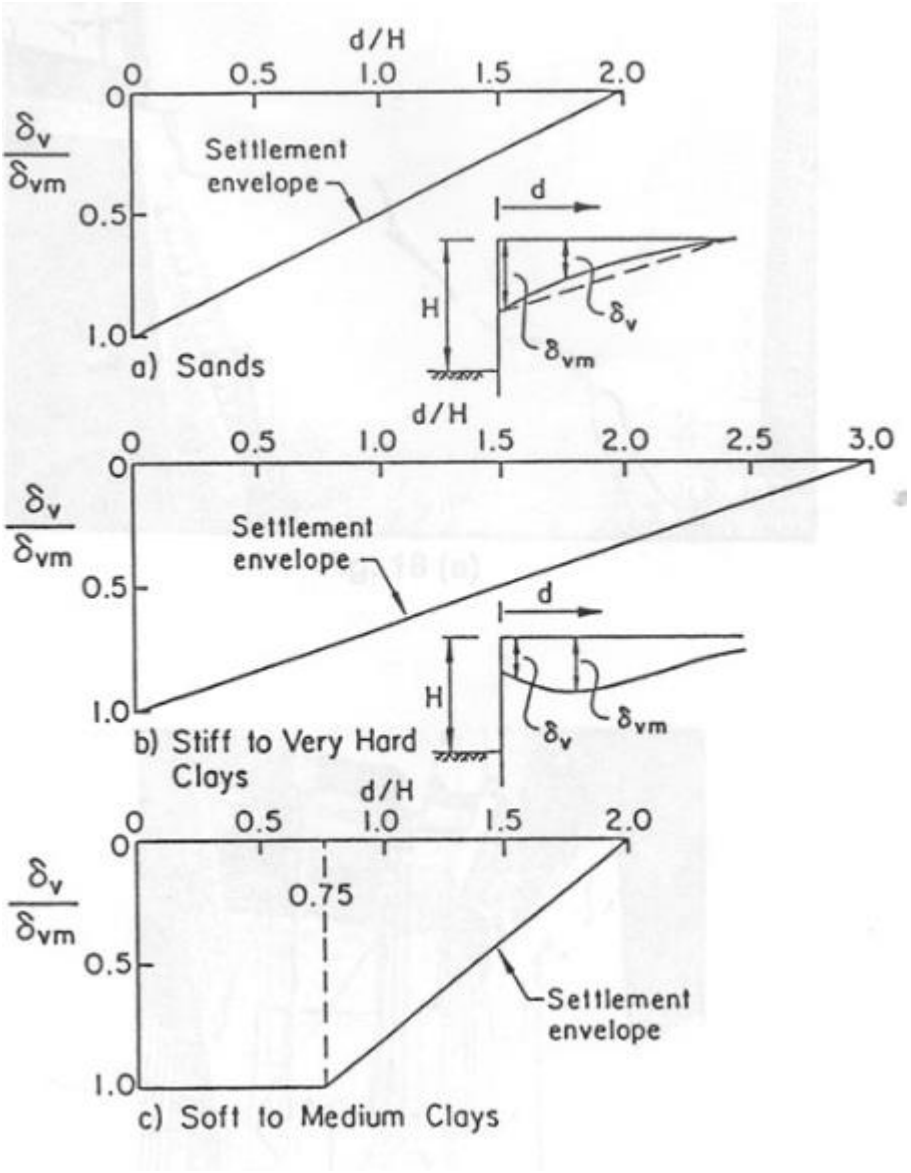

Figure 11: Dimensionless settlement profiles recommended for estimating the distribution of settlement adjacent to excavations in different soil types (from Clough and O'Rourke, 1990).

Clough and O'Rourke (1990) stated that if deep in ward movements are the predominant form of wall deformation, the settlements tend to be bounded by a trapezoidal displacement profile as in the case with deep excavations in soft to medium clay; and if cantilever movements predominate, as can occur for excavations in sands and stiff to very hard clay, then settlements tend to follow a triangular pattern.

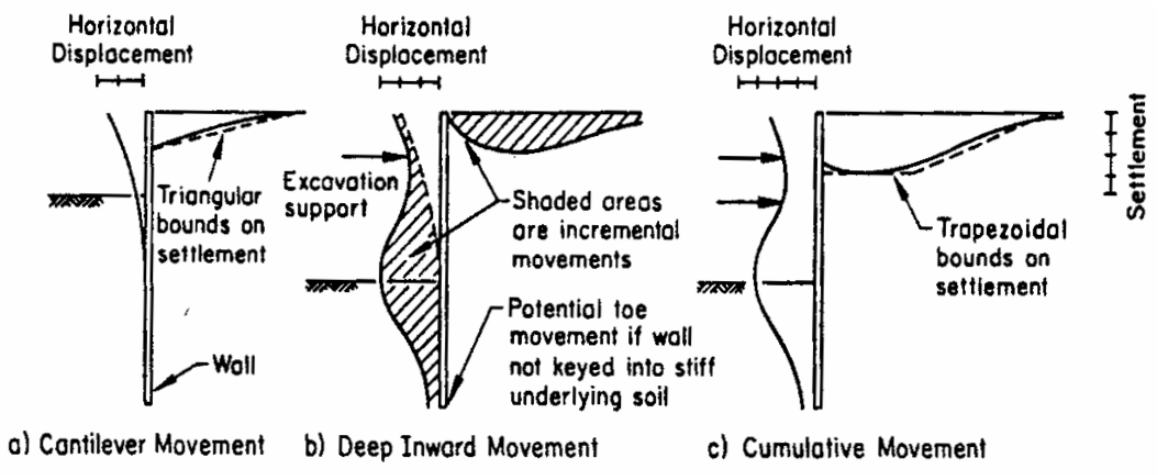

Figure 12: Typical Profiles of Movement for Braced and Tieback Walls (After Clough and O'Rourke, 1990).

2.5.1.4 Clough et al.'s Method

Clough et al. (1989) proposed a semi-empirical procedure for estimating movement at excavations in clay in which the maximum lateral wall movement δ_{hm} is evaluated relative to factor of safety (FS) and system stiffness, which is defined as follows:

$$\text{System stiffness } (\eta) = \frac{EI}{\gamma_w h^4}$$

Where;

EI - is the flexure rigidity per unit width of the retaining wall,
γ_w - the unit weight of water and
h - the average support spacing.

The factor of safety (FS) is defined according to Terzaghi (1943), as shown in Figure 7. It should be emphasized that FS is used as an index parameter. The system stiffness is defined as a function of the wall flexural stiffness, average vertical separation of supports, and unit weight of water, which is used as a normalizing parameter. Figure 13 shows δ_{hm} plotted relative to system stiffness for various FS. The family of curves in the figure is based on average condition, good workmanship, and the assumption that cantilever deformation of the wall contributes only a small fraction of the total movement. A method for estimating cantilever movement is also recommended by Clough et al. to add directly to those predicted by the Figure 13.

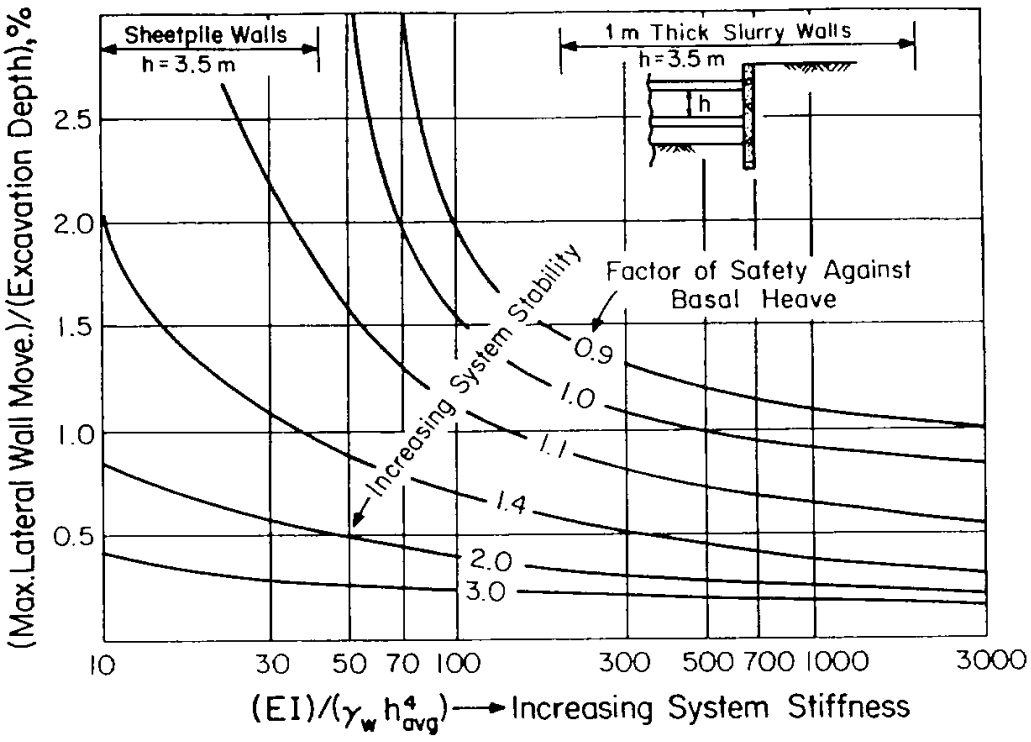

Figure 13: Lateral wall movements as a percentage of excavation depth versus system stiffness (After Clough, et al. 1989)

2.5.1.8 Long's Database

Long (2001) analyzed 296 case histories. His studies largely focus on validating results of Clough and O'Rourke (1990) for stiff soils with δ_{hm}/H=0.05-0.25% and δ_{vm}/H=0-0.2% on the Figure 14. For soft clay with low factor of safety against base stability, large movements of up to δ_{hm}/H = 3.2% may occur. These roughly followed the trends in Clough's chart despite scattering of the data. He stated that the deformations of deep excavations in non-cohesive soils as well as in stiff clay are independent of the stiffness of the wall and the support as well as the kind of support. The stiffness term only affects the deformation significantly when dealing with deep excavation in soft clays with a low factor of safety against base heave. Attempts were made by Long (2001) to validate the use of Adden brooke's flexibility number for quantifying stiffness of the support system. Results again show a similar trend as found in Clough's approach with wide scatter.

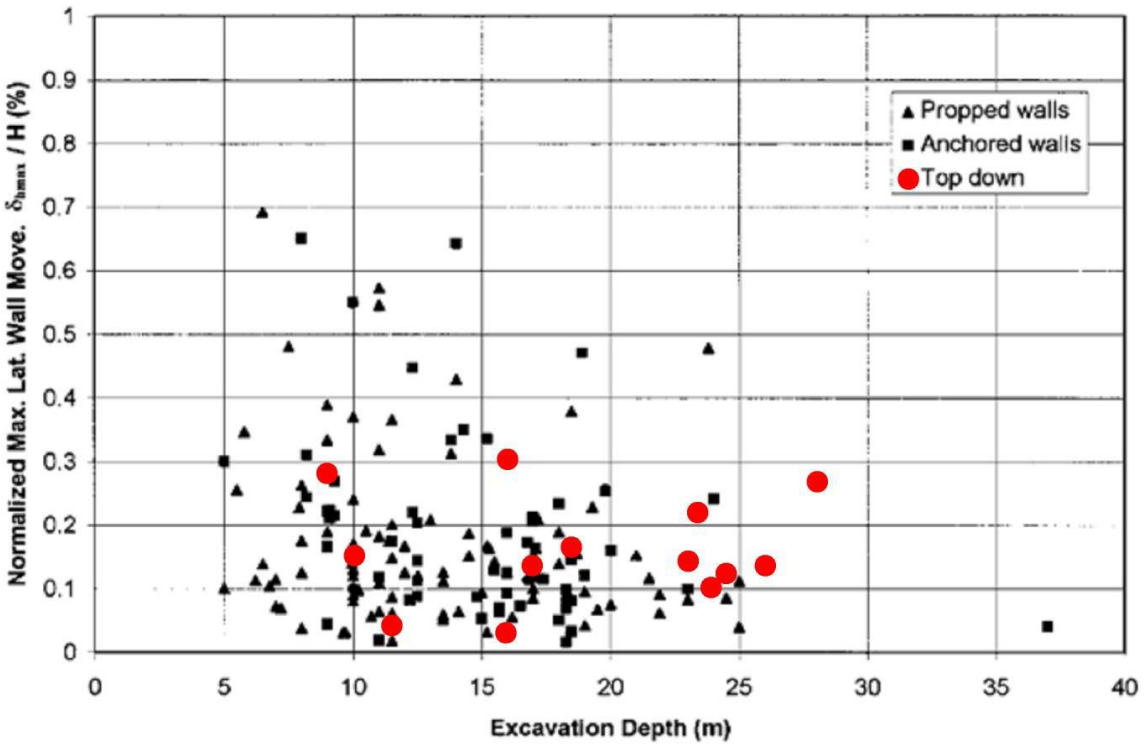

Figure 14: Normalized maximum lateral wall movement versus depth (taken from Long, 2001)

2.5.1.9 Moormann's Database

Moormann (2004) had carried out extensive empirical studies by taking 530 case histories of retaining wall and ground movement due to excavation in soft soil (C_u < 75kpa) into account. It is concluded that the maximum horizontal wall displacement (δ_{hm}) lie between 0.5% H and 1.0 % H, on average at 0.87% H (Figure 15 and Figure 16). The location of maximum horizontal displacement is at 0.5H to 1.0H below the ground. The maximum vertical settlement at the ground surface behind a retaining wall (δ_{vm}) lies in the range of0.1% H to 10% H, on average at 1.1% H. The settlement δ_{vm} occurs at a distance of less than 0.5 % H behind the wall, but there are cases in soft soil with this distance to be up to 2.0 H. The ratio δ_{vm}/δ_{hm} varies mainly between 0.5 and 1.0. The ground conditions and the excavation depth H are found to be the most influential parameter for deformation due to excavation. The retaining wall and ground movements seem to be largely independent of the system stiffness of the retaining system. Figure 17 shows the variation of normalized horizontal displacement with the system stiffness of the retaining structures. The results are then compared with the previous prediction by O'Rourke (1993). large scatter was observed. A calculated safety factor of about 1 could lead to observed maximum wall displacementsδh/H as low as 0.1%,even low as 0.1%,even though the value expected by

Clough et.al. was about 1% even for the stiffest support system.

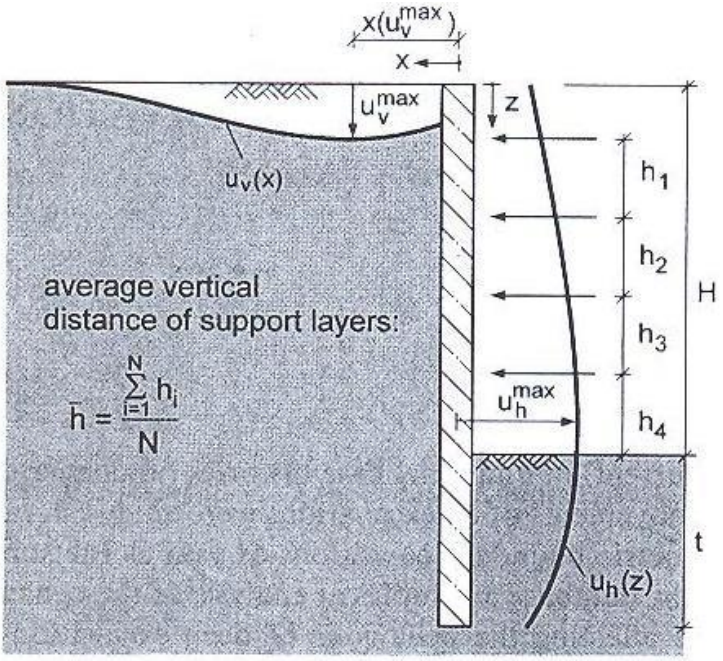

H [m] : max. depth of excavation (final stage)
t [m] : static relevant embedded length
h_i [m] : vertical spacing of support (struts, anchor)
u_h^{max} [m] : maximum horizontal wall displacement
u_v^{max} [m] : maximum vertical displacement at ground surface
N [-] : number of support layers

Figure 15: Definition of symbols by Moormann (2004)

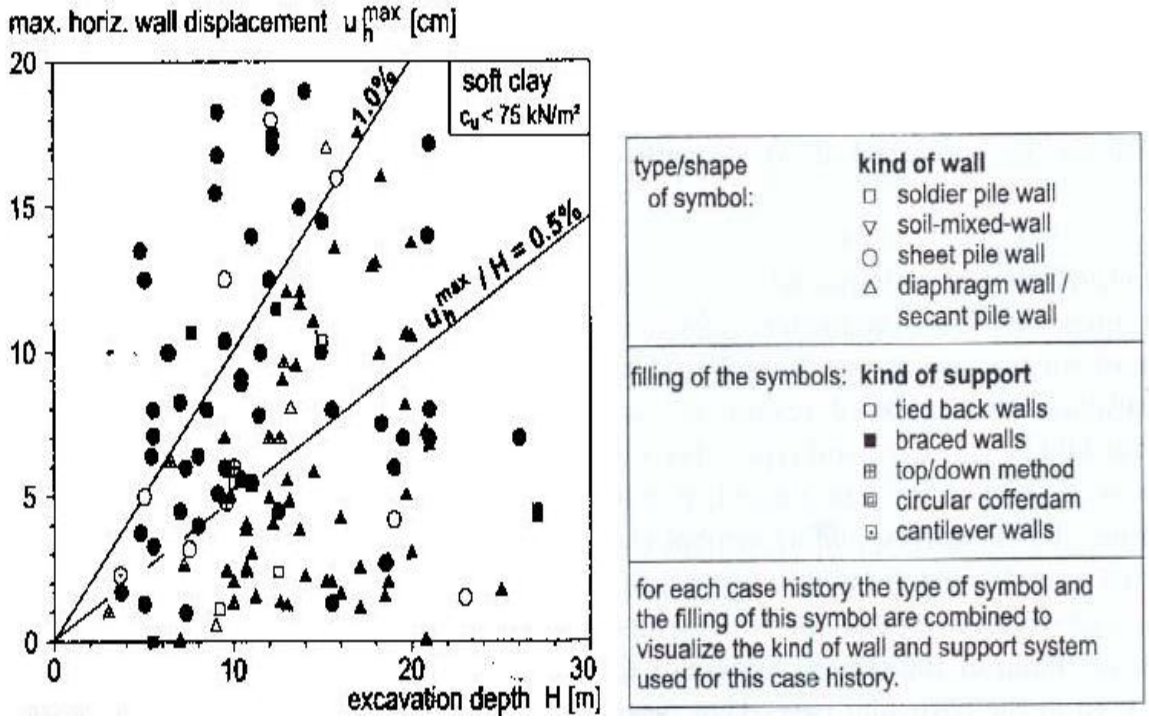

Figure 16: Variation of maximum horizontal displacement with excavation depth following Moormann (2004)

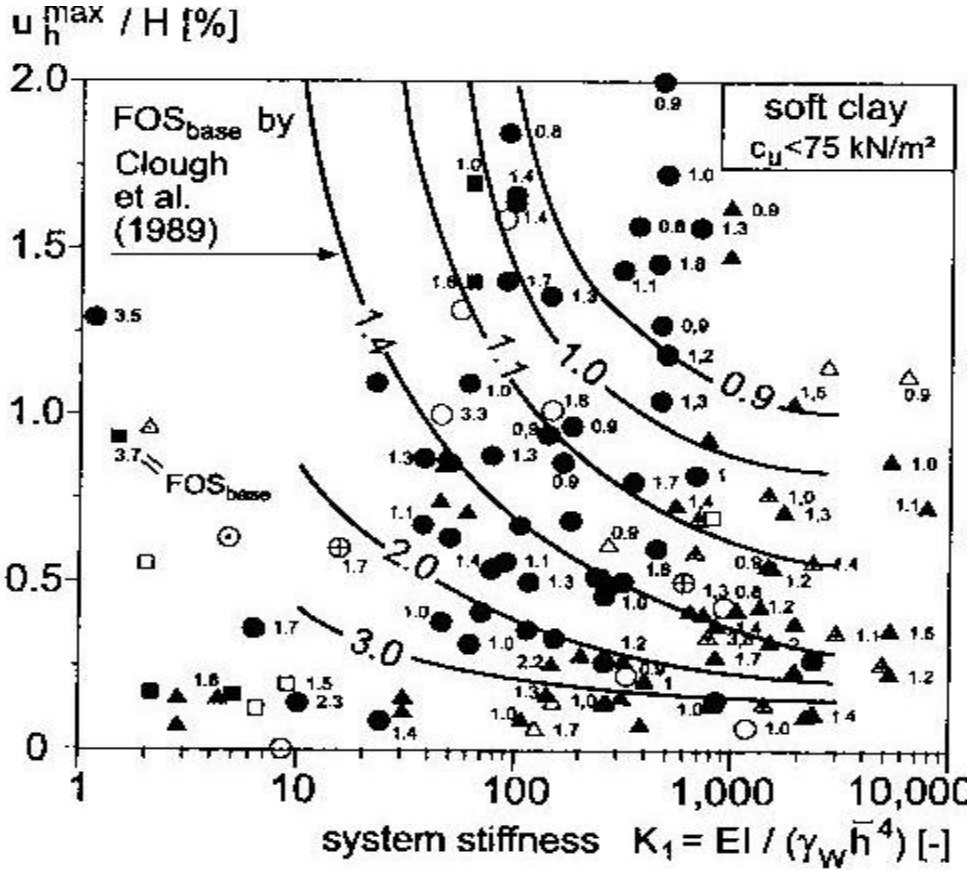

Figure 17: Variation of normalized maximum horizontal displacement with system stiffness following Moormann (2004) (For legend see figure 16)

2.6 Numerical studies

Effect of supporting structure

Mana and Clough (1981) carried out parametric studies on the effect of wall stiffness and strut spacing, the effect of strut stiffness, and the effect of excavation geometry such as excavation width and depth of the underlying firm layer, the effect of strut preloading and calculation of elastic soil stiffness on excavation induced deformation. Increasing the wall bending stiffness or decreasing strut spacing decreases movement. This effect is more significant when the factor of safety is low. Increasing the strut stiffness reduces movement, though the effect shows diminishing return at very high stiffness. Movement increases as excavation width and depth to an underlying firm layer increases. Use of preloads in the struts reduces movement, although there is a diminishing returns effect at higher preloads. Movement levels are strongly influenced by the soil modulus. Higher modulus leads to smaller movement.

Powrie and Li (1991) have carried out a series of numerical analyses on excavations singly propped at the crest of the retaining wall. The effect of soil, wall and prop stiffness and pre-excavation pressure coefficient were investigated. As the structure investigated was very stiff, so the magnitude of soil and wall movements was governed by the stiffness of the soil rather than that of the wall. A reduction in soil stiffness by a factor of 2 resulted in an increase in wall deformation almost by the same order of magnitude. On the other hand, wall movement was little affected by a 40% reduction in bending stiffness when the thickness of the wall was reduced from 1.5m to 1.25m. The assumed pre excavation lateral earth pressure significantly affected the prop loads and bending moment though the deformation would not increase much due to the accompanying increase in soil stiffness. The connection of the base slab to the retaining wall had an important influence on the bending moment profile of the slab. The provision of a quasi-rigid construction joint reduced the bending moment in the wall and the hogging moment at the center of the prop slab, but introduced a sagging moment in the slab at the connection to the wall.

CHAPTER 3

DEFORMATION CHARACTERISTICS AND PARAMETRIC STUDY OF DEEP EXCAVATION

3.1 Introduction

This part presents two -dimensional effects that the support system stiffness has on the behavior and performance of deep excavations. First, the Deformation characteristics (contiguous pile wall deformation and settlement variations) using contiguous pile wall parameters which is constructed in Addis Ababa, Lideta sub-city investigated on three types of soil, which have different shear strength parameters (Total and Effective shear strength parameters) and different drainage conditions (Drained and Undrained). In the second part the description and results of parametric study on the same three types of soil and with selected parameters are presented.

3.2 The Base Model Generation

A typical base model geometry and general dimensions for the study is shown in Figure 18. The model is simulated as a symmetrical plain strain finite element employing 15-noded triangular elements and half of the geometry with a width of 68 m and depth of 32 m.

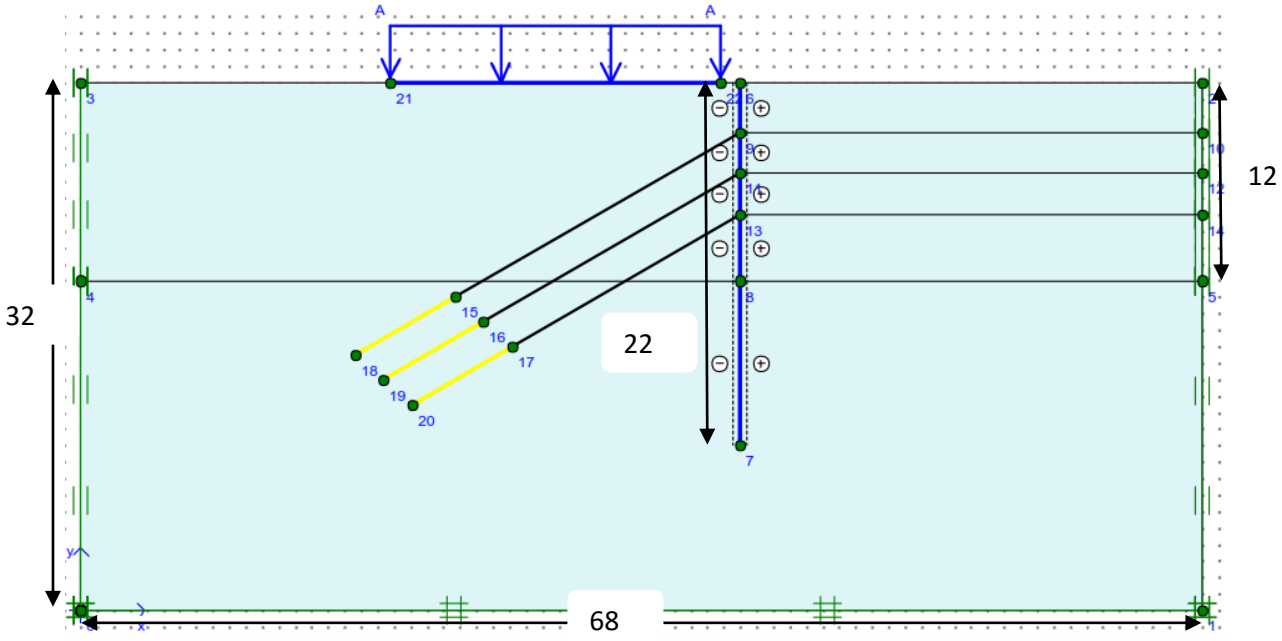

Figure 18: Typical Finite Element Model in PLAXIS for Deep Excavation

The soil is homogeneous layer (three types of soil) and the input parameters used in PLAXIS are presented in Table 5 below. Because of the low permeability of cohesive soil, the drainage conditions are Undrained with Effective & Total stresses and Drained with Effective stress drainage conditions are used in this study. The interface, R_{inter} is set to 0.5 for all clay layers (R_{inter} values gives a reduced interface friction & the cohesion in the adjacent soil).

Table 5: Soil parameters for Base Model

Parameter	Name	Unit	Soil Type								
			S_1			S_2			S_3		
Model utilized	Model	-	Mohr-Coulomb			Mohr-Coulomb			Mohr-Coulomb		
Type of material behaviour	Type	-	Undrained (Total Stress)	Undrained (Effective Stress)	Drained (Effective Stress)	Undrained (Total Stress)	Undrained (Effective Stress)	Drained (Effective Stress)	Undrained (Total Stress)	Undrained (Effective Stress)	Drained (Effective Stress)
Soil unit weight	γ_{unsat}	kN/m^3		16	16	16.5	16.5	16.5	17	17	17
	γ_{sat}	kN/m^3	19	19	19	19.3	19.3	19.3	19.6	19.6	19.6
Permeability in Hor. direction	K_x	m/day	0.001	0.001	0.001	0.0001	0.0001	0.0001	0.00001	0.00001	0.00001
Permeability in Ver. direction	K_y	m/day	0.001	0.001	0.001	0.0001	0.0001	0.0001	0.00001	0.00001	0.00001
Effective Young Modulus*	E'	kN/m^2		23,400	23,400		43,200	43,200	-	59,400	59,400
Undrained Young Modulus	E_u	kN/m^2	27,000	27,000		54,000	54,000		81,000	81,000	
Poisson's ratio	ν	-	0.35	0.3	0.3	0.35	0.2	0.2	0.35	0.1	0.1
Undrained Cohesion	C_u	kN/m^2	62	62	62	115	115	115	155	155	155
Effective Cohesion	C'	kN/m^2		30	30		60	60	-	90	90
Effective Friction angle	ϕ'	o	0	21	21	0	19	19	0	16	16
Dilatancy angle	ψ	o	0	0	0	0	0	0	0	0	0
Strength reduction factor	R_{inter}	-	0.5	0.5	0.5	0.5	0.5	0.5	0.5	0.5	0.5

Note:

***Effective Young Modulus, E'** $E' = \frac{2(1+\nu)}{3} E_u$ **(From Plaxis)**

The contiguous pile wall is modeled as elastic plate element. All parameters are computed from the actual deep excavation supported by contiguous pile wall implemented on Commercial Bank of Ethiopia, Lideta Office Building (3B+G+M+13 = 18 floors) found in Addis Ababa, Lideta Sub-City (Table 6).

The tie-back anchors are installed into contiguous pile wall. Each anchor is inclined at 30° with horizontal spacing ranged from 1.5m. The anchors assumed to have tensile strength, EA, of $200x10^6$ kN/m and pre-stress load of 250kN tie-back anchors. At the end of tie-back anchors, ground anchors of 7 m length are installed. Ground anchors, which have no bending stiffness but axial stiffness only, allow a continuous load transfer from the tie-back anchors to the ground along its entire length (Table 7).

Table 6: Contiguous pile wall parameter for Base Model

Parameter	Name	Unit	Contiguous pile
Concrete	Concrete class	-	C 30
Type of Material Behavior	Type	-	Elastic
Contiguous Pile Wall	Diameter	m	0.6
Reinforcement	Grade	-	S400
Diameter	D	m	0.016
Number of reinf.	No.	No.	8
Area of reinforcement	A_S	m^2	0.001609
Secant Modulus of Elasticity of concrete class C 30	E_C^*	kN/m^2	32,000,000
Secant Modulus of Elasticity of steel reinforcement	E_S^*	kN/m^2	200,000,000
Flexural Rigidity	EI^{**}	kNm^2/m	203,662.29
Normal Stiffness	EA	kN/m	9,051,428.57
Weight	W^{***}	(kN/m/m)	12.99

Note:

- *- E_C and E_S are taken from EBCS-2
- **- $EI = E_C I_g + E_s I_s$ where, $I_g = \pi r^4/4$ and I_g= gross moment of inertia, I_s= Moment of inertia of steel
- ***- $W = \gamma_C * d_{eq.} = \gamma_C * (12*(EI/EA))^{0.5}$,where $\gamma_C = 25kN/m^3$ (EBCS-2)

(W = weight per length of contiguous pile)

Table 7: Strut (Tie -back Anchor) Parameter for Base Model

Parameter	Name	Unit	Strut (Tie back Anchor)
Type of Material Behavior	Type	-	Elastic
Normal Stiffness	EA	kN/m	200,000,000
Spacing out of plane	L_S	m	1.50
Inclination	α	o	30

3.3 The Construction Phase

The sequence of construction activities at the site consists of wall installation, excavation, and support. The contiguous pile walls are installed before excavation. The installation is followed by grouting at the toe of the contiguous piles walls. Excavations inside the contiguous pile walls are proceeded in stages, which are alternated by the installation and preloading of anchors. Excavation and anchor installation, in which the excavations are presented as excavations I through IV from surface to formation level. For excavations I through III, each excavation stage is followed by a stage of anchor installation & preloading of anchors.

The typical phases in staged construction which are assumed to be carried out intervals of 3m, 2.5m (2 times) and 4m are shown below in Table 8:

Table 8: Calculation Phase of 2D non-linear Finite Element Analysis of case study on Contiguous Pile wall

Phase	Phase No.	Calculation type	Load input
Initial phase	0	-	-
Install wall	1	Plastic analysis	Staged construction
Excavate to first level RL-3.00 m	2	Plastic analysis	Staged construction
Install and prestress of tieback anchor at RL- 3.00m	3	Plastic analysis	Staged construction
Excavate to second level RL-5.50 m	4	Plastic analysis	Staged construction
Install and prestress of tieback anchor at RL- 5.50m	5	Plastic analysis	Staged construction
Excavate to third level RL-8.00 m	6	Plastic analysis	Staged construction
Install and prestress of tieback anchor at RL- 8.00m	7	Plastic analysis	Staged construction
Excavate to final level RL-12.00 m	8	Plastic analysis	Staged construction

3.4 Deformation characteristic of contiguous pile wall on soils commonly found in Addis Ababa

To analyze the characteristic/Base Model three neighboring structure loads have been considered, whose load are described in Table 9.

Table 9: Neighboring structure loads

Parameter	Unit	Load, L_1	Load, L_2	Load, L_3
Load	kN/m/m	56	75	94

The simulation of structure behavior is achieved by modelling it as a surface beam, taking into account both the bending stiffness and the axial stiffness of the structure.

The Model is proposed by Potts and Addenbrooke (1997) to study the influence of the stiffness of a structure located at the ground surface on constructing bored tunnels. They used a surface beam model. The beam used to simulate the structure assumed to be elastic and its interface with the soil to be rough.

Table 10: Neighboring structure stiffness parameter for base model

Parameter	Name	Unit	Beam/Plate
Type of Material Behavior	Type	-	Elastic
Axial Stiffness	EA	kN/m	640,000,000
Structure Stiffness	EI	kNm^2/m	180,000

Table 11: Distances between the face of excavation and the neighboring structure

Case	D_1	D_2	D_3	D_4	D_5
Distance (m)	1.2	2.4	3.6	4.8	6
H_e = 12m	(=0.1H_e)	(=0.2H_e)	(=0.3H_e)	(=0.4H_e)	(=0.5H_e)

3.5 Results of the Analysis

3.5.1 Lateral wall deflection

The variation of maximum lateral wall deflection with excavation-neighboring structure distance, depending on the type of structure loads and for three type of soils, drained with Effective stress, undrained with Effective stress & Undrained with Total stress drainage conditions are represented in Figure 19.

Table 12: Lateral wall deflection, Vertical settlement and Moment output from base model *(Drained with Effective stress)*

Soil Type S_1

Horizontal (δ_h), Vertical (δ_v) Deformation & Moment (M)			δ_h (mm)						δ_v (mm)						M (kNm/m)		
Load Type / Distance (m)			L_1	δ_h/H_e (%)	L_2	δ_h/H_e (%)	L_3	δ_h/H_e (%)	L_1	δ_v/H_e (%)	L_2	δ_v/H_e (%)	L_3	δ_v/H_e (%)	L_1	L_2	L_3
$D_1 = 0.1H_e$	1.2	0.1	45	0.37	50	0.42	55	0.46	128	1.07	128	1.07	128	1.07	240	249	251
$D_2 = 0.2H_e$	2.4	0.2	45	0.37	50	0.41	55	0.45	128	1.07	128	1.07	128	1.07	245	256	264
$D_3 = 0.3H_e$	3.6	0.3	44	0.37	49	0.41	54	0.45	128	1.07	128	1.07	128	1.07	249	260	274
$D_4 = 0.4H_e$	4.8	0.4	43	0.36	48	0.40	53	0.44	128	1.07	128	1.07	128	1.07	252	264	278
$D_5 = 0.5H_e$	6	0.5	43	0.36	47	0.39	51	0.43	128	1.07	128	1.07	128	1.07	255	268	281

Soil Type S_2

Horizontal (δ_h), Vertical (δ_v) Deformation & Moment (M)			δ_h (mm)						δ_v (mm)						M (kNm/m)		
Load Type / Distance (m)			L_1	δ_h/H_e (%)	L_2	δ_h/H_e (%)	L_3	δ_h/H_e (%)	L_1	δ_v/H_e (%)	L_2	δ_v/H_e (%)	L_3	δ_v/H_e (%)	L_1	L_2	L_3
$D_1 = 0.1H_e$	1.2	0.1	16	0.13	18	0.15	20	0.16	83	0.69	83	0.69	83	0.69	193	198	203
$D_2 = 0.2H_e$	2.4	0.2	16	0.13	17	0.14	19	0.16	83	0.69	83	0.69	83	0.69	195	200	207
$D_3 = 0.3H_e$	3.6	0.3	16	0.14	17	0.14	19	0.16	83	0.69	83	0.69	83	0.69	197	203	209
$D_4 = 0.4H_e$	4.8	0.4	16	0.14	17	0.14	18	0.15	83	0.69	83	0.69	83	0.69	198	205	212
$D_5 = 0.5H_e$	6	0.5	17	0.14	17	0.14	18	0.15	83	0.69	83	0.69	83	0.69	200	207	213

Soil Type S_3

Horizontal (δ_h), Vertical (δ_v) Deformation & Moment (M)			δ_h (mm)						δ_v (mm)						M (kNm/m)		
Load Type / Distance (m)			L_1	δ_h/H_e (%)	L_2	δ_h/H_e (%)	L_3	δ_h/H_e (%)	L_1	δ_v/H_e (%)	L_2	δ_v/H_e (%)	L_3	δ_v/H_e (%)	L_1	L_2	L_3
$D_1 = 0.1H_e$	1.2	0.1	10	0.08	10	0.08	10	0.08	67	0.56	67	0.56	67	0.56	188	193	198
$D_2 = 0.2H_e$	2.4	0.2	10	0.08	10	0.08	10	0.09	67	0.56	67	0.56	67	0.56	189	194	199
$D_3 = 0.3H_e$	3.6	0.3	10	0.08	10	0.08	10	0.09	67	0.56	67	0.56	67	0.56	191	196	201
$D_4 = 0.4H_e$	4.8	0.4	10	0.08	10	0.09	10	0.09	67	0.56	67	0.56	67	0.56	191	197	202
$D_5 = 0.5H_e$	6	0.5	10	0.08	10	0.09	11	0.09	67	0.56	67	0.56	67	0.56	192	198	203

Table 13: Lateral wall deflection, Vertical settlement and Moment output from base model *(Undrained with Effective stress)*

Soil Type S_1

Horizontal (δ_h), Vertical (δ_v) Deformation & Moment (M)			δ_h (mm)						δ_v (mm)						M (kNm/m)		
Load Type / Distance (m)			L_1	δ_h/H_e (%)	L_2	δ_h/H_e (%)	L_3	δ_h/H_e (%)	L_1	δ_v/H_e (%)	L_2	δ_v/H_e (%)	L_3	δ_v/H_e (%)	L_1	L_2	L_3
$D_1 = 0.1H_e$	1.2	0.1	69	0.58	76	0.63	90	0.75	53	0.44	66	0.55	86	0.72	191	214	252
$D_2 = 0.2H_e$	2.4	0.2	69	0.58	76	0.63	87	0.72	53	0.44	65	0.54	81	0.68	196	217	254
$D_3 = 0.3H_e$	3.6	0.3	70	0.58	76	0.63	85	0.71	53	0.44	64	0.53	78	0.65	200	221	253
$D_4 = 0.4H_e$	4.8	0.4	70	0.58	76	0.63	84	0.70	52	0.43	63	0.53	77	0.64	203	222	252
$D_5 = 0.5H_e$	6	0.5	70	0.58	76	0.63	84	0.70	52	0.43	62	0.52	76	0.63	205	222	249

Soil Type S_2

Horizontal (δ_h), Vertical (δ_v) Deformation & Moment (M)			δ_h (mm)						δ_v (mm)						M (kNm/m)		
Load Type / Distance (m)			L_1	δ_h/H_e (%)	L_2	δ_h/H_e (%)	L_3	δ_h/H_e (%)	L_1	δ_v/H_e (%)	L_2	δ_v/H_e (%)	L_3	δ_v/H_e (%)	L_1	L_2	L_3
$D_1 = 0.1H_e$	1.2	0.1	35	0.29	37	0.31	40	0.33	26	0.22	31	0.25	35	0.29	137	143	149
$D_2 = 0.2H_e$	2.4	0.2	35	0.29	38	0.31	40	0.33	26	0.22	30	0.25	35	0.29	139	146	153
$D_3 = 0.3H_e$	3.6	0.3	36	0.3	38	0.32	40	0.33	26	0.22	30	0.25	34	0.29	141	149	156
$D_4 = 0.4H_e$	4.8	0.4	36	0.3	38	0.32	40	0.34	26	0.22	30	0.25	34	0.28	143	151	159
$D_5 = 0.5H_e$	6	0.5	36	0.3	38	0.32	40	0.34	26	0.22	30	0.25	34	0.28	144	152	160

Soil Type S_3

Horizontal (δ_h), Vertical (δ_v) Deformation & Moment (M)			δ_h (mm)						δ_v (mm)						M (kNm/m)		
Load Type / Distance (m)			L_1	δ_h/H_e (%)	L_2	δ_h/H_e (%)	L_3	δ_h/H_e (%)	L_1	δ_v/H_e (%)	L_2	δ_v/H_e (%)	L_3	δ_v/H_e (%)	L_1	L_2	L_3
$D_1 = 0.1H_e$	1.2	0.1	24	0.20	26	0.22	28	0.23	18	0.15	21	0.17	24	0.20	118	122	127
$D_2 = 0.2H_e$	2.4	0.2	24	0.20	26	0.22	28	0.23	18	0.15	21	0.17	23	0.20	119	124	130
$D_3 = 0.3H_e$	3.6	0.3	25	0.20	26	0.22	28	0.23	18	0.15	21	0.17	23	0.19	121	126	132
$D_4 = 0.4H_e$	4.8	0.4	25	0.21	26	0.22	28	0.23	18	0.15	21	0.17	23	0.19	122	128	134
$D_5 = 0.5H_e$	6	0.5	25	0.21	26	0.22	28	0.23	18	0.15	21	0.17	23	0.19	122	128	134

Table 14: Lateral wall deflection, Vertical settlement and Moment output from base model *(Undrained with Total stress)*

Soil Type			Soil Type S_1														
Horizontal (δ_h), Vertical (δ_v) Deformation & Moment (M)			δ_h (mm)						δ_v (mm)						M (kNm/m)		
Load Type			L_1	δ_h/H_e (%)	L_2	δ_h/H_e (%)	L_3	δ_h/H_e (%)	L_1	δ_v/H_e (%)	L_2	δ_v/H_e (%)	L_3	δ_v/H_e (%)	L_1	L_2	L_3
Distance (m)																	
$D_1 = 0.1H_e$	1.2	0.1	85	0.71	109	0.91	896	7.46	68	0.57	97	0.81	938	7.82	285	323	923
$D_2 = 0.2H_e$	2.4	0.2	84	0.70	100	0.83	294	2.45	66	0.55	85	0.71	287	2.39	288	317	449
$D_3 = 0.3H_e$	3.6	0.3	84	0.70	95	0.79	175	1.46	64	0.53	78	0.65	159	1.33	291	315	393
$D_4 = 0.4H_e$	4.8	0.4	83	0.69	93	0.78	133	1.11	62	0.52	75	0.62	115	0.96	293	313	362
$D_5 = 0.5H_e$	6	0.5	82	0.69	92	0.76	112	0.93	60	0.5	72	0.60	94	0.79	292	310	339

Soil Type			Soil Type S_2														
Horizontal (δ_h), Vertical (δ_v) Deformation & Moment (M)			δ_h (mm)						δ_v (mm)						M (kNm/m)		
Load Type			L_1	δ_h/H_e (%)	L_2	δ_h/H_e (%)	L_3	δ_h/H_e (%)	L_1	δ_v/H_e (%)	L_2	δ_v/H_e (%)	L_3	δ_v/H_e (%)	L_1	L_2	L_3
Distance (m)																	
$D_1 = 0.1H_e$	1.2	0.1	37	0.31	40	0.34	43	0.36	27	0.22	31	0.26	35	0.29	189	195	202
$D_2 = 0.2H_e$	2.4	0.2	37	0.31	40	0.33	43	0.36	27	0.22	30	0.25	34	0.29	191	198	205
$D_3 = 0.3H_e$	3.6	0.3	37	0.31	40	0.33	43	0.36	26	0.22	30	0.25	34	0.28	193	201	208
$D_4 = 0.4H_e$	4.8	0.4	37	0.31	40	0.33	43	0.36	26	0.22	30	0.25	33	0.28	194	202	210
$D_5 = 0.5H_e$	6	0.5	37	0.31	40	0.33	42	0.35	26	0.22	30	0.25	33	0.28	195	203	211

Soil Type			Soil Type S_3														
Horizontal (δ_h), Vertical (δ_v) Deformation & Moment (M)			δ_h (mm)						δ_v (mm)						M (kNm/m)		
Load Type			L_1	δ_h/H_e (%)	L_2	δ_h/H_e (%)	L_3	δ_h/H_e (%)	L_1	δ_v/H_e (%)	L_2	δ_v/H_e (%)	L_3	δ_v/H_e (%)	L_1	L_2	L_3
Distance (m)																	
$D_1 = 0.1H_e$	1.2	0.1	25	0.21	27	0.22	29	0.24	18	0.15	20	0.17	23	0.19	151	156	161
$D_2 = 0.2H_e$	2.4	0.2	25	0.21	27	0.23	29	0.24	18	0.15	20	0.17	23	0.19	152	158	164
$D_3 = 0.3H_e$	3.6	0.3	25	0.21	27	0.22	29	0.24	18	0.15	20	0.17	22	0.19	154	159	165
$D_4 = 0.4H_e$	4.8	0.4	25	0.21	27	0.22	29	0.24	18	0.15	20	0.17	22	0.19	155	160	167
$D_5 = 0.5H_e$	6	0.5	25	0.21	27	0.22	29	0.24	18	0.15	20	0.17	22	0.19	155	161	167

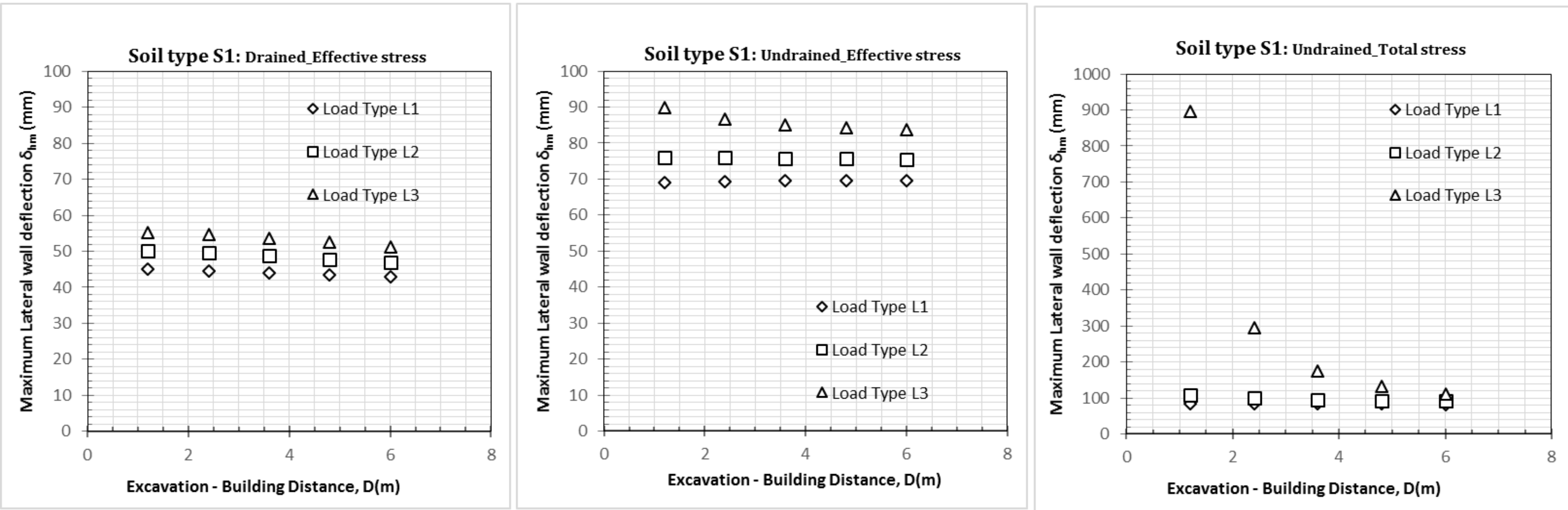

Figure 19: Variation of maximum lateral wall deflections with excavation-neigh boring structure distance *(for soil type S_1)*

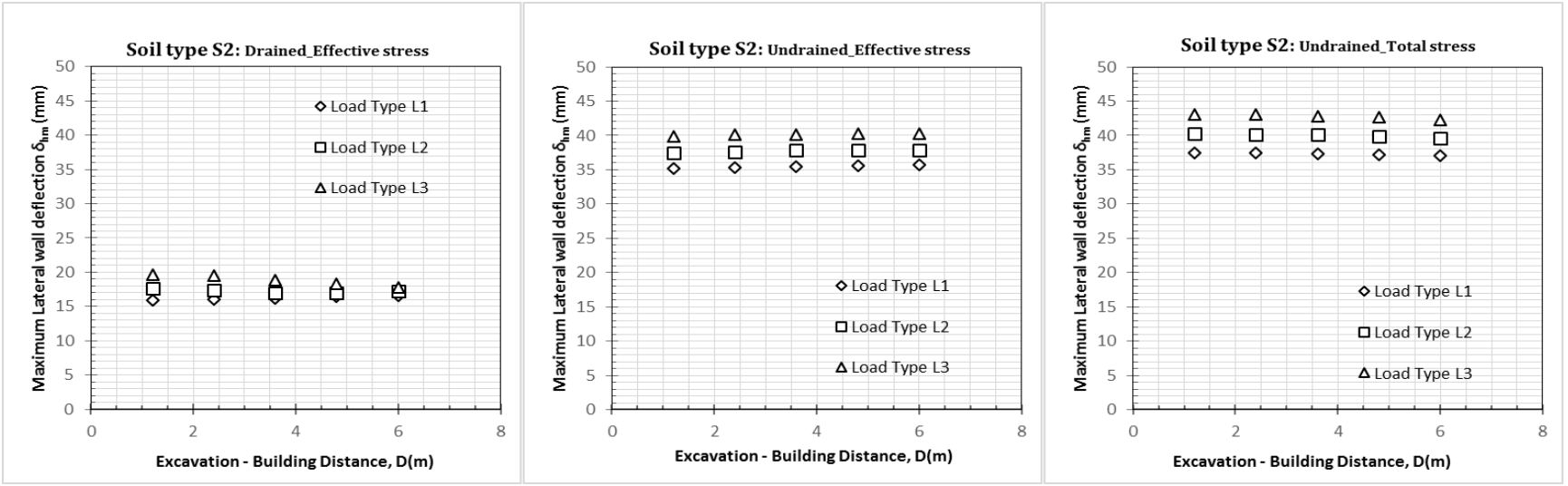

Figure 20: Variation of maximum lateral wall deflections with excavation-neigh boring structure distance *(for soil type S_2)*

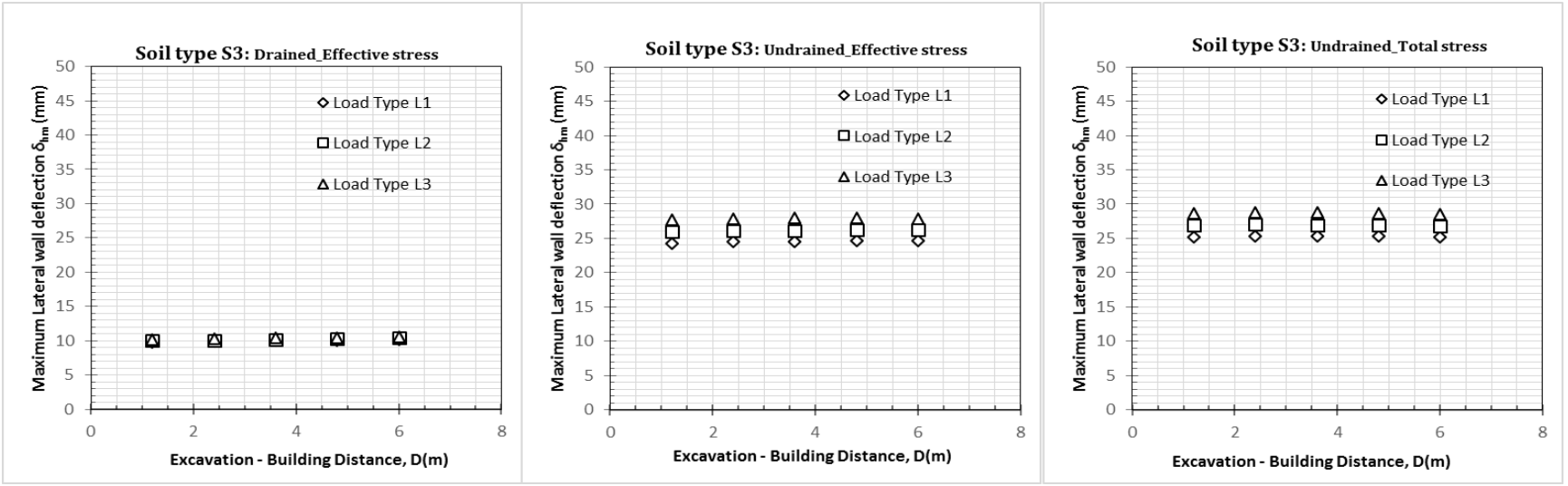

Figure 21: Variation of maximum lateral wall deflections with excavation-neigh boring structure distance *(for soil type S_3)*

From Figure 19, soil type S_1, the case for structure load type L_2, it can be seen that the maximum lateral wall deflection is about δ_{hm} = 50 mm *(Drained with effective stress)*, δ_{hm} = 76 mm *(Undrained with effective stress)* and δ_{hm} = 109 mm *(undrained with total stress)* occurs when the structure is positioned at a distance D_1 (= $0.1H_e$ = 1.2m) and a minimum lateral wall deflection of δ_{hm} = 47 mm *(Drained with effective stress,* a decrease of about 6.0%*)*, δ_{hm} = 76 mm *(Undrained with effective stress,* a decrease of about 0.0%*)* and δ_{hm} = 92 mm *(undrained with total stress,* a decrease of about 15.6%*)* occurs in the case the structure is positioned at a distance D_5 (= $0.5H_e$ =6m) from face of excavation.

Similarly, from Figure 20, for soil type S_2, the case for structure load type L_2, it can be seen that, the maximum lateral wall deflection is about δ_{hm} = 18 mm *(Drained with effective stress)*, δ_{hm} = 38 mm *(Undrained with effective stress)* and δ_{hm} = 40 mm *(Undrained with total stress)* occurs in the case the structure is positioned at a distance D_1 (= $0.1H_e$ = 1.2m) and a minimum lateral wall deflection of δ_{hm} = 17 mm *(Drained with effective stress,* a decrease of about 5.56%*)* (), δ_{hm} = 38 mm *(Undrained with effective stress,* a decrease of about 0.0%*)* and δ_{hm} = 40 mm *(Undrained with total stress,* a decrease of about 0.0%*)* occurs in the case the structure is positioned at a distance D_5 (= $0.5H_e$ =6m) from face of excavation.

Similarly, from Figure 21, for soil type S_3, the case for building load type L_2, it can be seen that, the maximum lateral wall deflection is about δ_{hm} = 10 mm *(Drained with effective stress)*, δ_{hm} = 26 mm *(Undrained with effective stress)* and δ_{hm} = 27 mm *(Undrained with total stress)* occurs in the case the structure is positioned at a distance D_1 (= $0.1H_e$ = 1.2m) and a minimum lateral wall deflection of δ_{hm} = 10 mm *(Drained with effective stress,* a decrease of about 0.0%*)* , δ_{hm} = 26 mm *(Undrained with effective stress,* a decrease of about 0.0%*)* and δ_{hm} = 27 mm *(Undrained with total stress,* a decrease of about 0.0%*)* occurs in the case the structure is positioned at a distance D_5 (= $0.5H_e$ =6m) from face of excavation.

This shows, due to soil stiffness variation, with the same building load, increasing neighboring building distance-excavation has more effect on maximum lateral wall deflection in soil type S_1 than soil type S_2 & S_3. Moreover, specifically for soil type S_1, with the same structure load, increasing neighboring structure distance-excavation has more effect on maximum lateral wall deflection in *Undrained with total stress drainage condition* than drained with effective stress & Undrained with effective stress drainage conditions.

Following normalization of lateral wall deflection, with the excavation depth and graph represented on Figure 22, 23 and 24, for soil types S_1, S_2 and S_3 respectively. we can observe the relationship between normalized lateral wall deflection and neighboring structure-distance from face of excavation can be expressed by exponential decay function of equation on Table 15 so that to select preliminary contiguous pile wall and soil parameters for design.

Table 15: Equation of normalized maximum lateral wall deflection in terms of neighboring structure distance from face of excavation

Soil type	Drainage conditions	Load type		
		L_1	L_2	L_3
S_1	Drained with Effective stress	$\frac{\delta_{hm}}{H_e} = 0.38e^{-0.119(D/H_e)}$	$\frac{\delta_{hm}}{H_e} = 0.4264e^{-0.168(D/H_e)}$	$\frac{\delta_{hm}}{H_e} = 0.4714\ e^{-0.186\ (D/H_e)}$
	Undrained with Effective stress	$\frac{\delta_{hm}}{H_e} = 0.576e^{0.0167\ (D/H_e)}$	$\frac{\delta_{hm}}{H_e} = 0.6339e^{-0.013(D/H_e)}$	$\frac{\delta_{hm}}{H_e} = 0.7532e^{-0.172(D/H_e)}$
	Undrained with Total stress	$\frac{\delta_{hm}}{H_e} = 0.7154e^{-0.084(D/H_e)}$	$\frac{\delta_{hm}}{H_e} = 0.9202e^{-0.415(D/H_e)}$	$\frac{\delta_{hm}}{H_e} = 8.5763e^{-4.947(D/H_e)}$
S_2	Drained with Effective stress	$\frac{\delta_{hm}}{H_e} = 0.1307e^{0.1146(D/H_e)}$	$\frac{\delta_{hm}}{H_e} = 0.1466e^{-0.073(D/H_e)}$	$\frac{\delta_{hm}}{H_e} = 0.1695e^{-0.264(D/H_e)}$
	Undrained with Effective stress	$\frac{\delta_{hm}}{H_e} = 0.2923e^{0.0375(D/H_e)}$	$\frac{\delta_{hm}}{H_e} = 0.3113e^{0.0337(D/H_e)}$	$\frac{\delta_{hm}}{H_e} = 0.3324e^{0.0227(D/H_e)}$
	Undrained with Total stress	$\frac{\delta_{hm}}{H_e} = 0.3136e^{-0.028(D/H_e)}$	$\frac{\delta_{hm}}{H_e} = 0.3368e^{-0.035(D/H_e)}$	$\frac{\delta_{hm}}{H_e} = 0.3617e^{-0.048(D/H_e)}$
S_3	Drained with Effective stress	$\frac{\delta_{hm}}{H_e} = 0.0813e^{0.0752(D/H_e)}$	$\frac{\delta_{hm}}{H_e} = 0.0825e^{-0.0885(D/H_e)}$	$\frac{\delta_{hm}}{H_e} = 0.0836e^{-0.11(D/H_e)}$
	Undrained with Effective stress	$\frac{\delta_{hm}}{H_e} = 0.2022e^{0.0371(D/H_e)}$	$\frac{\delta_{hm}}{H_e} = 0.216e^{0.0253(D/H_e)}$	$\frac{\delta_{hm}}{H_e} = 0.2311e^{0.0169(D/H_e)}$
	Undrained with Total stress	$\frac{\delta_{hm}}{H_e} = 0.2107e^{-0.004(D/H_e)}$	$\frac{\delta_{hm}}{H_e} = 0.2252e^{-0.011(D/H_e)}$	$\frac{\delta_{hm}}{H_e} = 0.2401e^{-0.016(D/H_e)}$

For instance; to estimate the maximum lateral wall deflection 15m from face of 30m deep excavation (For soil type S_1 – Drained with effective stress condition and structure load type L_3).

$$\frac{Distance\ from\ Excavation}{Excavation\ depth} = \frac{15}{30} = 0.5$$

From Equation on Figure 22, for soil type S_1-drained with effective stress drainage condition and structure load type L_3;

$$\frac{\delta_{hm}}{H_e} = 0.4714\, e^{-0.186(D/H_e)}$$

$$\frac{\delta_{hm}}{H_e} = 0.4714\, e^{-0.186*0.5} = 0.43\%$$

Therefore, the expected maximum lateral wall deflection, δ_{hm} = 0.0043*30 = 0.13 m

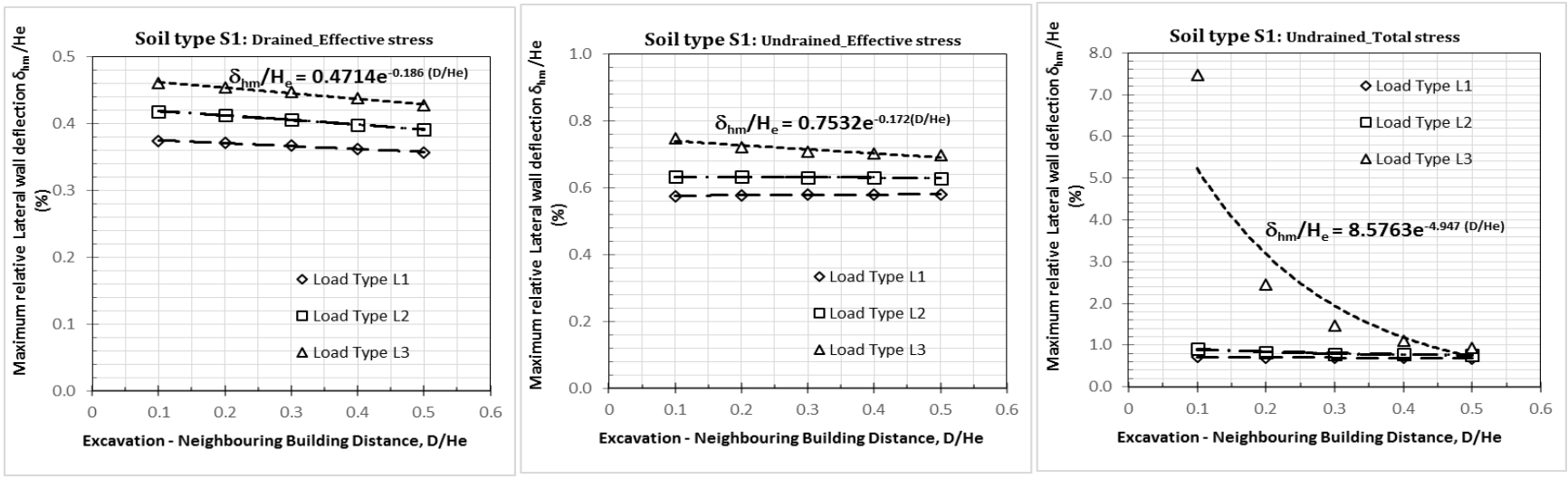

Figure 22: Variation of normalized maximum lateral wall deflections with relative structure distance – excavation *(for soil type S_1)*

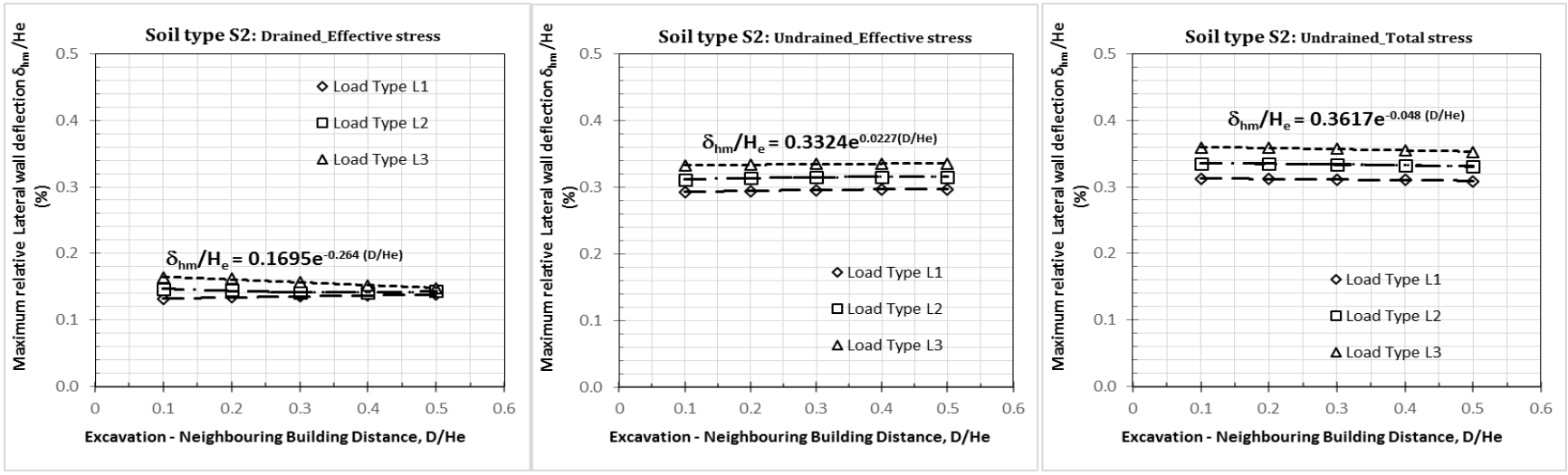

Figure 23: Variation of normalized maximum lateral wall deflections with relative structure distance – excavation *(for soil type S_2)*

Figure 24: Variation of normalized maximum lateral wall deflections with relative structure distance – excavation *(for Soil Type S_3)*

3.5.2 Settlements of the neighboring structure

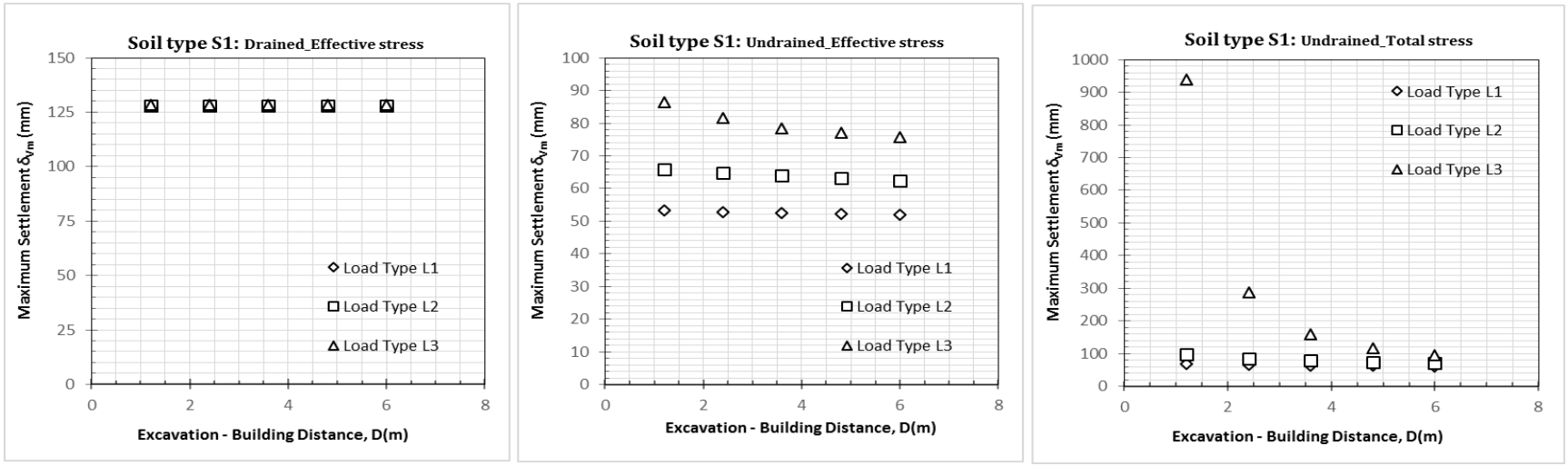

Figure 25: Variation of maximum settlement with excavation-neighboring structure distance *(for soil type S_1)*

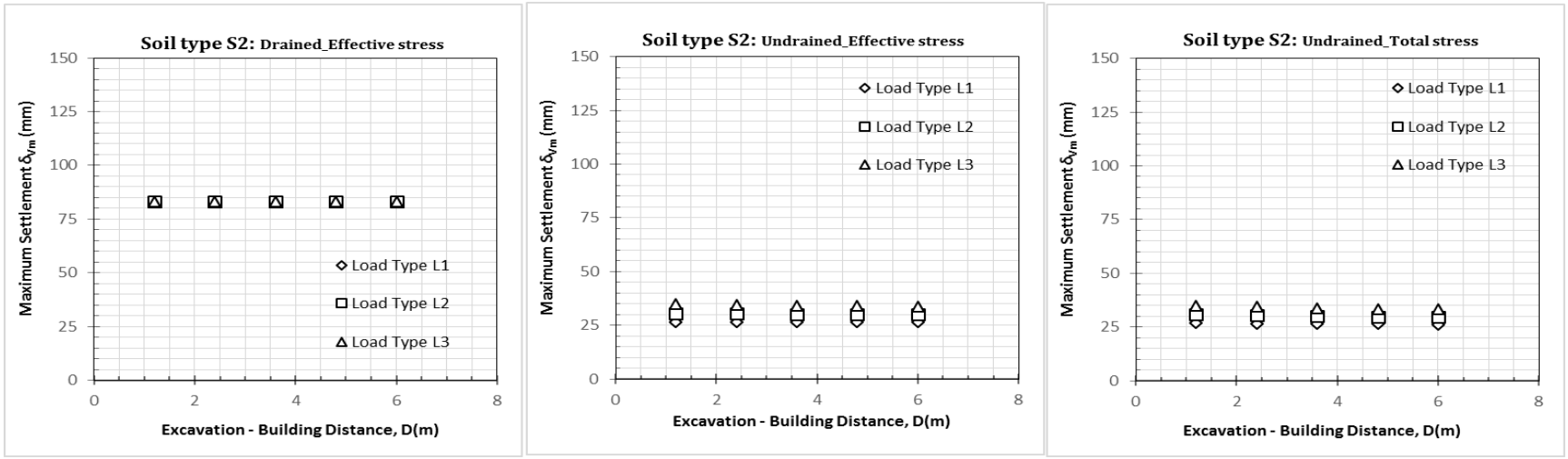

Figure 26: Variation of maximum settlement with excavation-neighboring structure distance *(for soil type S_2)*

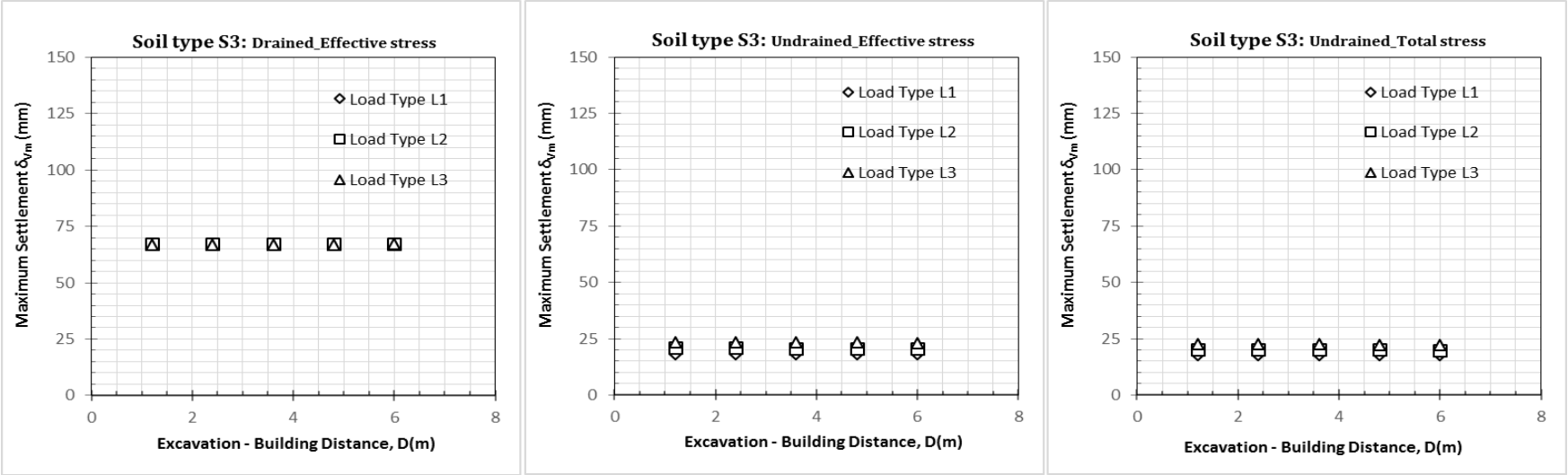

Figure 27: Variation of maximum settlement with excavation-neighboring structure distance *(for soil type S_3)*

Figure 25, 26 and 27 show the variations in maximum settlement are identified varying the distance of structure from face of excavation for soil type S_1, S_2 & S_3 respectively. It can be seen that maximum settlement decreases with the increase in distance of structure from face of excavation.

Figure 25 represents the distribution of maximum settlement in the ground and structure system for soil type S_1. It can be seen that the magnitude of maximum settlement is more pronounced in Undrained with effective stress condition.

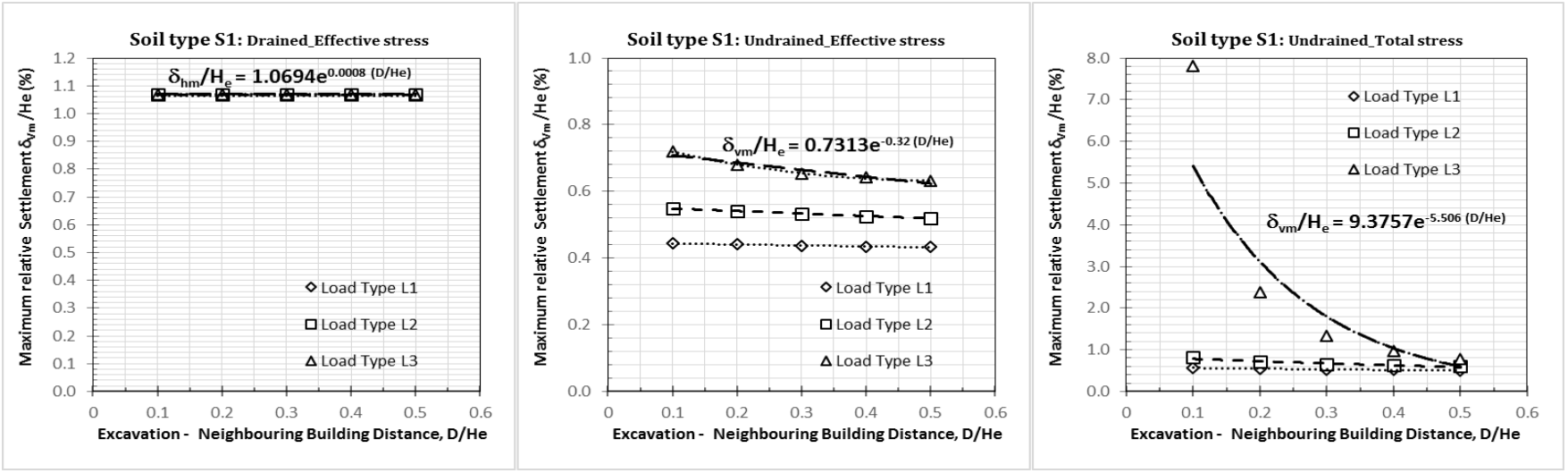

Figure 28: Variation of Normalized maximum settlement with relative structure distance-excavation *(for soil type S_1)*

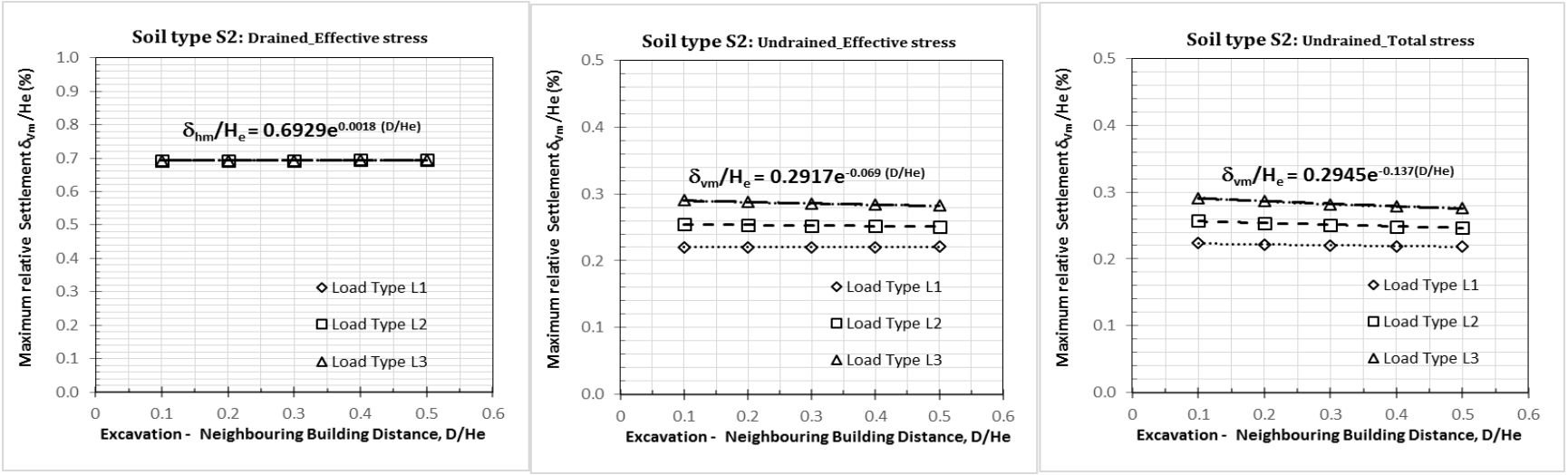

Figure 29: Variation of Normalized maximum settlement with relative structure distance-excavation *(for soil type S_2)*

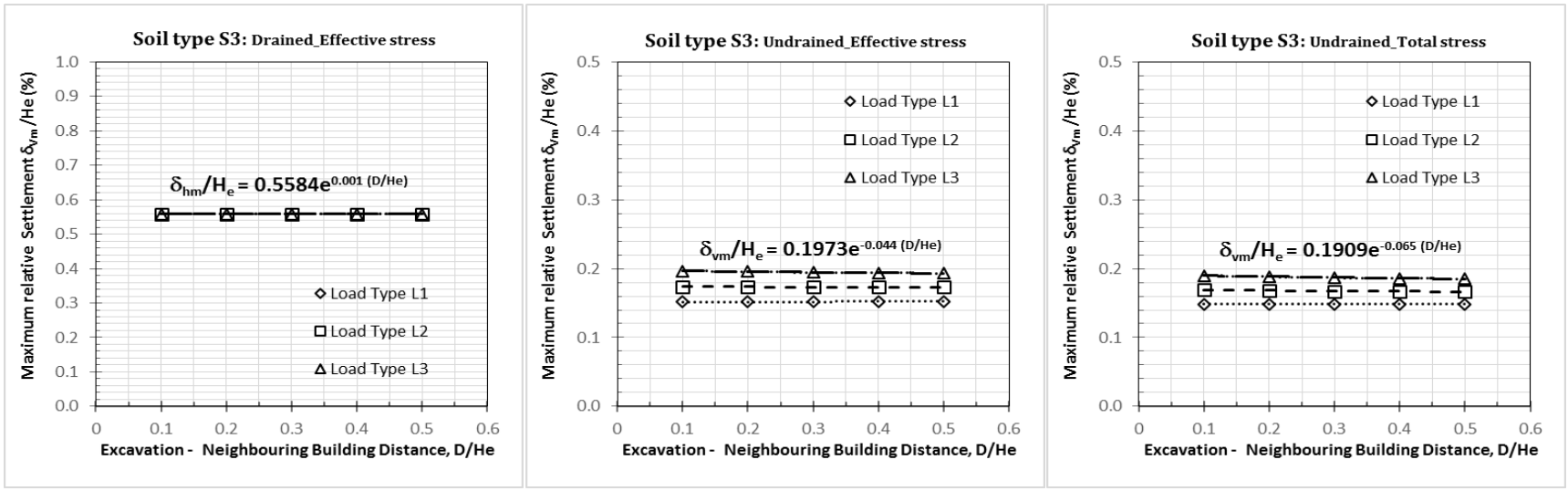

Figure 30: Variation of Normalized maximum settlement with relative structure distance-excavation *(for soil type S_3)*

Figure 28, 29 &30, show the variations in maximum normalized settlement (divided by the excavation depth) are identified varying the distance of structure from face of excavation for soil type S_1, S_2 & S_3 respectively. It can be seen that, maximum normalized settlement decreases with increasing structure distance from face of excavation.

Moormann (2004) had carried out extensive empirical studies by taking 530 case histories of retaining wall and ground movement due to excavation in soft soil (C_u < 75kpa) into account. It is concluded that;

"*The maximum horizontal wall displacement (δ_{hm}) lie between 0.5%H and 1.0 %H, on average at 0.87%H (Figure 15 and Figure 16).The location of maximum horizontal displacement is at 0.5H to 1.0H below the ground."*

This study summarizes, for all load types L_1,L_2 &L_3; lateral wall deflection,δ_{hm} on soft soil type S_1 (C_u = 62 kpa) lie between 0.36%H_e & 0.46%H_e, 0.58%H_e & 0.75%H_e and 0.69%H_e & 7.46%H_e for Drained with effective stress, Undrained with effective stress and Undrained with total stress drainage conditions respectively. Hence, according to Moormann studies, *maximum horizontal wall displacement* lies outside the range, only for Undrained with total stress drainage condition.

"*The maximum vertical settlement at the ground surface behind a retaining wall (δ_{vm}) lies in the range of 0.1%H to 10%H, on average at 1.1%H. The settlement δ_{vm} occurs at a distance of less than 0.5%H behind the wall, but there are cases in soft soil with this distance to be up to 2.0H. The ratio δ_{vm}/δ_{hm} varies mainly between 0.5 and 1.0."*

This study summarizes, for all load types L_1, L_2 & L_3; maximum settlement, δ_{vm} on soft soil type S_1 (C_u = 62 kpa), lie between 1.07%H_e & 1.073%H_e, 0.43%H_e & 0.72%H_e and 0.5%H_e & 7.82%H_e for Drained with effective stress, Undrained with effective stress and Undrained with total stress drainage conditions respectively. Hence, according to Moormann studies, *maximum vertical settlement* lies within the range.

Long (2001) analyzed 296 case histories. His studies largely focus on validating results of Clough and O'Rourke (1990) for stiff soils with δ_{hm}/H = 0.05-0.25% and δ_{vm}/H=0-0.2% on the Figure 14.

This study summarizes, for all load types and all drainage conditions; lateral wall deflection, δ_{hm}, on stiff soil type S_2 (C_u = 115 kpa) and S_3 (C_u = 155 kpa) lie between 0.13%H_e & 0.16%H_e and 0.08%H_e & 0.09%H_e respectively. Hence, according to Long (2001) studies, *maximum horizontal wall displacement* lies within the range (0.05%H – 0.25%H).

Similarly, this study summarizes, for all load types and all drainage conditions; maximum settlement, δ_{vm}, on stiff soil type S_2 (C_u = 115 kpa) and S_3 (C_u = 155 kpa) lie between 0.69%H_e & 0.694%H_e and 0.56%H_e & 0.564%H_e respectively. Hence, according to Long (2001) studies, *maximum vertical settlement* lies outside the range (0%H – 0.2%H).

Following normalization of maximum settlement, with the excavation depth & graph represented on Figure 28, 29 and 30, for soil types S_1, S_2 and S_3 respectively. We can observe the relationship between normalized settlement and neighboring structure-distance from face of excavation be expressed by exponential decay function of the equation on Table 16 so that to select preliminary contiguous pile wall and soil parameters for design.

Table 16: Equation of normalized maximum settlements in terms of neighboring structure distance from face of excavation.

Soil type	Drainage conditions	Load type		
		L_1	L_2	L_3
S_1	Drained with Effective stress	$\frac{\delta_{vm}}{H_e} = 1.065\,e^{0.0005\,(D/H_e)}$	$\frac{\delta_{vm}}{H_e} = 1.0673\,e^{0.0006\,(D/H_e)}$	$\frac{\delta_{vm}}{H_e} = 1.0694e^{-0.0008(D/H_e)}$
	Undrained with Effective stress	$\frac{\delta_{vm}}{H_e} = 0.4467e^{-0.066(D/H_e)}$	$\frac{\delta_{vm}}{H_e} = 0.5563e^{-0.14(D/H_e)}$	$\frac{\delta_{vm}}{H_e} = 0.7313e^{-0.32(D/H_e)}$
	Undrained with Total stress	$\frac{\delta_{vm}}{H_e} = 0.5846e^{-0.312(D/H_e)}$	$\frac{\delta_{vm}}{H_e} = 0.8403e^{-0.737(D/H_e)}$	$\frac{\delta_{vm}}{H_e} = 9.3757e^{-5.506(D/H_e)}$
S_2	Drained with Effective stress	$\frac{\delta_{vm}}{H_e} = 0.6932\,e^{0.001(D/H_e)}$	$\frac{\delta_{vm}}{H_e} = 0.6931e^{0.0012(D/H_e)}$	$\frac{\delta_{vm}}{H_e} = 0.6929e^{-0.0018(D/H_e)}$
	Undrained with Effective stress	$\frac{\delta_{vm}}{H_e} = 0.22\,e^{0.0049\,(D/H_e)}$	$\frac{\delta_{vm}}{H_e} = 0.2552e^{-0.034(D/H_e)}$	$\frac{\delta_{vm}}{H_e} = 0.2917e^{-0.069(D/H_e)}$
	Undrained with Total stress	$\frac{\delta_{vm}}{H_e} = 0.2242e^{-0.055(D/H_e)}$	$\frac{\delta_{vm}}{H_e} = 0.2588e^{-0.099(D/H_e)}$	$\frac{\delta_{vm}}{H_e} = 0.2945e^{-0.137(D/H_e)}$
S_3	Drained with Effective stress	$\frac{\delta_{vm}}{H_e} = 0.5591$	$\frac{\delta_{vm}}{H_e} = 0.5588\,e^{0.0003(D/H_e)}$	$\frac{\delta_{vm}}{H_e} = 0.5584\,e^{0.001(D/H_e)}$
	Undrained with Effective stress	$\frac{\delta_{vm}}{H_e} = 0.1512\,e^{0.0175(D/H_e)}$	$\frac{\delta_{vm}}{H_e} = 0.174e^{-0.016(D/H_e)}$	$\frac{\delta_{vm}}{H_e} = 0.1973e^{-0.044(D/H_e)}$
	Undrained with Total stress	$\frac{\delta_{vm}}{H_e} = 0.1484e^{-0.004(D/H_e)}$	$\frac{\delta_{vm}}{H_e} = 0.1694e^{-0.036(D/H_e)}$	$\frac{\delta_{vm}}{H_e} = 0.1909e^{-0.065(D/H_e)}$

For instance; to estimate the maximum settlement 15m from face of 30m deep excavation (For soil type S_1 – Drained with effective stress condition and structure load type L_3).

$$\frac{Distance\ from\ Excavation}{Excavation\ depth} = \frac{15}{30} = 0.5$$

From Equation on Figure 28, for soil type S_1-drained with effective stress condition and structure load type L_3;

$$\frac{\delta_{vm}}{H_e} = 1.0964\,e^{0.0008\,(D/H_e)}$$

$$\frac{\delta_{vm}}{H_e} = 1.0964\,e^{0.0008\,*\,0.5} = 1.1\%$$

Therefore, the expected maximum lateral wall deflection, δ_{vm} = 0.011*30 = 0.33m

3.5.3 The relation between the retaining wall lateral displacements and the neighboring structure settlements

For well-constructed excavations, the magnitude of the ground's lateral and vertical movements are correlated. In order to show the relationship between the maximum lateral wall deflection and settlement, data in Table 12, 13 & 14 are plotted in Figure 31, 32 & 33 respectively and show that the magnitude of the maximum settlement is about 0.43 to 10.44 times that of the maximum lateral wall deflection. This indicates that the magnitude of the maximum settlement is partially different from the general pattern, which shows that the maximum lateral and vertical movements are of the same order of magnitude (Moormann, 2004).

The data from Moormann, lies between the lines of δ_{vm}/δ_{hm} = 0.5 and δ_{vm}/δ_{hm}= 1.0. However, in drained with effective stress condition in three types of soils, S_1, S_2 & S_3 both lateral and vertical displacement are larger than the displacement data from Moormann, 2004.

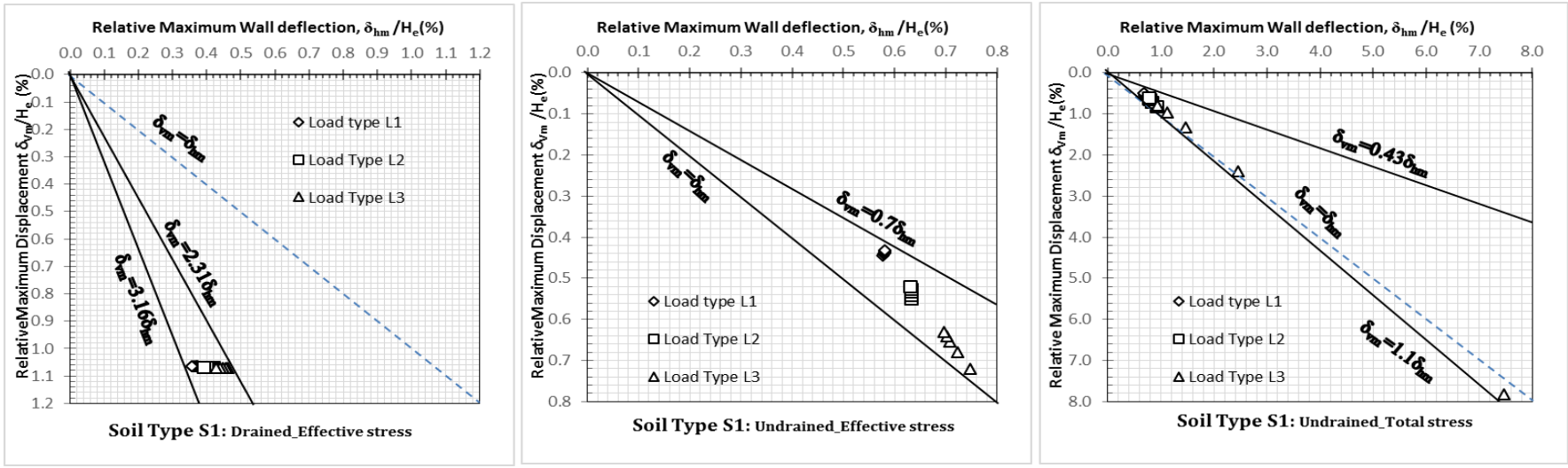

Figure 31: Normalized maximum retaining wall deflections with normalized maximum settlement *(for soil type S_1)*

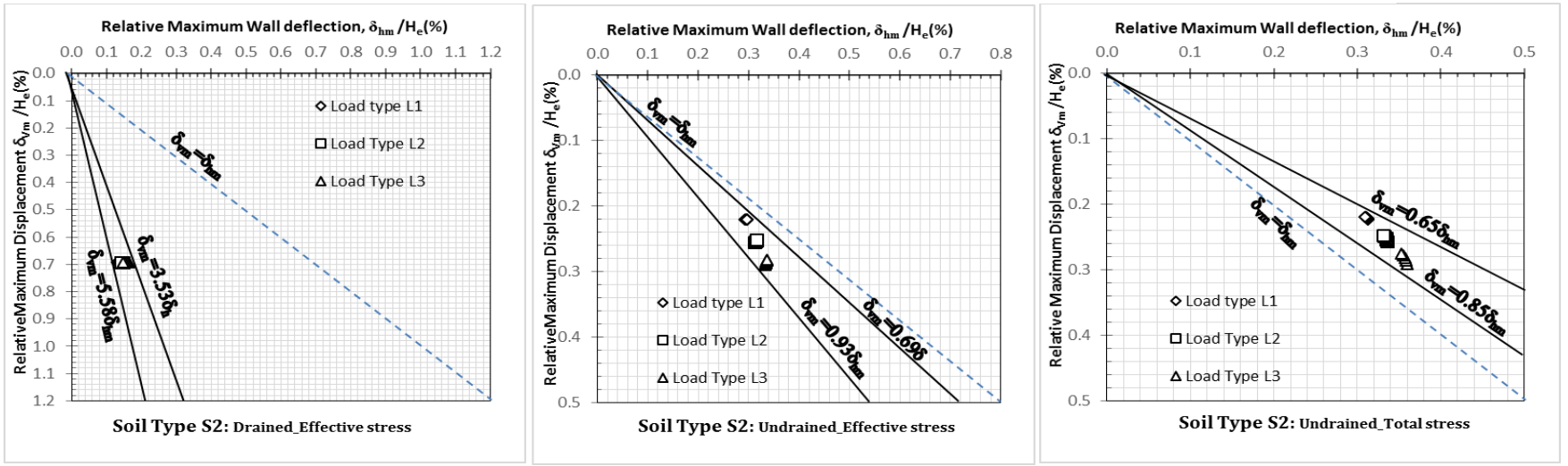

Figure 32: Normalized maximum retaining wall deflections with normalized maximum settlement *(for soil type S_2)*

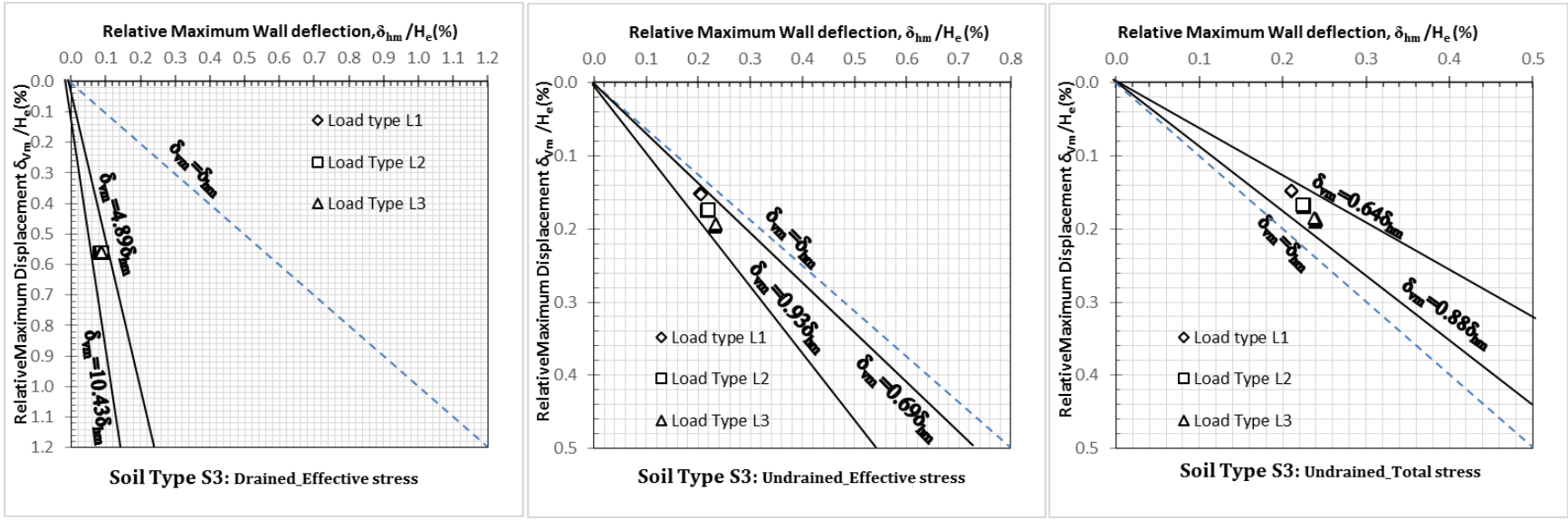

Figure 33: Normalized maximum retaining wall deflections with normalized maximum settlement *(for soil type S_3)*

3.5.4 Angular distortion and Horizontal strain

Table 17: Angular distortion and Horizontal strain *(Drained with Effective stress)*

Building Length, L = 20m

Soil Type		Soil Type S_1												Soil Type S_2												Soil Type S_3											
Horizontal (δ_h), Vertical (δ_v) Deformation & Moment / Load Type		δ_h @ L1 (mm)	$\varepsilon_h = \delta_h/L$ ($x10^{-3}$) (mm)	δ_h @ L2 (mm)	$\varepsilon_h = \delta_h/L$ ($x10^{-3}$) (mm)	δ_h @ L3 (mm)	$\varepsilon_h = \delta_h/L$ ($x10^{-3}$) (mm)	δ_v @ L1 (mm)	$\beta = \delta_v/L$ ($x10^{-3}$) (mm)	δ_v @ L2 (mm)	$\beta = \delta_v/L$ ($x10^{-3}$) (mm)	δ_v @ L3 (mm)	$\beta = \delta_v/L$ ($x10^{-3}$) (mm)	δ_h @ L1 (mm)	$\varepsilon_h = \delta_h/L$ ($x10^{-3}$) (mm)	δ_h @ L2 (mm)	$\varepsilon_h = \delta_h/L$ ($x10^{-3}$) (mm)	δ_h @ L3 (mm)	$\varepsilon_h = \delta_h/L$ ($x10^{-3}$) (mm)	δ_v @ L1 (mm)	$\beta = \delta_v/L$ ($x10^{-3}$) (mm)	δ_v @ L2 (mm)	$\beta = \delta_v/L$ ($x10^{-3}$) (mm)	δ_v @ L3 (mm)	$\beta = \delta_v/L$ ($x10^{-3}$) (mm)	δ_h @ L1 (mm)	$\varepsilon_h = \delta_h/L$ ($x10^{-3}$) (mm)	δ_h @ L2 (mm)	$\varepsilon_h = \delta_h/L$ ($x10^{-3}$) (mm)	δ_h @ L3 (mm)	$\varepsilon_h = \delta_h/L$ ($x10^{-3}$) (mm)	δ_v @ L1 (mm)	$\beta = \delta_v/L$ ($x10^{-3}$) (mm)	δ_v @ L2 (mm)	$\beta = \delta_v/L$ ($x10^{-3}$) (mm)	δ_v @ L3 (mm)	$\beta = \delta_v/L$ ($x10^{-3}$) (mm)
Distance (m)																																					
$D_1 = 0.1H_e$	1.2	45	2.250	50	2.510	55	2.7645	128	6.391	128	6.404	128	6.417	16	0.793	18	0.881	20	0.982	83	4.160	83	4.159	83	4.158	10	0.491	10	0.500	10	0.507	67	3.355	67	3.353	67	3.351
$D_2 = 0.2H_e$	2.4	45	2.229	50	2.480	55	2.729	128	6.391	128	6.404	128	6.418	16	0.803	17	0.868	19	0.974	83	4.160	83	4.160	83	4.159	10	0.495	10	0.504	10	0.513	67	3.355	67	3.353	67	3.352
$D_3 = 0.3H_e$	3.6	44	2.203	49	2.435	54	2.6865	128	6.392	128	6.405	128	6.418	16	0.813	17	0.848	19	0.944	83	4.160	83	4.160	83	4.160	10	0.500	10	0.508	10	0.519	67	3.355	67	3.353	67	3.352
$D_4 = 0.4H_e$	4.8	43	2.175	48	2.392	53	2.634	128	6.392	128	6.405	128	6.419	16	0.821	17	0.847	18	0.913	83	4.161	83	4.161	83	4.161	10	0.502	10	0.513	10	0.524	67	3.355	67	3.353	67	3.352
$D_5 = 0.5H_e$	6	43	2.146	47	2.350	51	2.5635	128	6.392	128	6.406	128	6.419	17	0.831	17	0.860	18	0.888	83	4.161	83	4.161	83	4.161	10	0.506	10	0.518	11	0.530	67	3.355	67	3.354	67	3.353

Table 18: Angular distortion and Horizontal strain *(Undrained with Effective stress)*

Building Length, L = 20m

Soil Type		Soil Type S_1												Soil Type S_2												Soil Type S_3											
Horizontal (δ_h), Vertical (δ_v) Deformation & Moment / Load Type		δ_h @ L1 (mm)	$\varepsilon_h = \delta_h/L$ ($x10^{-3}$) (mm)	δ_h @ L2 (mm)	$\varepsilon_h = \delta_h/L$ ($x10^{-3}$) (mm)	δ_h @ L3 (mm)	$\varepsilon_h = \delta_h/L$ ($x10^{-3}$) (mm)	δ_v @ L1 (mm)	$\beta = \delta_v/L$ ($x10^{-3}$) (mm)	δ_v @ L2 (mm)	$\beta = \delta_v/L$ ($x10^{-3}$) (mm)	δ_v @ L3 (mm)	$\beta = \delta_v/L$ ($x10^{-3}$) (mm)	δ_h @ L1 (mm)	$\varepsilon_h = \delta_h/L$ ($x10^{-3}$) (mm)	δ_h @ L2 (mm)	$\varepsilon_h = \delta_h/L$ ($x10^{-3}$) (mm)	δ_h @ L3 (mm)	$\varepsilon_h = \delta_h/L$ ($x10^{-3}$) (mm)	δ_v @ L1 (mm)	$\beta = \delta_v/L$ ($x10^{-3}$) (mm)	δ_v @ L2 (mm)	$\beta = \delta_v/L$ ($x10^{-3}$) (mm)	δ_v @ L3 (mm)	$\beta = \delta_v/L$ ($x10^{-3}$) (mm)	δ_h @ L1 (mm)	$\varepsilon_h = \delta_h/L$ ($x10^{-3}$) (mm)	δ_h @ L2 (mm)	$\varepsilon_h = \delta_h/L$ ($x10^{-3}$) (mm)	δ_h @ L3 (mm)	$\varepsilon_h = \delta_h/L$ ($x10^{-3}$) (mm)	δ_v @ L1 (mm)	$\beta = \delta_v/L$ ($x10^{-3}$) (mm)	δ_v @ L2 (mm)	$\beta = \delta_v/L$ ($x10^{-3}$) (mm)	δ_v @ L3 (mm)	$\beta = \delta_v/L$ ($x10^{-3}$) (mm)
Distance (m)																																					
$D_1 = 0.1H_e$	1.2	69	3.457	76	3.795	90	4.489	53	2.666	66	3.299	86	4.320	35	1.758	37	1.871	40	1.996	26	1.322	31	1.529	35	1.742	24	1.216	26	1.297	28	1.386	18	0.909	21	1.043	24	1.180
$D_2 = 0.2H_e$	2.4	69	3.470	76	3.797	87	4.338	53	2.644	65	3.243	81	4.075	35	1.768	38	1.882	40	2.006	26	1.321	30	1.520	35	1.725	24	1.224	26	1.304	28	1.393	18	0.910	21	1.041	23	1.173
$D_3 = 0.3H_e$	3.6	70	3.479	76	3.792	85	4.247	53	2.625	64	3.193	78	3.925	36	1.776	38	1.890	40	2.010	26	1.321	30	1.514	34	1.711	25	1.229	26	1.308	28	1.397	18	0.911	21	1.038	23	1.167
$D_4 = 0.4H_e$	4.8	70	3.482	76	3.786	84	4.212	52	2.609	63	3.153	77	3.849	36	1.782	38	1.895	40	2.014	26	1.322	30	1.510	34	1.701	25	1.233	26	1.310	28	1.398	18	0.913	21	1.037	23	1.163
$D_5 = 0.5H_e$	6	70	3.480	76	3.777	84	4.18	52	2.597	62	3.119	76	3.789	36	1.784	38	1.896	40	2.015	26	1.324	30	1.508	34	1.694	25	1.234	26	1.311	28	1.395	18	0.916	21	1.037	23	1.160

Table 19: Angular distortion and Horizontal strain *(Undrained with Total stress)*

Building Length, L = 20m

Soil Type S_1

Horizontal (δ_h), Vertical (δ_v) Deformation & Moment / Load Type / Distance (m)		δ_h @ L1 (mm)	$\varepsilon_h = \delta_h/L$ (x10^{-3}) (mm)	δ_h @ L2 (mm)	$\varepsilon_h = \delta_h/L$ (x10^{-3}) (mm)	δ_h @ L3 (mm)	$\varepsilon_h = \delta_h/L$ (x10^{-3}) (mm)	δ_v @ L1 (mm)	$\beta = \delta_v/L$ (x10^{-3}) (mm)	δ_v @ L2 (mm)	$\beta = \delta_v/L$ (x10^{-3}) (mm)	δ_v @ L3 (mm)	$\beta = \delta_v/L$ (x10^{-3}) (mm)
$D_1 = 0.1H_e$	1.2	85	4.255	109	5.449	896	44.78	68	3.412	97	4.867	938	46.909
$D_2 = 0.2H_e$	2.4	84	4.222	100	4.978	294	14.715	66	3.290	85	4.238	287	14.342
$D_3 = 0.3H_e$	3.6	84	4.187	95	4.761	175	8.769	64	3.182	78	3.909	159	7.974
$D_4 = 0.4H_e$	4.8	83	4.154	93	4.659	133	6.6675	62	3.092	75	3.728	115	5.772
$D_5 = 0.5H_e$	6	82	4.114	92	4.576	112	5.607	60	3.011	72	3.589	94	4.714

Soil Type S_2

Distance (m)		δ_h @ L1 (mm)	$\varepsilon_h = \delta_h/L$ (x10^{-3}) (mm)	δ_h @ L2 (mm)	$\varepsilon_h = \delta_h/L$ (x10^{-3}) (mm)	δ_h @ L3 (mm)	$\varepsilon_h = \delta_h/L$ (x10^{-3}) (mm)	δ_v @ L1 (mm)	$\beta = \delta_v/L$ (x10^{-3}) (mm)	δ_v @ L2 (mm)	$\beta = \delta_v/L$ (x10^{-3}) (mm)	δ_v @ L3 (mm)	$\beta = \delta_v/L$ (x10^{-3}) (mm)
$D_1 = 0.1H_e$	1.2	37	1.873	40	2.011	43	2.157	27	1.341	31	1.542	35	1.748
$D_2 = 0.2H_e$	2.4	37	1.873	40	2.009	43	2.152	27	1.330	30	1.521	34	1.717
$D_3 = 0.3H_e$	3.6	37	1.868	40	2.004	43	2.142	26	1.320	30	1.504	34	1.691
$D_4 = 0.4H_e$	4.8	37	1.862	40	1.995	43	2.131	26	1.315	30	1.491	33	1.670
$D_5 = 0.5H_e$	6	37	1.852	40	1.983	42	2.116	26	1.312	30	1.482	33	1.655

Soil Type S_3

Distance (m)		δ_h @ L1 (mm)	$\varepsilon_h = \delta_h/L$ (x10^{-3}) (mm)	δ_h @ L2 (mm)	$\varepsilon_h = \delta_h/L$ (x10^{-3}) (mm)	δ_h @ L3 (mm)	$\varepsilon_h = \delta_h/L$ (x10^{-3}) (mm)	δ_v @ L1 (mm)	$\beta = \delta_v/L$ (x10^{-3}) (mm)	δ_v @ L2 (mm)	$\beta = \delta_v/L$ (x10^{-3}) (mm)	δ_v @ L3 (mm)	$\beta = \delta_v/L$ (x10^{-3}) (mm)
$D_1 = 0.1H_e$	1.2	25	1.262	27	1.348	29	1.435	18	0.891	20	1.014	23	1.140
$D_2 = 0.2H_e$	2.4	25	1.265	27	1.350	29	1.438	18	0.889	20	1.009	23	1.130
$D_3 = 0.3H_e$	3.6	25	1.265	27	1.350	29	1.437	18	0.888	20	1.004	22	1.122
$D_4 = 0.4H_e$	4.8	25	1.264	27	1.347	29	1.433	18	0.888	20	1.001	22	1.115
$D_5 = 0.5H_e$	6	25	1.260	27	1.342	29	1.426	18	0.890	20	1.000	22	1.111

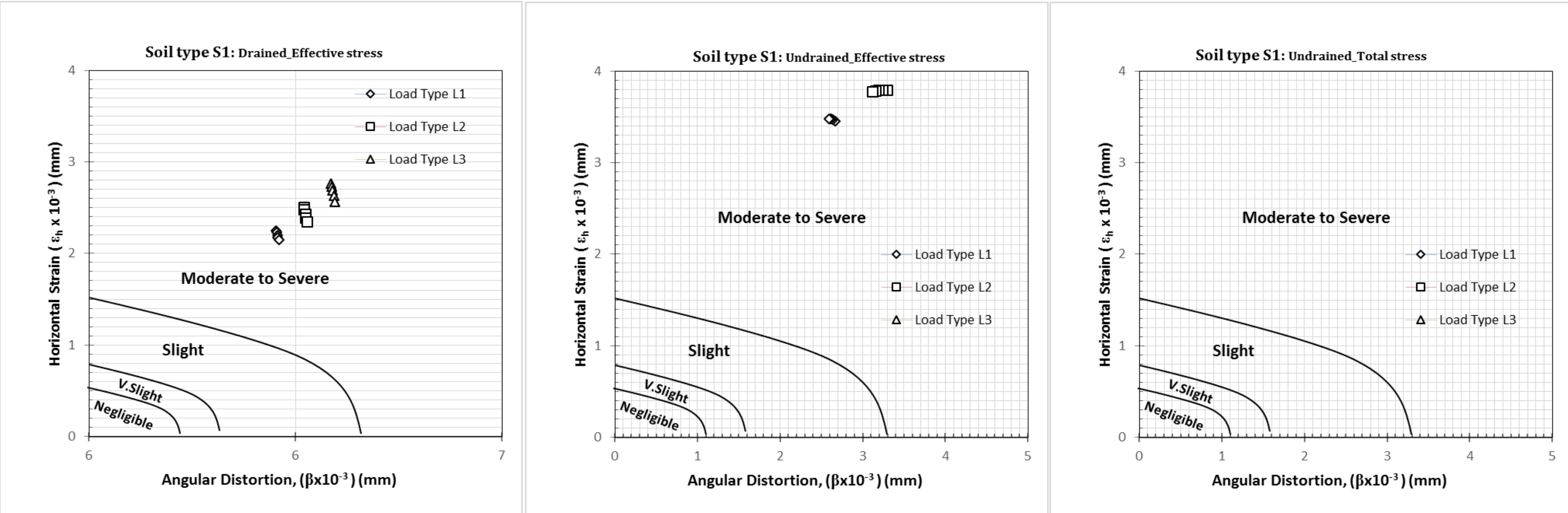

Figure 34: Angular distortions with Horizontal strain *(for soil type S_1)*

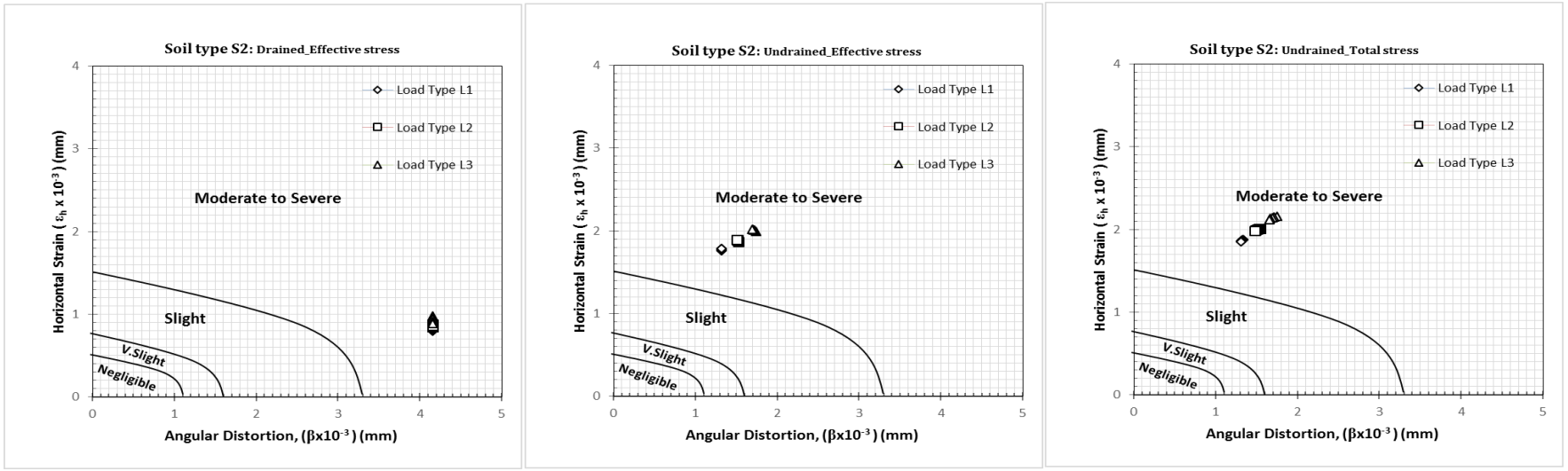

Figure 35: Angular distortions with Horizontal strain *(for soil type S_2)*

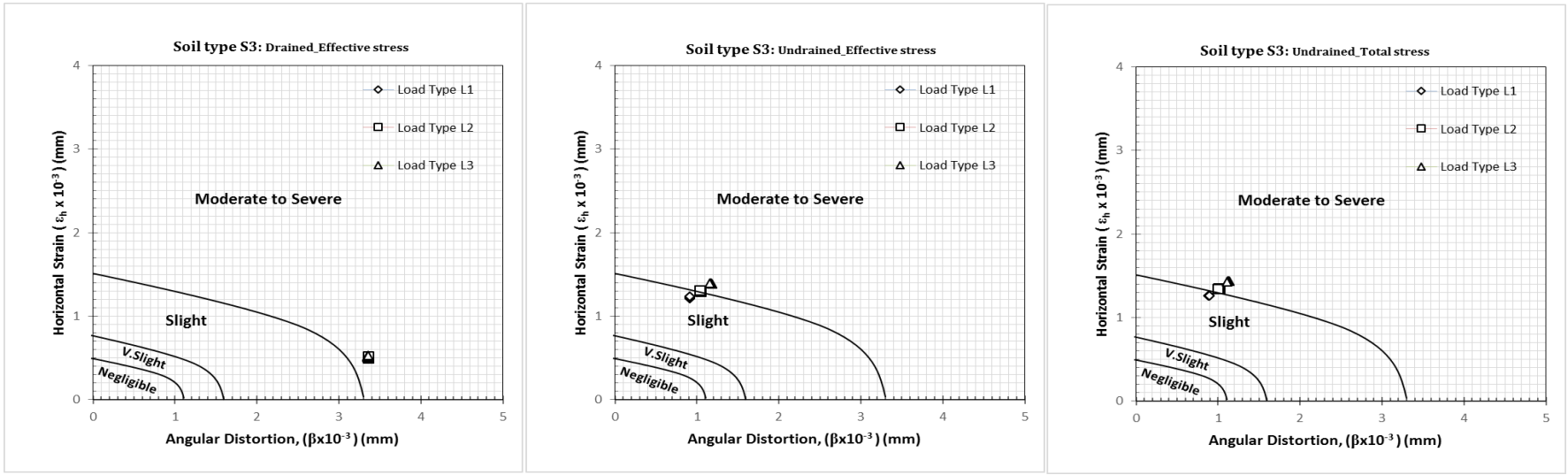

Figure 36: Angular distortions with Horizontal strain *(for soil type S_3)*

Various damage category criteria have been proposed such as the methods of Rankin (1988), Boscardin & Cording (1989) and Boone (1996). For design purpose, the designer should normally limit the angular distortion and horizontal strain such that the damage category does not exceed 'Slight" in Table 2. The damage category is based on the work of Burland et al. (1977) and is shown in Table 1. Therefore, the limiting value of angular distortion (β) and horizontal strain (ε) for the slight category is 3.3×10^{-3} and 1.5×10^{-3} respectively.

Figure 35, 36 &37, show the variations in angular distortions are identified varying horizontal strains for three soil types S_1, S_2 & S_3 respectively. It can be seen that soil types S_1 and S_2, angular distortions and horizontal strains categorized as moderate to severe damage category and in soil type S_3 angular distortions and horizontal strains categorized as slight to moderate damage category as per the method of Boscardin & Cording (1989) and Boone (1999).

3.6 Parametric study of deep excavation supported by contiguous pile wall

Previously reviewed studies show that soil type is a key factor in performance of deep excavations. Soil type is important because the performance of deep excavations is governed by the interaction between the soil and the support system. Support systems for deep excavation consist of two main components. The first is a retaining structure. The second component is the support provided for the retaining structure. The stiffness of the support system is governed by individual stiffness of the components. Thus, parameters are identified accordingly.

The models used for the parametric study are identical to the original models, except for certain parameters being changed in order to determine the impact of these specific parameters. Soil type, diameter of contiguous pile wall, anchor spacing and anchor pre-stress force are the variables considered in the parametric study. When one of the above parameters is varied, the rest are kept constant. The issue of heave is not addressed in this parametric study as PLAXIS does not include this parameter in the calculation.

Table 20: Contiguous Pile wall parameters considered for parametric study

Parameter	Name	Unit	Contiguous pile		
			Dia. 0.4m	Dia. 0.6m	Dia. 0.8m
Concrete	Concrete class	-	C 30	C 30	C 30
Type of Material Behavior	Type	-	Elastic	Elastic	Elastic
Contiguous Pile Wall	Diameter	m	0.4	0.6	0.8
Reinforcement	Grade	-	S400	S400	S400
Diameter	D	m	0.016	0.016	0.016
Number of reinf.	No.	No.	6	8	11
Area of reinforcement	A_S	m^2	0.001207	0.001609	0.002213
Secant Modulus of Elasticity of concrete class C 30	E_C*	kN/m^2	32,000,000	32,000,000	32,000,000
Secant Modulus of Elasticity of steel reinforcement	E_S*	kN/m^2	200,000,000	200,000,000	200,000,000
Flexural Rigidity	EI**	kNm^2/m	40,232.43	203,662.29	643,664.22
Normal Stiffness	EA	kN/m	4,022,857.14	9,051,428.57	16,091,428.57
Weight	W***	(kN/m/m)	8.661	12.991	17.321

Note:

- *- E_C and E_S are taken from EBCS-2
- **- $EI = E_C I_g + E_s I_s$ where, $I = \pi r^4/4$ and I_g= gross moment of inertia, I_s= Moment of inertia of steel
- ***- $W = \gamma_C * d_{eq.} = \gamma_C * (12*(EI/EA))^{0.5}$,where γ_C= $25kN/m^3$ (EBCS-2)

(W = weight per length of contiguous pile)

Table 21: The neighboring structure load considered in the parametric study

Parameter	Unit	Load, L_1	Load, L_2	Load, L_3
Load	kN/m/m	56	75	94

Table 22: Strut spacing considered in the parametric study

Parameter	L_{S1}	L_{S2}	L_{S3}
Spacing out of plane, L_S (m)	1.5	2	2.50

Table 23: Strut pre-stress force considered in the parametric study

Parameter	F_{max1}	F_{max2}	F_{max3}
Prestress load, F_{max} (kN)	150	250	350

3.6.1 Effect of change in diameter of contiguous pile wall

For all the analyses conducted in this section of parametric study, the following quantities or features were kept the same:

- All soil types parameters, i.e. S_1, S_2 & S_3
- Tie-back anchor (strut) spacing, L_S = 1.5 m
- Neighboring structure load, type L_2 = 75 kN/m/m
- Neighboring structure distance-excavation, D= $0.1H_e$ = 1.2m
- Construction sequences (as described at section 3.3)

Table 24: Lateral wall deflection, Settlement and bending moment output from base model analysis *(soil type S_1)*

Soil type S_1

Strut spacing, L_s = 1.5m ,

Neighboring Load, L_2 = 75 kN/m/m

Neighboring Load distance-excavation, $D_1 = 0.1H_e$ = 1.2 m

Diameter (m)		Lateral wall deflection			Vertical displacement			Moment		
		δ_h (mm)			δ_v (mm)			M (kNm/m)		
		Und_Eff.	Drai_Eff	Und_Tot.	Und_Eff.	Drai_Eff	Und_Tot.	Und_Eff.	Drai_Eff	Und_Tot.
D_1	0.40	75.87	53.15	103.32	64.68	128.02	86.10	83.95	120.48	117.94
D_2	0.60	75.90	50.20	108.97	65.97	128.08	97.33	213.66	248.77	323.25
D_3	0.80	75.60	49.24	131.45	67.38	128.13	127.14	423.01	383.63	641.93

Table 25: Lateral wall deflection, Settlement and bending moment output from base model analysis *(soil type S_2)*

Soil type S_2

Strut spacing, L_s = 1.5m ,

Neighboring Load, L_2 = 75 kN/m/m

Neighboring Load distance-excavation, $D_1 = 0.1H_e$ = 1.2 m

Diameter (m)		Lateral wall deflection			Settlement			Moment		
		δ_h (mm)			δ_v (mm)			M (kNm/m)		
		Und_Eff.	Drai_Eff	Und_Tot.	Und_Eff.	Drai_Eff	Und_Tot.	Und_Eff.	Drai_Eff	Und_Tot.
D_1	0.40	37.76	19.65	41.50	30.39	83.21	30.56	56.94	100.38	74.31
D_2	0.60	37.41	17.61	40.21	30.57	83.18	30.83	142.89	198.29	195.26
D_3	0.80	37.25	16.84	39.44	30.83	83.15	31.18	275.20	294.16	374.93

Table 26: Lateral wall deflection, Settlement and bending moment output from base model analysis (*soil type S_3)*

Soil type S_3 Strut spacing, L_s = 1.5m , Neighboring Load, L_2 = 75 kN/m/m Neighboring Load distance-excavation, $D_1 = 0.1H_e$ = 1.2 m										
Diameter (m)		**Lateral wall deflection**			**Settlement**			**Settlement**		
		δ_h (mm)			**δ_v (mm)**			**M (kNm/m)**		
		Und_Eff.	**Drai_Eff**	**Und_Tot.**	**Und_Eff.**	**Drai_Eff**	**Und_Tot.**	**Und_Eff.**	**Drai_Eff**	**Und_Tot.**
D_1	0.40	26.57	10.59	27.96	20.82	67.11	20.27	53.33	96.74	57.90
D_2	0.60	25.94	10.00	26.95	20.86	67.06	20.28	122.39	193.24	155.94
D_3	0.80	25.70	10.00	26.26	20.94	67.02	20.33	233.25	286.12	300.18

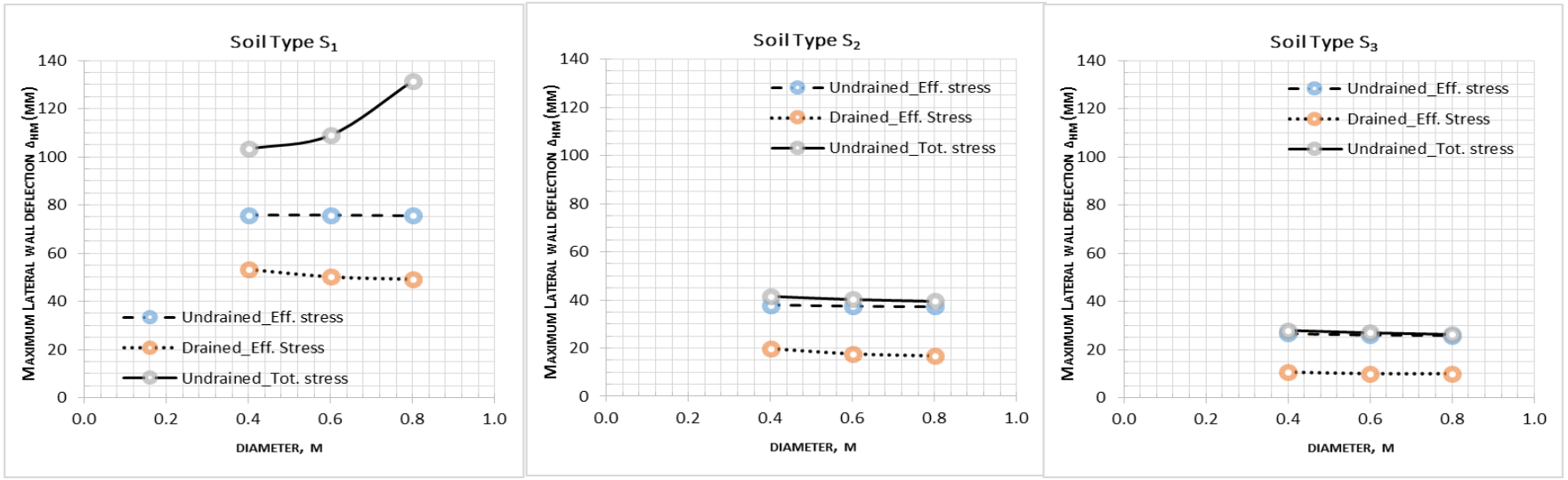

Figure 37: Maximum lateral wall deflection with contiguous pile wall diameter

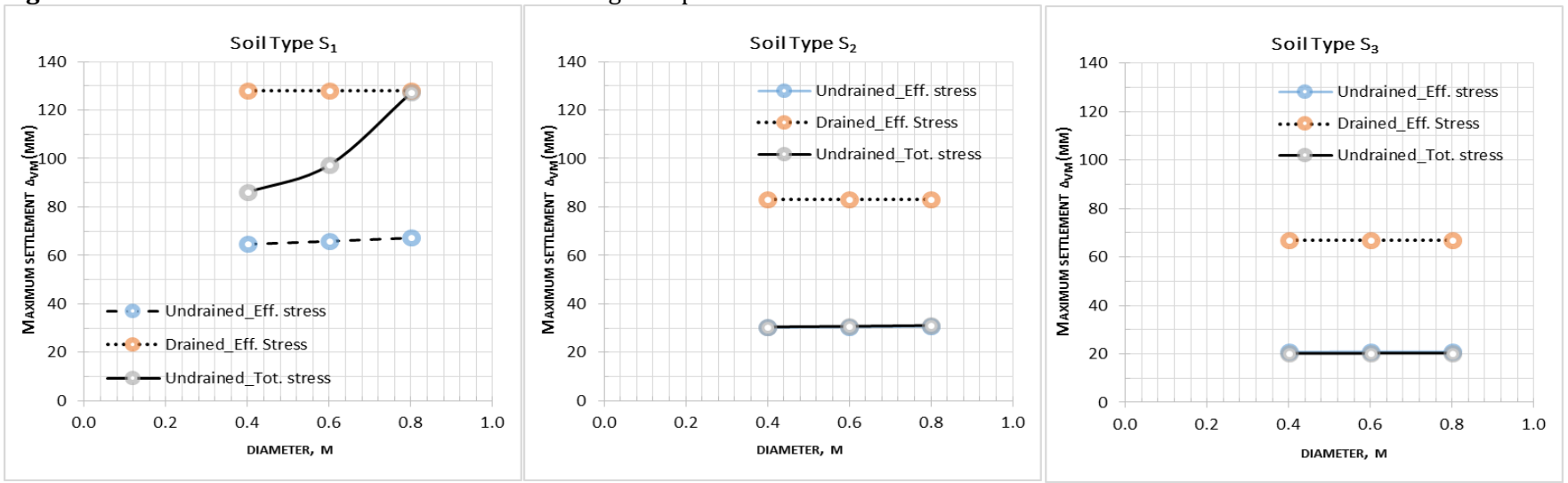

Figure 38: Maximum settlement with contiguous pile wall diameter

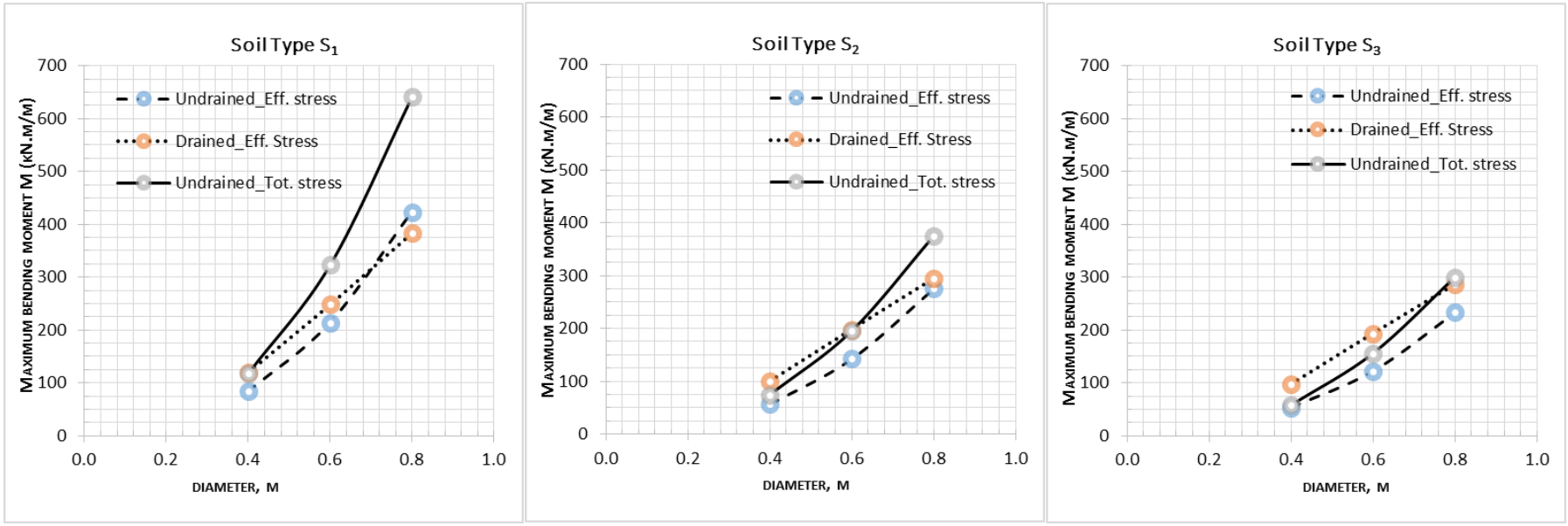

Figure 39: Maximum bending moment with contiguous pile wall diameter

From Figures 38, 39 & 40, the effect of change in diameter of contiguous pile wall with the change in soil types has presented as follows;

Lateral wall deflection:

- In soil type S_1, S_2 and S_3; in all drainage conditions except undrained with total stress drainage condition in soil type S_1, lateral wall deflection decreases when the diameter of contiguous pile wall is increased. In soil type S_1, undrained with total stress, lateral wall deflection increase when the diameter of contiguous pile wall is increased. Like increment of lateral wall deflection with diameter of contiguous pile wall bending moment is increases in all soil types S_1, S_2, & S_3.

Settlement:

- In soil type S_1, S_2, S_3; in all drainage conditions, except in undrained with total stress drainage condition in soil type S_1, settlement slightly increases when the diameter of contiguous pile wall is increased and in drained with effective stress condition. Like increment of maximum settlement with diameter of contiguous pile wall, bending moment is increases in all soil types S_1, S_2, & S_3. In soil type S_1, undrained with total stress, deflection increase when the diameter of contiguous pile wall is increased.

It is understood that, a large diameter contiguous pile wall is able to resist horizontal deformation better but at the expense of induced greater bending moment. In other words, a stiffer contiguous pile wall also needs greater bending strength. In terms of cost, it worth noting that the maximum lateral wall deflection and settlement of the contiguous pile wall does not reduce appreciably but the maximum bending moment continues to increase when the diameter of contiguous pile wall is increased. This implies that it is not economical to increase the stiffness of the contiguous pile wall beyond a certain maximum value.

Long's (2001) empirical data base on 296 case histories

"The **deformations of deep excavations** in non-cohesive soils as well as in stiff clay are **independent of the stiffness of the wall and the support as well as the kind of support."**

Powerie and Li (1991) numerical studies

"**The magnitude of soil and wall movements** was governed by **the stiffness of the soil rather than that of the wall."**

3.6.2 Effect of change in strut spacing

For all the analyses conducted in this section of parametric study, the following quantities or features were kept the same:

- All soil types parameters, i.e. S_1, S_2 & S_3
- Diameter of contiguous pile wall, D = 0.6 m
- Neighboring structure load, L_2 = 75 kN/m/m
- Neighboring structure distance-excavation, D = $0.1H_e$ = 1.2m
- Construction sequences (as described at section 3.3)

Table 27: Lateral wall deflection, Settlement and bending moment output from model analysis *(soil type S_1)*

Soil type S_1

Contiguous pile wall diameter, D = 0.6 m

Neighboring Load, L_2 = 75 kN/m/m

Neighboring Load distance-excavation, $D_1 = 0.1H_e$ = 1.2 m

Strut Spacing, L_s (m)		Lateral wall deflection δ_h (mm)			Settlement δ_v (mm)			Moment M (kNm/m)		
		Und_Eff.	Drai_Eff	Und_Tot.	Und_Eff.	Drai_Eff	Und_Tot.	Und_Eff.	Drai_Eff	Und_Tot.
L_s	1.5	75.90	50.20	108.97	65.97	128.08	97.33	213.66	248.77	323.25
L_s	2.0	75.97	50.36	110.08	66.08	128.09	98.37	214.29	248.55	325.09
L_s	2.5	76.02	50.57	111.02	66.16	128.10	99.27	214.70	249.37	326.42

Table 28: Lateral wall deflection, Settlement and bending moment output from model analysis *(soil type S_2)*

Soil type S_2

Contiguous pile wall diameter, D = 0.6 m

Neighboring Load, L_2 = 75 kN/m/m

Neighboring Load distance-excavation, $D_1 = 0.1H_e$ = 1.2 m

Strut Spacing, L_s (m)		Lateral wall deflection δ_h (mm)			Settlement δ_v (mm)			Moment M (kNm/m)		
		Und_Eff.	Drai_Eff	Und_Tot.	Und_Eff.	Drai_Eff	Und_Tot.	Und_Eff.	Drai_Eff	Und_Tot.
L_s	1.5	37.41	17.61	40.21	30.57	83.18	30.83	142.89	198.29	195.26
L_s	2.0	37.44	17.84	40.33	30.61	83.19	30.94	142.71	198.22	194.57
L_s	2.5	37.45	18.01	40.41	30.64	83.21	31.02	142.57	198.45	194.09

Table 29: Lateral wall deflection, Settlement and bending moment output from model analysis *(soil type S_3)*

Soil type S_3

Contiguous pile wall diameter, D = 0.6 m

Neighboring Load, L_2 = 75 kN/m/m

Neighboring Load distance-excavation, $D_1 = 0.1H_e$ = 1.2 m

Strut Spacing, L_s (m)		Lateral wall deflection δ_h (mm)			Settlement δ_v (mm)			Moment M (kNm/m)		
		Und_Eff.	Drai_Eff	Und_Tot.	Und_Eff.	Drai_Eff	Und_Tot.	Und_Eff.	Drai_Eff	Und_Tot.
L_s	1.5	25.94	10.00	26.95	20.86	67.06	20.28	122.39	193.24	155.94
L_s	2.0	25.97	9.86	27.02	20.90	67.07	20.35	122.06	193.45	155.44
L_s	2.5	25.97	9.79	27.07	20.90	67.09	20.40	122.06	193.55	155.21

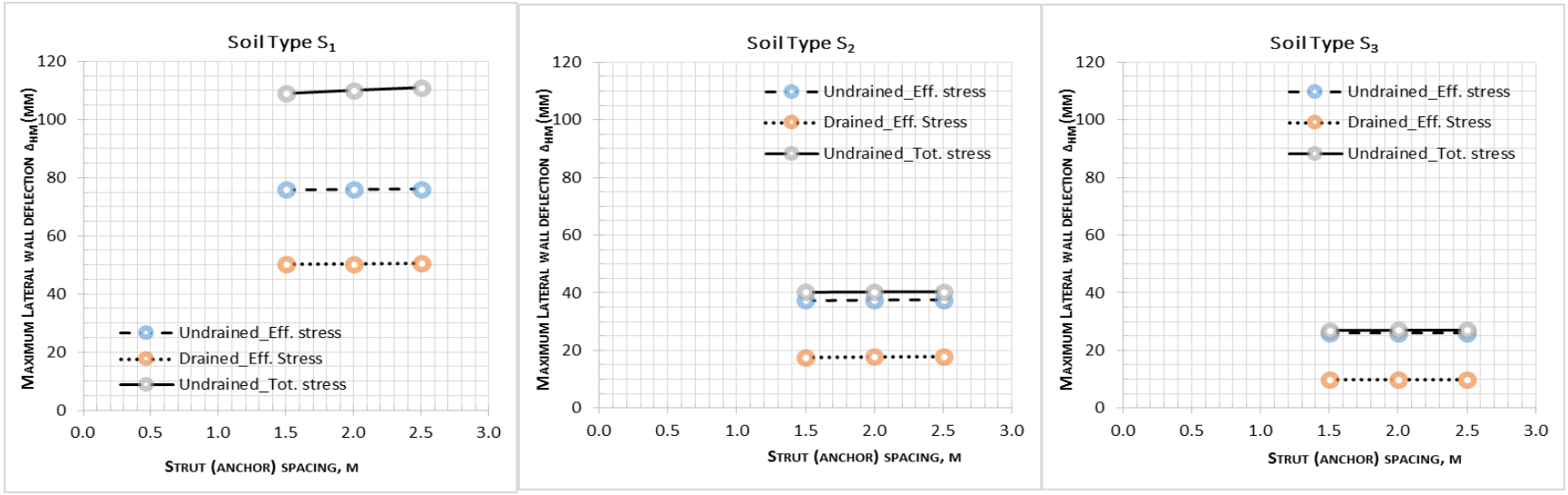

Figure 40: Maximum lateral wall deflection with strut (tie-back anchor) spacing

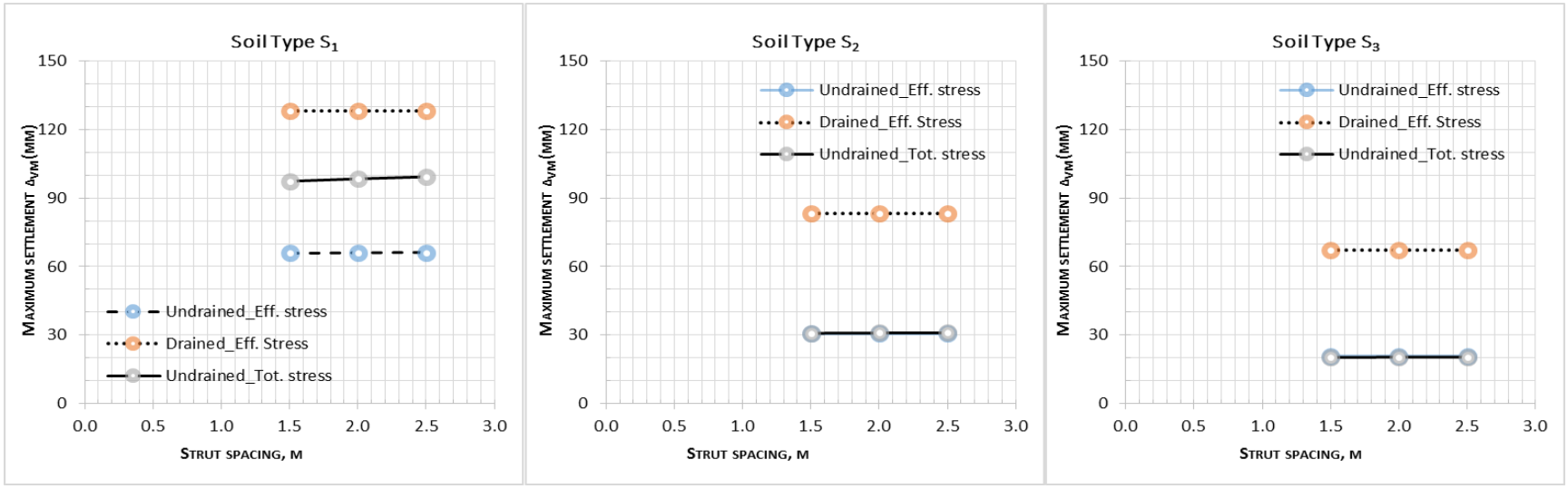

Figure 41: Maximum settlement with strut (tie-back anchor) spacing

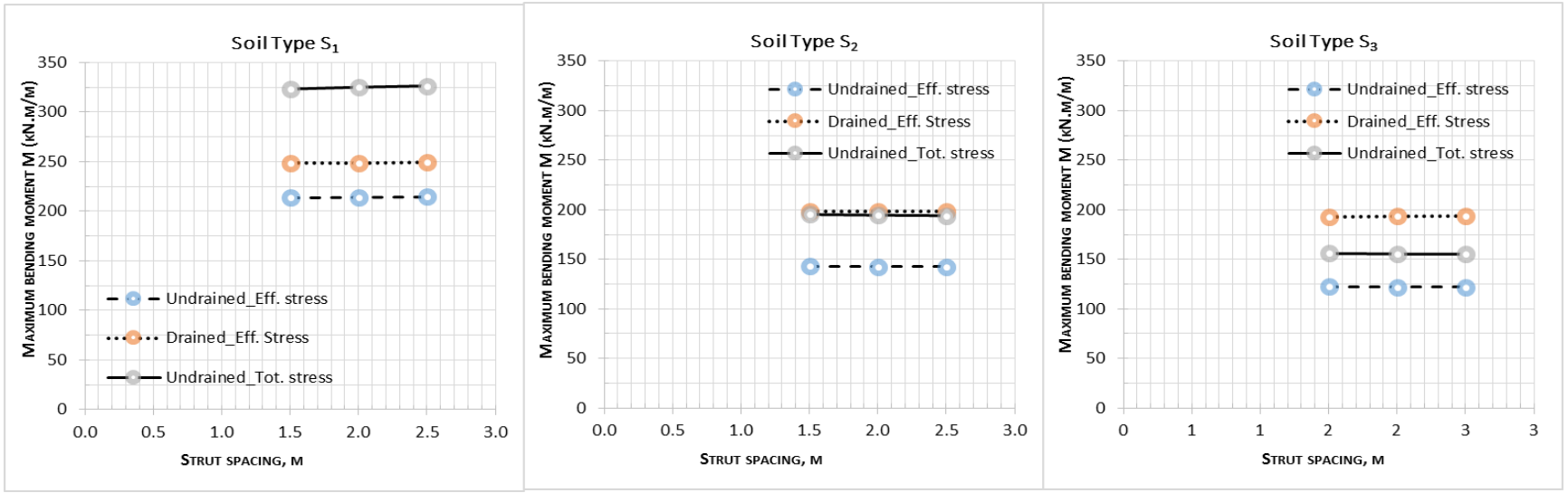

Figure 42: Maximum bending moment with strut (tie-back anchor) spacing

From Figure 41, 42 & 43, the effect of change in anchor spacing with the change in soil types have presented as follows;

Maximum lateral wall deflection:

- In soil type S_1, S_2 and S_3; in all drainage conditions except soil type S_3, drained with effective stress drainage condition, lateral wall deflection slightly increases when anchor spacing is increased. Following this, contiguous pile wall bending moment also slightly increases when anchor spacing is increased. In soil type S_3, drained with effective stress, lateral wall deflection slightly decreases when anchor spacing is increased. Consequently, contiguous pile wall bending moment also slightly decreases when anchor spacing is increased.

Maximum settlement:

- In soil type S_1, S_2 and S_3; in all drainage conditions except soil type S_3, drained with effective stress drainage condition, settlement slightly increases when anchor spacing is increased. Contiguous pile wall bending moment also slightly increases when anchor spacing is increased.

For instance, in soil type S_1, undrained with effective stress drainage condition; for the change of 2.0 m to 2.5 m horizontal anchor spacing, it is shown that an increase in lateral wall deflection from 75.97 mm to 76.02 mm, i.e. 0.07% increment, and an increase in settlement from 66.08 mm to 66.16 mm i.e. 0.12% increment is observed as well as an increase in bending moment from 214.29 kN.m/m to 214.70 kN.m/m i.e. 0.19% increment is observed. This shows, the lateral wall deflection, settlement and bending moment of the contiguous pile wall did not reduce appreciably when the strut spacing change from 2m to 2.5m.

Moormann's (2004) empirical data base on 530 case histories

"**The retaining wall and ground movements** seem to be **largely independent of the system stiffness of the retaining system**."

Mana and Clough (1981) numerical studies

"Increasing the wall bending stiffness or decreasing strut spacing decreases movement. This effect is **more significant when the factor of safety is low"**

3.6.3 Effect of change in strut (tie-back anchor) pre-stress force

In this section, the effect of strut (tie-back anchor) pre-stress force on the performance of deep excavation supported by contiguous pile wall will be studied.

For all the analyses conducted in this section of parametric study, the following quantities or features are kept the same:

- All soil types parameters, i.e. S_1, S_2 & S_3
- Diameter of contiguous pile wall, D = 0.6 m
- Tie-back anchor spacing, L_S = 1.5 m
- Neighboring structure Load, L_2 = 75 kN/m/m
- Neighboring structure distance-excavation, D = $0.1H_e$ = 1.2m
- Construction sequences (as described at section 3.3)

Table 30: Lateral wall deflection, Settlement and bending moment output from base model analysis *(soil type S_1)*

Soil Type S_1

Contiguous pile wall diameter, D = 0.6 m

Neighboring Load, L_2 = 75 kN/m/m

Neighboring Load distance-excavation, $D_1 = 0.1H_e$ = 1.2 m

Strut Prestress Load (kN)		Lateral wall deflection δ_h (mm)			Settlement δ_v (mm)			Moment M (kNm/m)		
		Und_Eff.	Drai_Eff	Und_Tot.	Und_Eff.	Drai_Eff	Und_Tot.	Und_Eff.	Drai_Eff	Und_Tot.
F_{max}	150	79.76	56.49	130.64	71.81	128.09	118.35	207.93	243.27	345.79
F_{max}	250	75.90	50.20	108.97	65.97	128.08	97.33	213.66	248.77	353.25
F_{max}	350	74.24	45.21	99.04	61.30	128.06	87.27	229.94	256.77	366.45

Table 31: Lateral wall deflection, Settlement and bending moment output from base model analysis *(soil type S_2)*

Soil type S_2

Contiguous pile wall diameter, D = 0.6 m

Neighboring Load, L_2 = 75 kN/m/m

Neighboring Load distance-excavation, $D_1 = 0.1H_e$ = 1.2 m

Strut Prestress Load (kN)		Lateral wall deflection δ_h (mm)			Settlement δ_v (mm)			Moment M (kNm/m)		
		Und_Eff.	Drai_Eff	Und_Tot.	Und_Eff.	Drai_Eff	Und_Tot.	Und_Eff.	Drai_Eff	Und_Tot.
F_{max}	150	38.74	21.67	42.20	32.78	83.89	32.89	128.20	193.78	183.26
F_{max}	250	37.41	17.61	40.21	30.57	83.18	30.83	142.89	198.29	195.26
F_{max}	350	36.85	15.84	38.68	28.41	81.20	28.82	159.23	229.84	210.64

Table 32: Lateral wall deflection, Settlement and bending moment output from base model analysis *(soil type S_3).*

Soil type S_3

Contiguous pile wall diameter, D = 0.6 m

Neighboring Load, L_2 = 75 kN/m/m

Neighboring Load distance-excavation, $D_1 = 0.1H_e$ = 1.2 m

Strut Prestress Load (kN)		Lateral wall deflection δ_h (mm)			Settlement δ_v (mm)			Moment M (kNm/m)		
		Und_Eff.	Drai_Eff	Und_Tot.	Und_Eff.	Drai_Eff	Und_Tot.	Und_Eff.	Drai_Eff	Und_Tot.
F_{max}	150	27.18	12.05	28.37	22.45	67.76	21.74	110.42	186.30	145.88
F_{max}	250	25.94	10.00	26.95	20.86	67.06	20.28	122.39	193.24	155.94
F_{max}	350	25.27	9.68	25.79	19.33	65.10	18.91	137.07	201.69	169.26

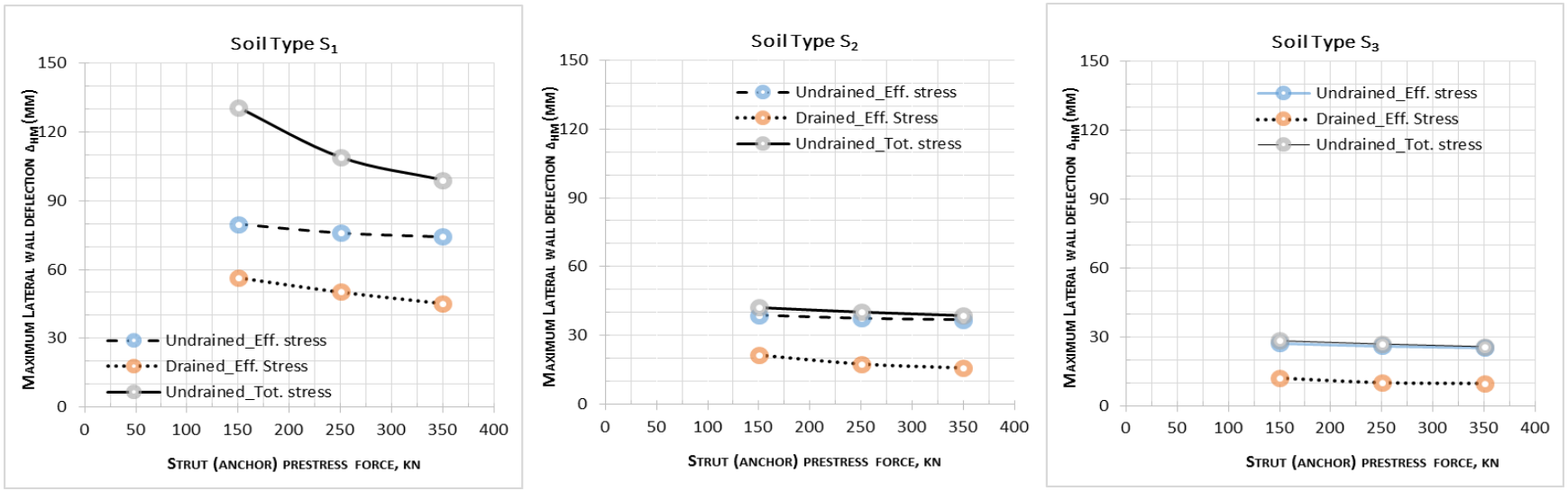

Figure 43: Maximum lateral wall deflection with strut (tie-back anchor) pre-stress force

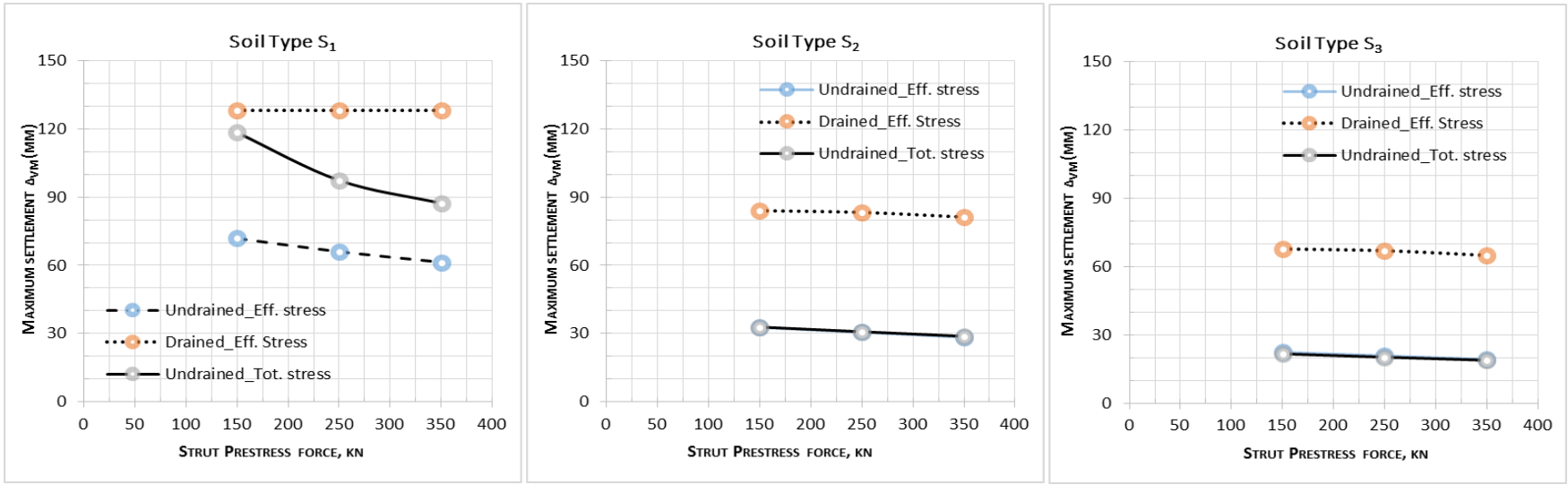

Figure 44: Maximum settlement with strut (tie-back anchor) pre-stress force

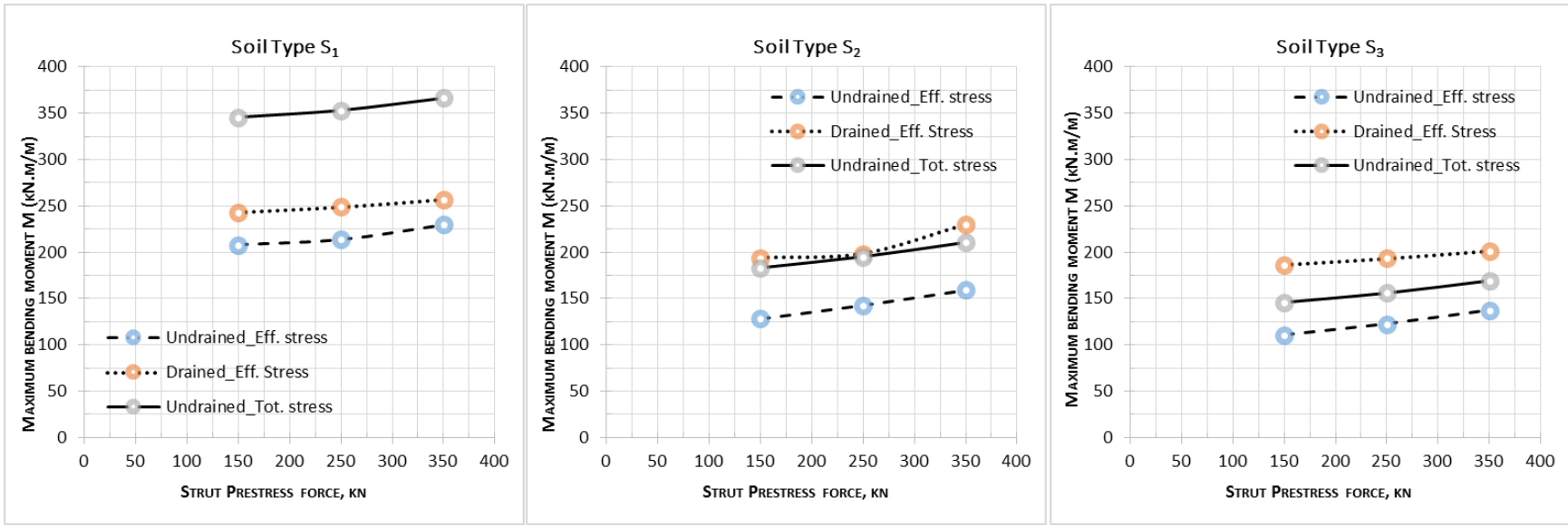

Figure 45: Maximum bending moment with strut (tie-back anchor) pre-stress force

This parameter helps to identify the force required for the support system to be stable from ground movements. From Figures 44, 45 & 46, the effect of change in anchor pre-stress force with the change in soil types have presented as follows;

Maximum lateral wall deflection and settlement:

- In soil type S_1, S_2 and S_3; in all drainage conditions, both lateral wall deflection and settlement decreases when anchor pre-stress force is increased. Following this, contiguous pile wall bending moment also increases when anchor pre-stress force is increased. However, in all soil types S_1, S_2 &S_3, undrained with total stress, lateral wall deflection and settlement decrement are pronounced when anchor spacing is increased.

For instance, in soil type S_1, undrained with total stress drainage condition; for the change of 250 kN to 350 kN anchor pre-stress force, it is shown that a decrease in lateral wall deflection from 108.97 mm to 99.04 mm, i.e. 9.11% decrement, and decrease in settlement from 97.33 mm to 87.27 mm i.e. 10.34% decrement is observed as well as an increase in bending moment from 353.25 kN.m/m to 366.45 kN.m/m i.e. 3.60% increment is observed. This shows, the lateral wall deflection, settlement and bending moment of contiguous pile wall does reduce appreciably when the strut pre-stress force changes from 250 kN to 350 kN.

Mana and Clough (1981)

"Increasing the wall bending stiffness or decreasing strut spacing decreases movement. This effect is more significant when the factor of safety is low. **Increasing the strut stiffness reduces movement, though the effect shows diminishing return at very high stiffness**."

CHAPTER 4
CONCLUSIONS AND RECOMMENDATIONS

4.1 Conclusions

- The maximum lateral wall deflection, maximum settlement and bending moment decreases with increasing soil stiffness from soil type S_1 to S_2 to S_3. This shows, the ground deformations around a deep excavation are significantly influenced by the type of soil. It is important, therefore, to obtain accurate laboratory test results and appropriate estimation of soil parameters in order to obtain accurate estimates of soil displacement around deep excavations.
- The performance of deep excavation affected by neighboring building load and the structure distance from face of excavation. The excavation project must meet the corresponding requirements regarding the deformations induced by neighboring structures.
- A stiff contiguous pile wall is required for controlling horizontal ground movements resulting from deep excavation. However, when choosing a support system for the deep excavation, it should be kept in mind that even if the stiffest of contiguous pile wall will reduce horizontal displacement of the ground. Selecting big contiguous pile wall diameter alone does not eliminate all the horizontal ground movements.
- Applying tie-back anchors significantly reduces ground deformation around deep excavation. However, decreasing anchor spacing beyond optimum limit do not reduce ground deformation appreciably.
- Struts (tie-back anchor) are usually pre-stressed to minimize wall deflections and ground movements. However, the effects of anchor pre-stress force on soft soil, like on soil type S_1, displacement around deep excavations should be further investigated by using different soil models.

4.2 Recommendations

- In order to reduce the risk of failure (ultimate limit state) of deep excavations and that of damaging neighboring buildings or structures (serviceability limit state), the design of retaining works should be done by thoroughly analyzing the induced deformation.
- The designer should select proper deep excavation support system and parameters based on neighboring structure load, influence zone of excavations and type of soil.
- The simplified method provides a very good approach for engineers to calculate the ground settlement for preliminary design. However, for detailed design, advanced numerical analyses with proper soil models are recommended.

References

Addenberooke, T.I., Potts, D. M. and Dabee, B. (2000). Displacement flexibility number for multi-propped retaining wall design. Journal of Geotechnical and Geo-environmental engineering, Vol. 126, No. 8, August, 2000, pp 718-726.

Bjerrum, L. (1963), Discussion *Proc. Eur. Conf. SM&FE*, Wiesbaden, 2, p.135.

Boone, S.J. (1996, Ground-movement-related building damage. *Journal of Geotechnical Engineering*, ASCE, Vol.122, No.11, 886-896.

Boone, S.J., Westland, J, & Nusink, R.1999. Comparative evaluation of building response to an adjacenet braced excavation. *Can. Geotech. J.* 36: 210-233.

Boscardin, M.D. & Cording. E.J. 1989, Building response to excavation-induced settlement. *Journal of Geotechnical Engineering*. Vol. 115, No. 1: 1-21.

Borin, D. L. (1989), Wallap-*computer program for the stability analysis of retaining walls*. Geosolve.

Bowles, J.E. 1988. Foundation analysis and design. 4th ed., McGraw-Hill Book Company, New York.

Briaud, J., & Kim, B. (1998). Beam Column Method for Tieback Walls. (ASCE, Ed.) *Journal of Geotechnical and Geo Environmental Engineering*, *124* (1), 67–79.

Brinkgreve, R., Broere, W., & Waterman, D. (2004). *PLAXIS 2-D Professional Version 8.0 - User's Manual.* PLAXIS b.v., The Netherlands.

Britto, A.M. & Gunn, M.J. (1987) *Critical State Soil Mechanics via Finite elements*. Ellis Horwood Ltd, Chichester.

Burland, J.B. & Wroth, C.P. (1975), Settlement of buildings and associated damage. *State-of-the-art review*, *Proc. Conf. Settlement of Structures*, Cambridge, Pentech Press, London, p. 611.

Burland, J.B. and Wroth, C.P. (1974) "Settlement of buildings and associated damage." *Proc Conf. on Settlement of Structures*, Pentech Press, London, England.

Clough, G.W., Smith, E. W. and Sweeney, B. P. (1989) Movement control of excavation support system by iterative design. Foundation Engineering Current Principles and Practices, Vol.2 ASCE, New York, NY, 1989, pp.869-882.

Clough, G.W. and O'Rourke, T. D., (1990). Construction induced movements of in situ walls. In Proc. Design and performance of earth retaining structure, ASCE Special conference, Ithaca, New York, pp 439-470.

Goh, A.T.C. (1994). Estimating basal heave stability for braced excavation in soft clay. Technical note, Journal of Geotechnical Engineering, Vol. 120, No.8, August, 1994, 1430-1436.

Goldberg, D.T., Jaworski, W.E., and Gordon, M.D. (1976). Lateral support systems and underpinning. Rep. FHWA-RD-75-128, Federal Highway Administration, Washington D.C.

Gue, S.S. & Tan, Y.C. (1998), Performance of Anchored Diaphragm Walls for Deep Basement in Kuala *Lumpur, Malaysia, Proceedings of the 13th southeast Asian Geotechnical Conferences,* Taipei. (accepted for publication in November, 1998)

Hashash, Y. M. A., and Whittle, A. J. (1996). Ground movement prediction for deep excavations in soft clay. J. Geotech. Eng., 122(6), pp.474-486.

Institution of Structural Engineers (1989), *Soil-Structure Interaction* - The Real Behavior of Structures. Institution of Structural Engineers, London, 120p.

Institution of Structural Engineers (1975), *Design and Construction of Deep Basements*. Institution of Structural Engineers, London, 64p.

ITASCA (1991), FLAC Fast *Lagrangian analysis of Continua*: *user's manual* (Version 3). ITASCA, Minneapolis.

Japan National Railways Public Corporation (1979), *Standard of design and construction of retaining structures* (in Japanese).

Jen, L. C. (1998). The design and performance of deep excavation in clay. Ph.D thesis, MIT.

Long, M. (2001). Database for retaining wall and ground movements due to deep excavation. J. Geotech. & Geoenviron. Engrg, ASCE, Vol. 127(3), 203-224.

Mana, A. I. and Clough, G. W. (1981). Prediction of movements for braced cuts in clay. J. Geotech. Engrg, ASCE, 107(6): 759-777.

Matuso, M. and Kawamura, K. (1981), Predictions for the settlements around the excavations. *Proc. Of the 26th Symposium of JSSMFE on comparing measurements and predictions of ground deformation due to excavation or embankment*, pp. 61-68 (in Japanese).

Maruoka, M. and Ikuta, Y. (1986), Surface settlements caused by excavations in alluvial deposit. *Proc. Of the 21st annual meeting of JSSMFE,* pp. 1369-1370 (in Japanese).

Meyerhof, G.G. (1956), Discussion paper by Skempton et al. 'Settlement analysis of six structures in Chicago and London', *Proc. ICE, 5*, No.1, p. 170.

Moormann, C. (2004). Analysis of wall and ground movement due to deep excavation in soft soil based on a new worldwide database. Soils and Foundations, Vol. 44, No. 1, 87-98.

Naito, T. et al. (1958), *Reports of the research committee for preventing public disaster on the surface settlement due to excavation works*, Architectural Institute of japan (in Japanese)

Ng, C. W.W., (1998). Observed Performance of multi-propped excavation in stiff clay. J. Geotech & Geoenviron. Engrg. Vol.124 (9). pp. 889-905.

Ou, C.Y. And Chiou, D.C. And Wu, T.S. (1996). Three dimensional finite element analysis of deep excavations. Journal of geotechnical engineering, Vol 122, No.5, May, 1996, pp337-345.

Pappin, J.W., Simpson, B., Felton, P.J., and Raison, C, (1986), Numerical analysis of flexible retaining walls. Symp. On Computer Applications in geotechnical Engineering. The Midland Geotechnical Society, Birmingham Univ., pp. 195-212.

Pappin, J.W. et al. (1985), Numerical analysis of flexible retaining wall. Proc. Conf. Numerical Methods in Engineering Theory and applications, Swansea, 789-802.

Peck, R. B., (1969). Deep excavation and tunneling in soft ground. In Proc. of 7th ICSMFE, State-of-the-Art volume, Mexican City, pp.225-290.

Poulos. H.G. & Chen, L.T. (1997), Pile response to excavation-induced lateral soil movement. *Journal of Geotechnical and Geo-Environmental Engineering*, ASCE, Vol. 123, No.2, 94-99.

Powrie, W. and Li, E.S.F. (1991) Finite element analyses of an in situ wall propped at formation level, Geotechnique, Vol. 41, No. 4, pp. 499-514.

Rowe, P.W. (1952) Anchored sheet pile walls. Proc. ICE. 1:27-70.

Skempton, A.W. & macDonald, D.H. (1956), Allowable settlement of buildings. Proc. *ICE*, part 3, 5, P.727.

S.S Gue & Y.C. Tan (1998), Design and construction considerations for Deep Excavation, SSP Geotechnics Sdn Bhd

Sugimoto, T. (1986), Prediction of the maximum settlements of ground surface by open cuts. Proc. Of JSCE, No.373/VI-5, pp.113-120 (in Japanese).

Sugimoto, T. & sasaki, S. (1987), *Relationship between the maximum movements of walls and the maximum settlements of ground surface. Proc. Of the 22nd annual meeting of JSSMFE*, pp.1261-1262 (in Japanese).

Teferra, A. (1992). *Foundation Engineering.* Addis Ababa: Addis Ababa University Press.

Terzaghi, K. (1943). Theoretical soil mechanics, John Wiley, New York

Terzaghi, K., (1943). Theoretical soil mechanics, John Wiley & Sons, Inc., New York, N.Y.

Terzaghi, K. And Peck, R. B., (1967). Soil Mechanics in engineering practice, John Wiley and Sons, Inc., New York, Toronto, London. pp.729.

Tan, S.A. 2007. 2-Day Workshop on Advanced Computational Geotechnics: Finite Element Analysis, *Course Notes*. Petaling Jaya, Selangor, Malaysia.

Tan, Y.C. (1997), Deformation of anchored Diaphragm walls for Deep Basement at Berjaya Star City, Kuala Lumpur, *Proceedings of the Third Asian Young Geotechnical Engineers Conference 1997*, Singapore, pp. 121-130.

Whittle, A. J. (1993). Evaluation of a constitutive model for over-consolidated clays. Geotechnique, 43(2): 289-313.

Wong, K.S. and Broms, B.B. (1989). Lateral wall deflections or braced excavation in clay. J. Geotech. Engrg., Vol. 115, No.6, June, 1989, pp.853-870.

Appendices

Appendix 2: Soil Models

A.1.1 Mohr-Coulomb Model

The Mohr-Coulomb model coded in PLAXIS version 8.0 is based on an elastic perfectly-plastic mode which is constitutive law with a fixed yield surface, i.e. a yield surface that is fully defined by model parameters and not affected by (plastic) straining. For stress state represented by points within the yield surface, the behavior is purely elastic and all strains are reversible. There is no hardening or softening law required for the Mohr-Coulomb model as it is assumed to be perfectly plastic. A plastic yield function, *f*, is introduced as a function of stress and strain that can often be presented as a surface in principal stress space as shown in Figure A.46.

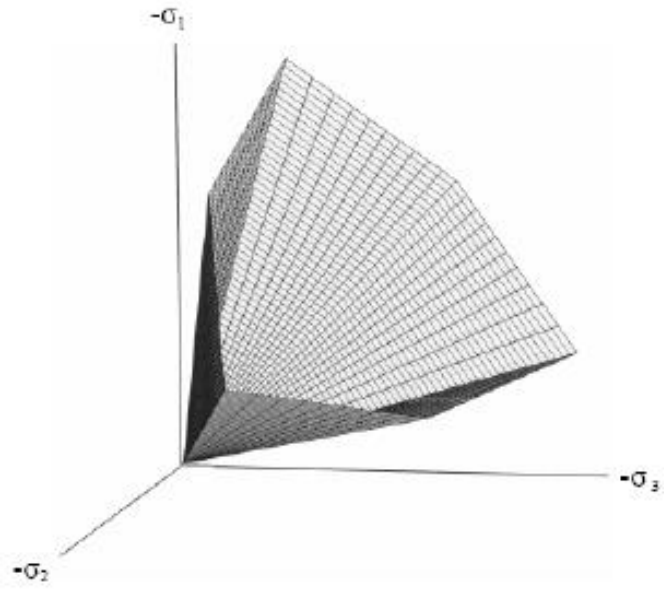

Figure A.46: The Mohr-Coulomb yield surface in principal stress space (c = 0)

The strains and strain rates are decomposed into an elastic part and a plastic part in theory of elasto plasticity:

$$\underline{\varepsilon} = \underline{\varepsilon}^{e} + \underline{\varepsilon}^{p} \qquad \dot{\underline{\varepsilon}} = \dot{\underline{\varepsilon}}^{e} + \dot{\underline{\varepsilon}}^{p} \quad \ldots\ldots\ldots\ldots\ldots\ldots \qquad (A.1.1.1)$$

The Mohr-Coulomb model requires five parameters. Parameters related to elastic behavior are E and ν, whereas parameters related to plastic behavior are c and f, and ψ, angle of dilatancy. These parameters with their standard units are listed in Table A.33:

Table A.33: Mohr Coulomb parameters with their standard units

PARAMETER		UNIT
E	Young's Modulus	[kN/m^2]
ν	Poisson's ratio	[-]
Φ	Friction angle	[°]
C	Cohesion	[kN/m^2]
ψ	Dilatancy angle	[°]

PLAXIS uses the Young's modulus as the basic stiffness modulus in the Mohr-Coulomb model. E_{ur} which tend to increase with the confining pressure is needed for unloading modeling such as in the case of excavations. This behavior in turn results in the deep soil layers tend to have greater stiffness than shallow layers. Hence, when using a constant stiffness modulus to represent soil behavior, a value that is consistent with the stress level and the stress path development should be chosen.

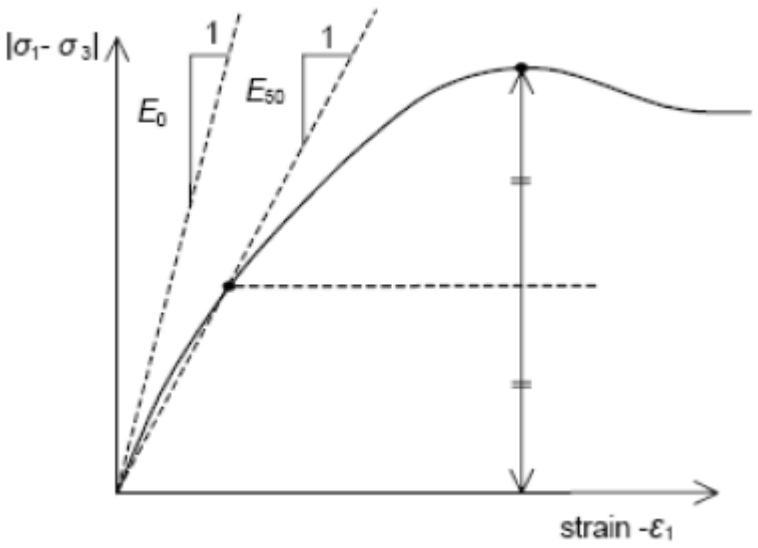

Figure A.47: Definition of E_0 and E_{50} for standard drained tri-axial test result

Although standard drained tri-axial tests may yield a significant rate of volume decrease at the very beginning of axial loading, but PLAXIS recommended the use of a high value initial value of Poisson's ratio (ν) when using the Mohr-Coulomb model.

In general, for unloading conditions, however, PLAXIS suggested to use values in the Range between 0.15 and 0.25.

PLAXIS can handle cohesion less sands (c = 0), but some options will not perform well. To avoid complications, non-experienced users are advised to enter at least a small value (use c > 0.2 kPa). The friction angle, F, is entered in degrees. High friction angles, as sometimes obtained for dense sands, will substantially increase plastic computational effort.

PLAXIS suggested using this model as first analysis of the problem considered by approximating a constant average stiffness for each layer of soil to obtain a first impression of deformations.

A.1.2 Soil Hardening Model

Soil response to loading is highly nonlinear and highly dependent on the magnitude of stress. This behavior has a significant influence on the stresses and displacements developed within the reinforced structure. Nonlinear elastic (hyperbolic) model can be expected to provide acceptable prediction of the behavior of soil at relatively low shear stress levels. The soil stiffness modeled in this manner increases with increasing confining pressure and decreases with increasing stress level as shown in Figure below. A very low stiffness is assigned to elements with stress condition at failure.

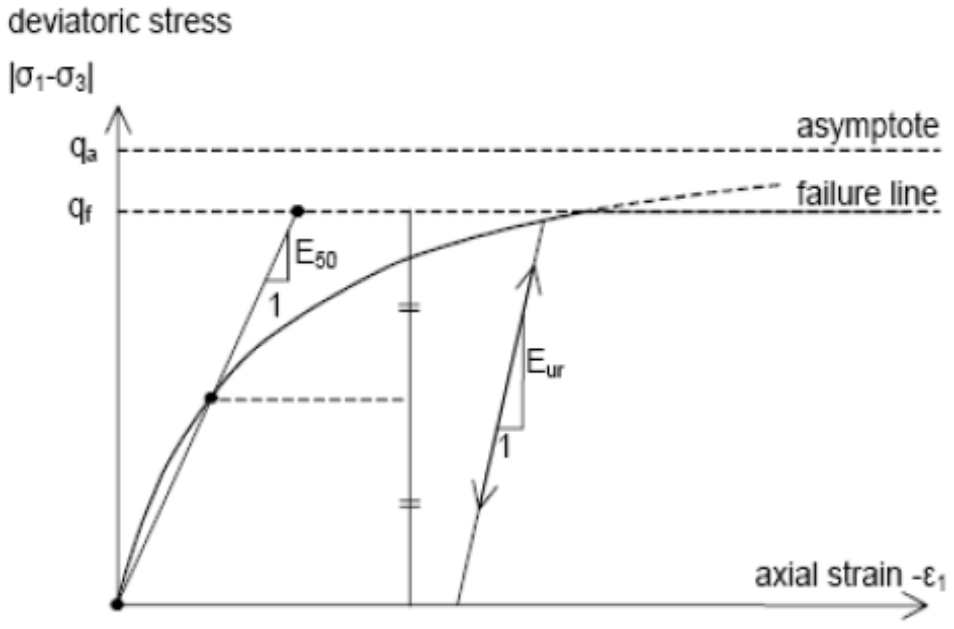

Figure A.48: Hyperbolic stress-strain relation in primary loading for a standard drained tri-axial test

The hyperbolic model is relatively simple, well validated and reliable to represent soil behavior. Similar to the Mohr-Coulomb model, limiting states of stress in the HS model are described in terms of effective stress parameters, i.e. the friction angle, ϕ, the cohesion, c, and the dilatancy angle, ψ, or in terms of undrained shear strength of soil, S_u, by specifying zero values for f and ψ and setting C equal to S. The soil stiffness, however, is described much more accurately in the HS model by using three different input stiffness values – the tri-axial loading stiffness, E_{50}^{ref}, the tri-axial unloading/reloading stiffness, E_{ur}^{ref}, and the odometer loading stiffness, E. Unlike the Mohr-Coulomb model, the HS model also accounts for stress-dependency of soil stiffness, i.e. the elastic stiffness values increase with confining stress in the HS model.

The HS model allows for plastic volume change (volumetric hardening) as well as plastic shearing due to deviatoric loading (shear hardening). Compared with the Mohr-Coulomb model, the unloading behavior of the soil is better taken into account in the HS model. The HS model may be used to calculate realistic pressure distribution below raft foundations and behind soil retaining structures (Brinkgreve et al. 2004).

The HS model does not account for softening in which the modulus decreases with strain whereas strain hardening model for which the modulus increase with strain. The use of the HS model generally results in longer calculation time than the Mohr Coulomb model since the material stiffness matrix is formed and decomposed in each calculation step.

Some parameters required in the strain hardening model are the (Effective) cohesion [c, kN/m^2], (effective) angle of internal friction [F, °] and the angle of dilatancy [ψ, °]. The basic parameters for soil stiffness in soil hardening model are the secant stiffness in standard drained triaxial test [E^{ref}_{50}, kN/m^2], the tangent stiffness for primary odometer loading [E^{ref}_{oed}, kN/m^2] and power for stress-level dependency of stiffness [m]. Table below shows the parameters used in the soil hardening model with their respective unit.

Table A.34: Advanced parameters with their standard units and default setting for Hardening Soil Model

SOIL PARAMETER AND RESPECTIVE DEFAULT SETTING		UNIT
E_{ref}^{50}	Secant stiffness in standard drained triaxial test	[KN/M^2]
E_{oed}^{ref}	Tangent stiffness for primary oedometer loading (default $E_{oed}^{ref} = E_{50}^{ref}$)	[KN/M^2]
m	Power for stress-level dependency of stiffness	[-]
E_{ur}^{ref}	Unloading/reloading stiffness (default $E_{ur}^{ref}=3\ E_{50}^{ref}$)	[KN/M^2]
v_{ur}	Poisson's ratio for unloading-reloading (default $V_{ur}=0.2$)	[-]
P^{ref}	Reference stress for stiffness (default $P^{ref}=100$ stress units)	[KN/M^2]
K_o^{nc}	K_0-value for normal consolidation (default $K_o^{nc} = 1 - \sin\phi$)	[-]
R_f	Failure ratio q_f/q_a (default $R_f=0.9$)	[-]
$\sigma_{tension}$	Tensile strength (default $\sigma_{tension} = 0$ stress units)	[KN/M^2]
$\sigma_{increment}$	As in Mohr-Coulomb model (default $\sigma_{increment} = 0$)	[KN/M^2]

Appendix 2: PLAXIS Software Output

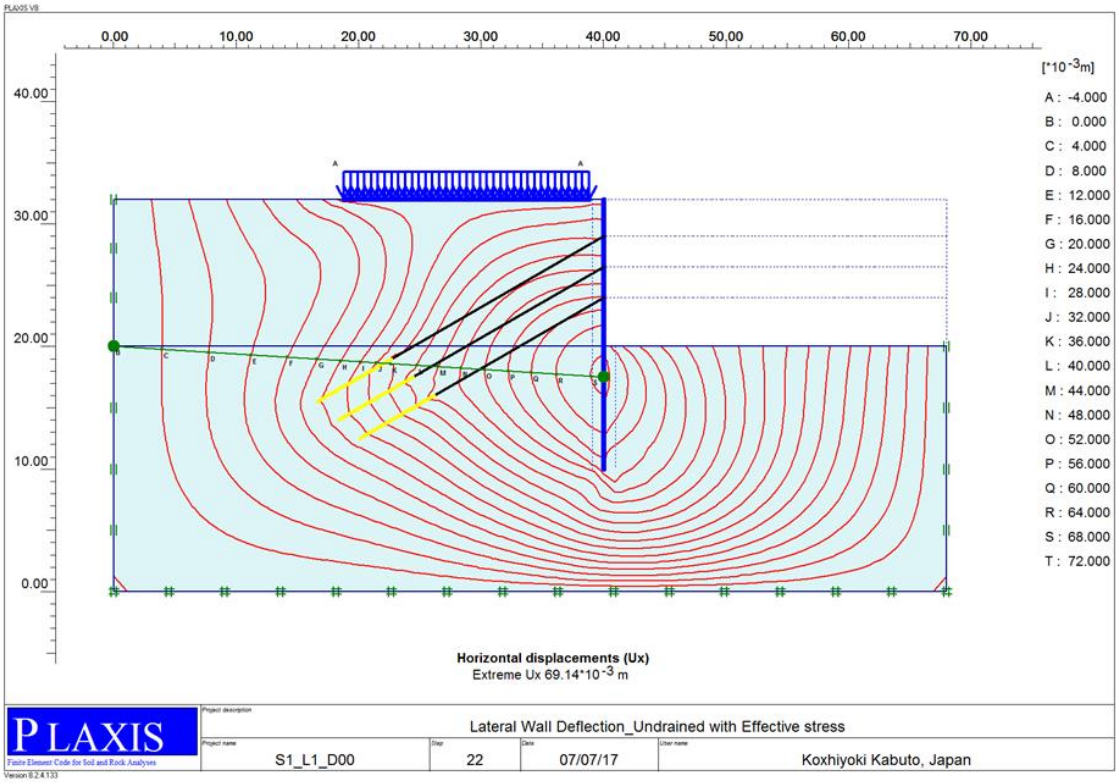

Figure A49: Lateral wall deflection of Soil 1_Undrained with Effective stress @ **Load 1** & Distance 1

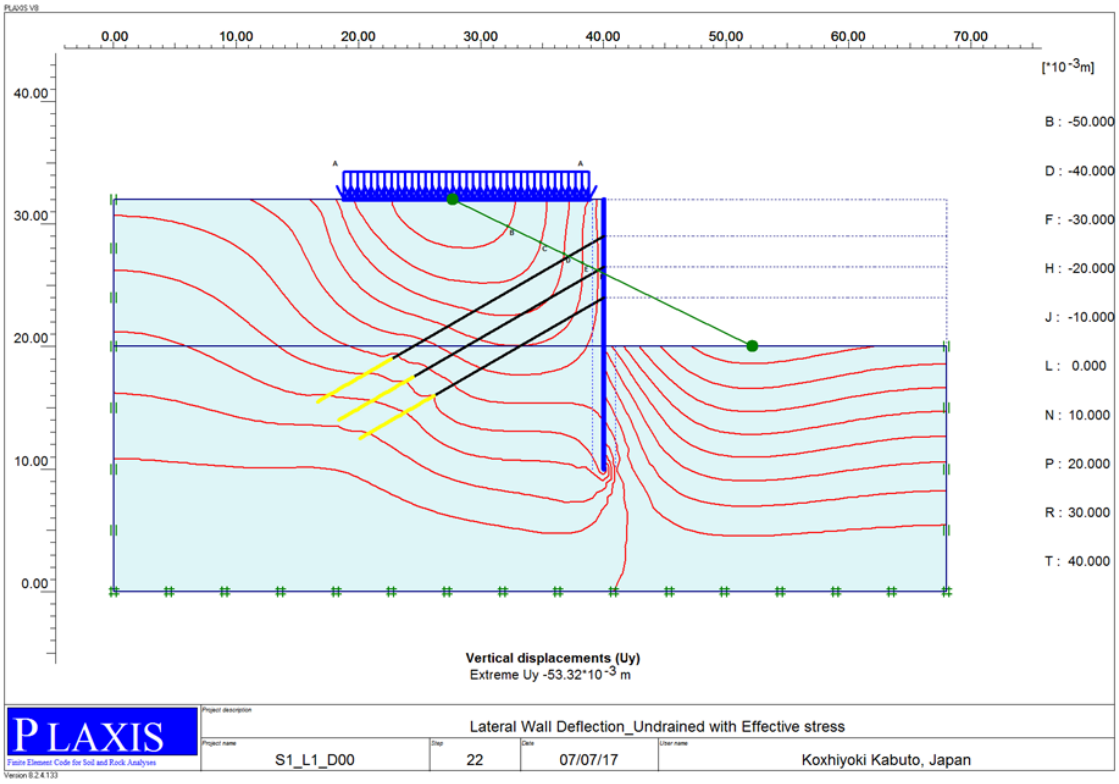

Figure A50*:* Vertical Settlement of Soil 1_Undrained with Effective stress @ **Load 1** & Distance 1

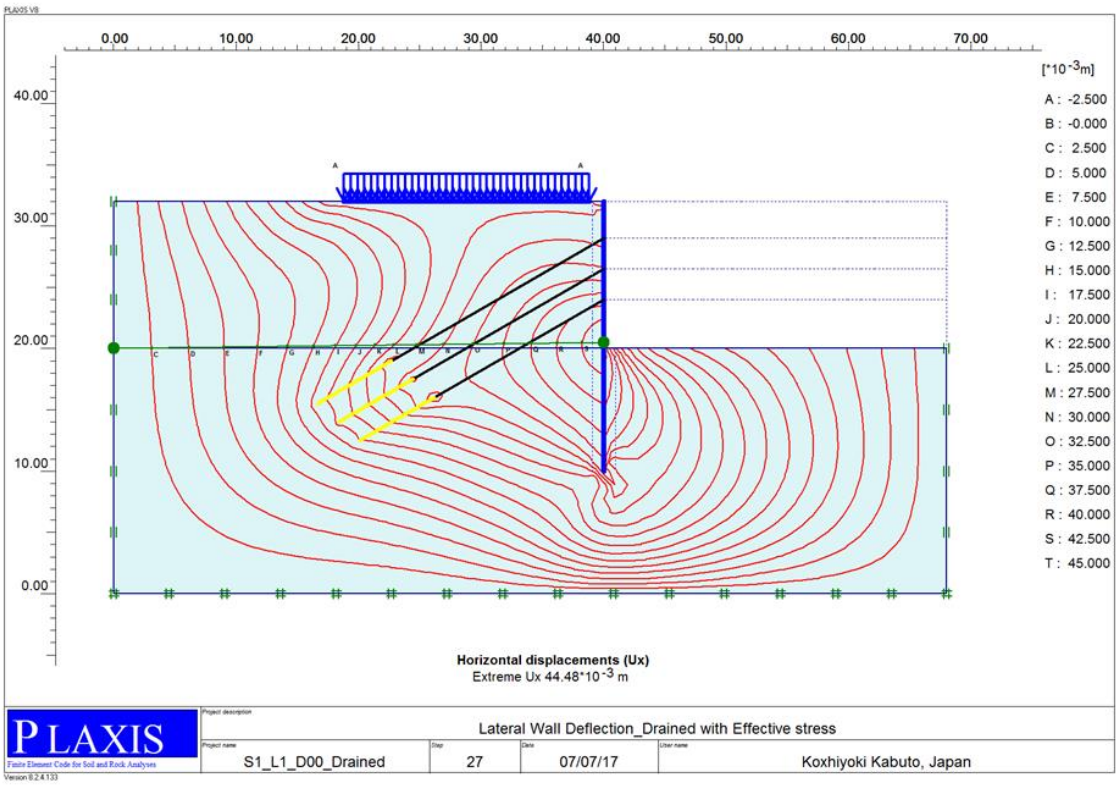

Figure A51: Lateral wall deflection of Soil 1_Drained with Effective stress @ **Load 1** & Distance 1

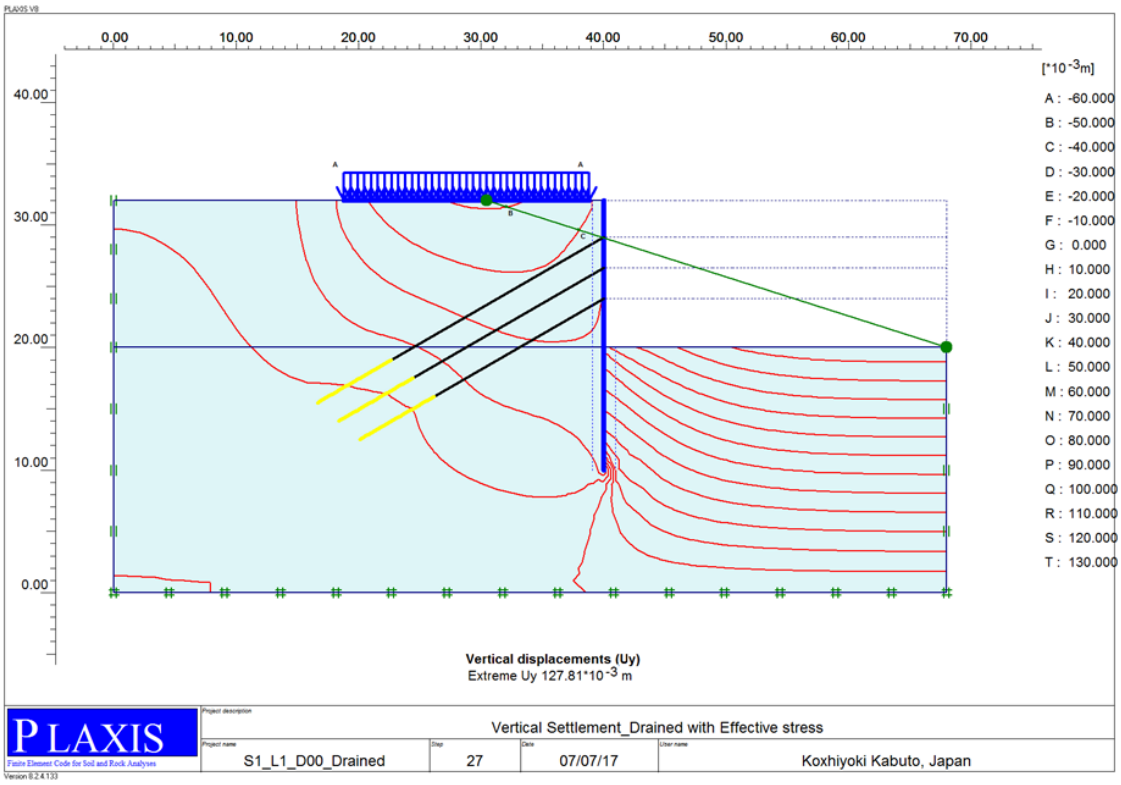

Figure A52: Vertical Settlement of Soil 1_Drained with Effective stress @ **Load 1** & Distance 1

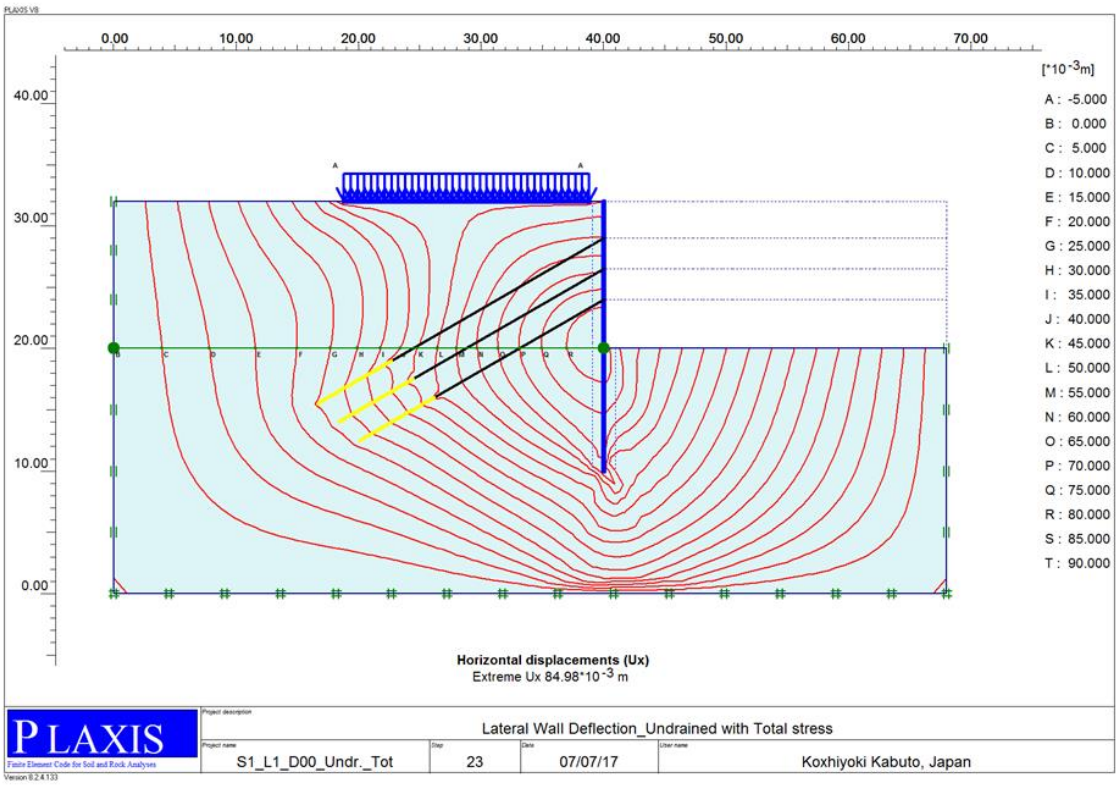

Figure A53: Lateral wall deflection of Soil 1_Undrained with Total stress @ **Load 1** & Distance 1

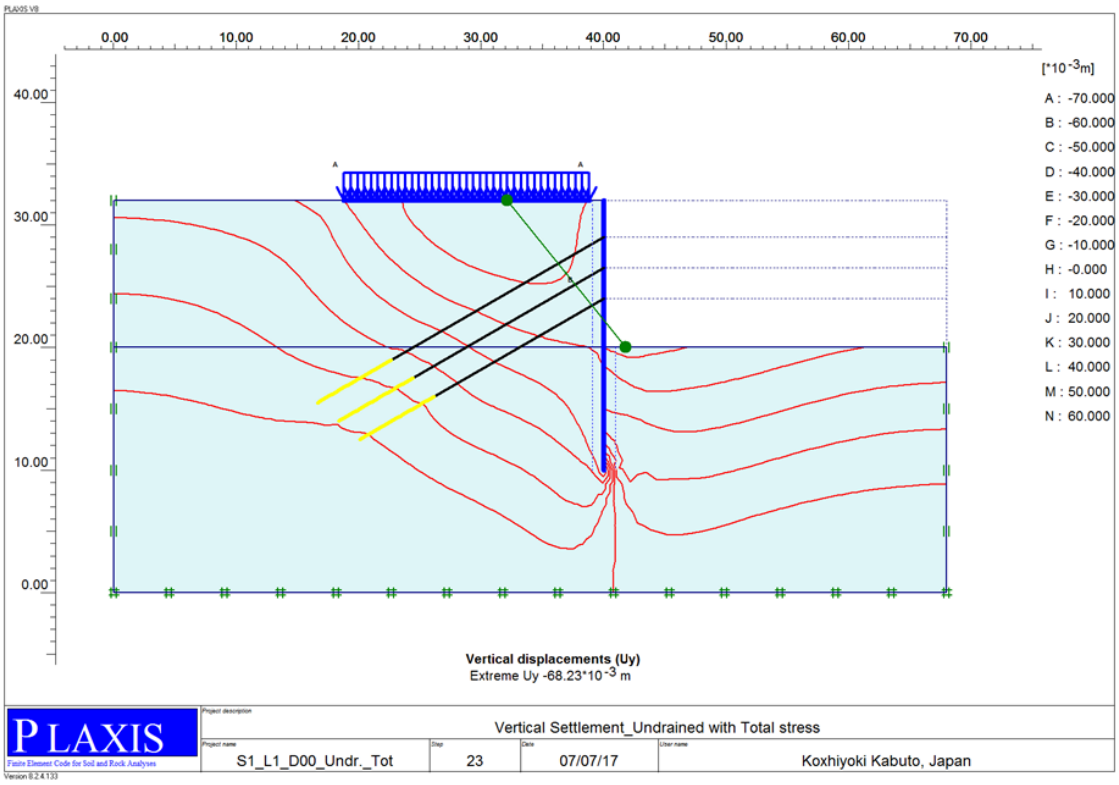

Figure A54: Vertical Settlement of Soil 1_Undrained with Total stress @ **Load 1** & Distance 1

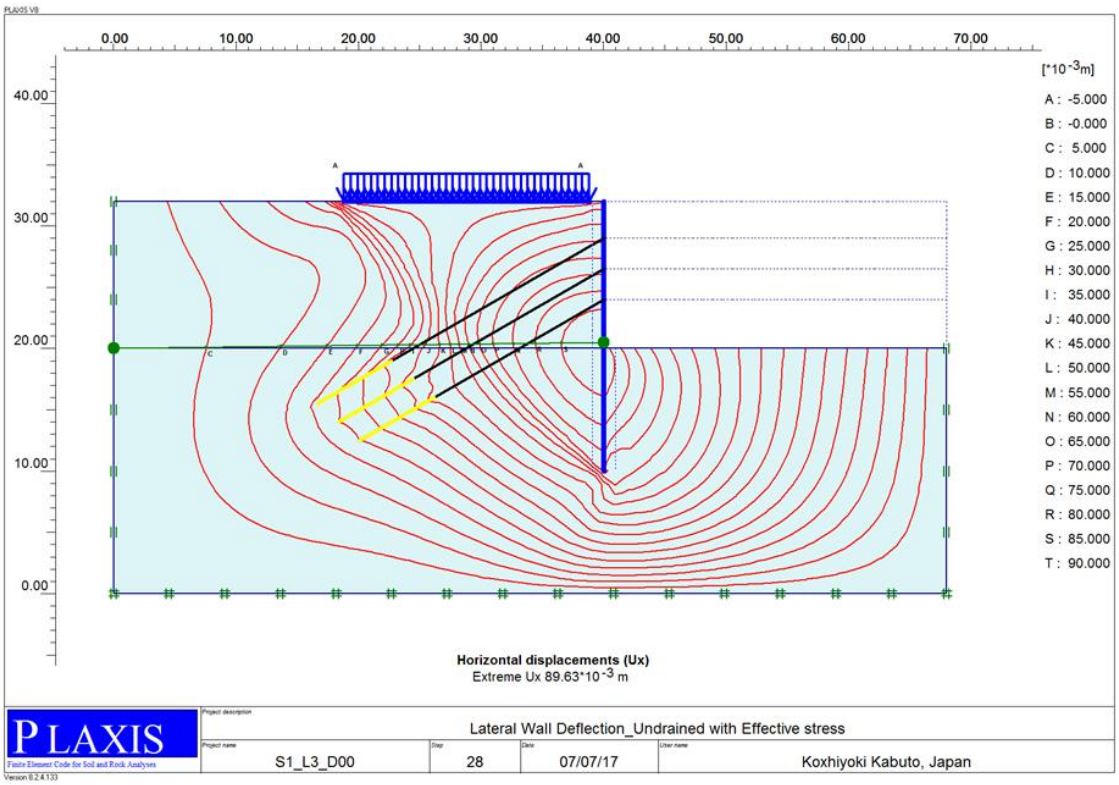

Figure A55: Lateral wall deflection of Soil 1_Undrained with Effective stress @ **Load 3** & Distance 1

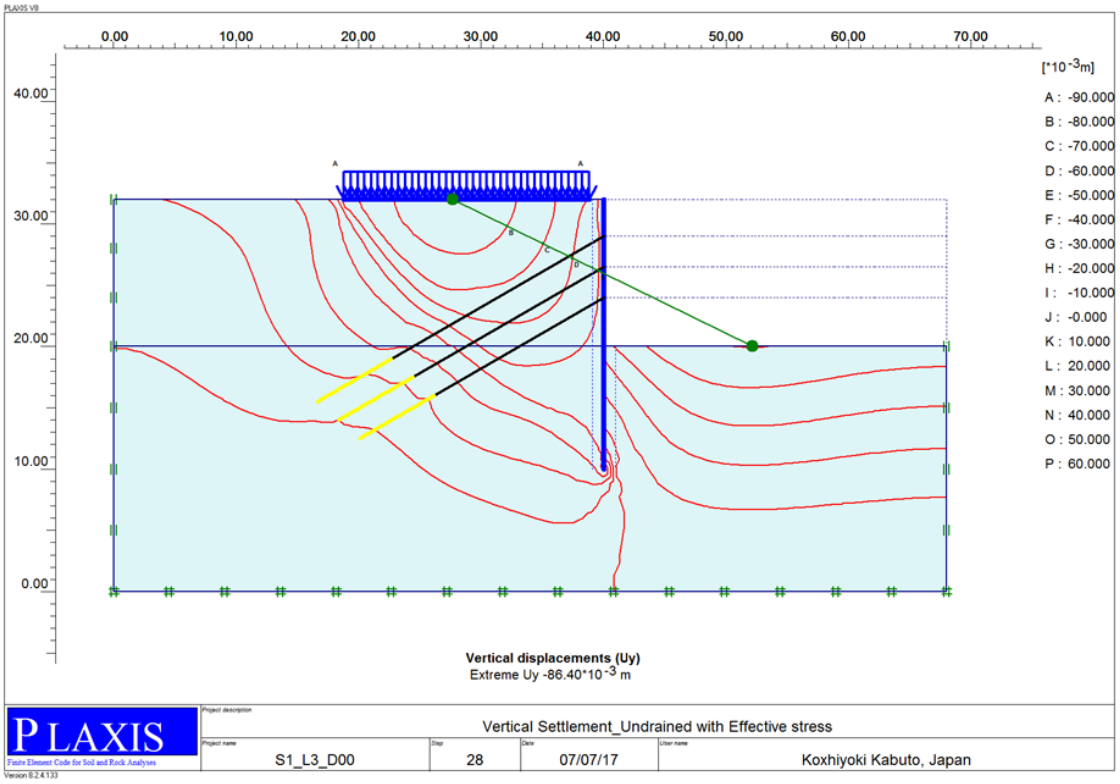

Figure A56: Vertical Settlement of Soil 1_Undrained with Effective stress @ **Load 3** & Distance 1

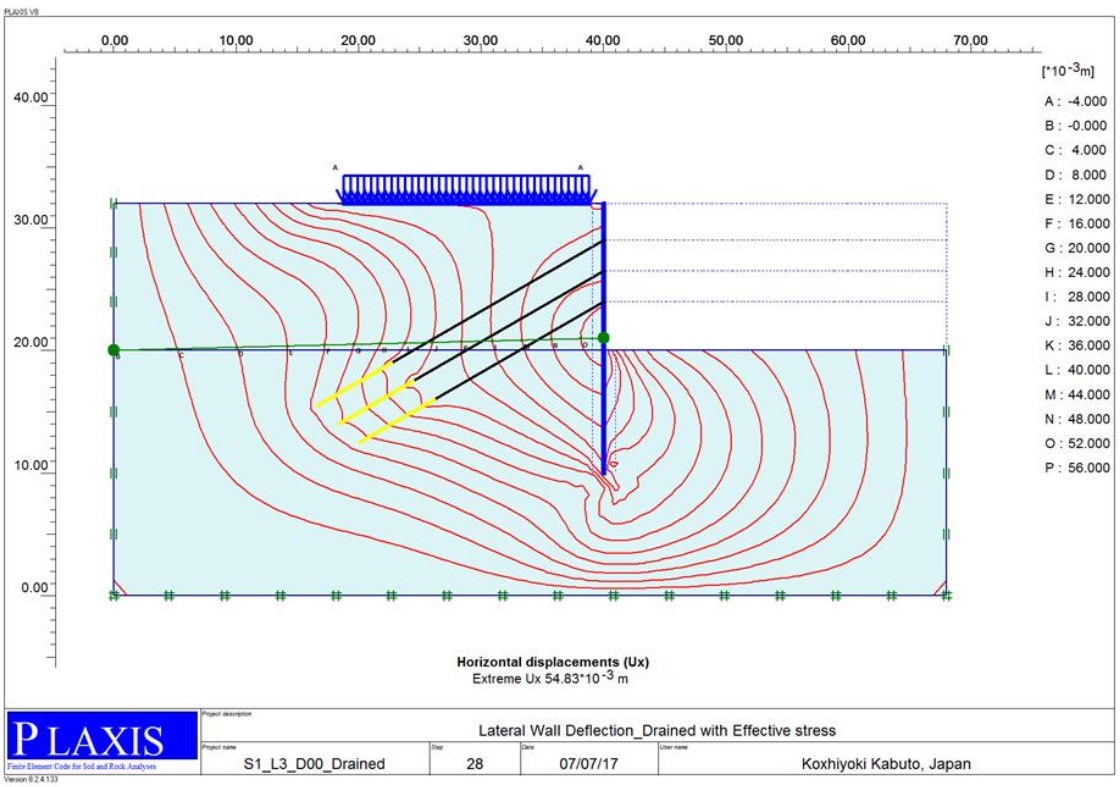

Figure A57: Lateral wall deflection of Soil 1_Drained with Effective stress @ **Load 3** & Distance 1

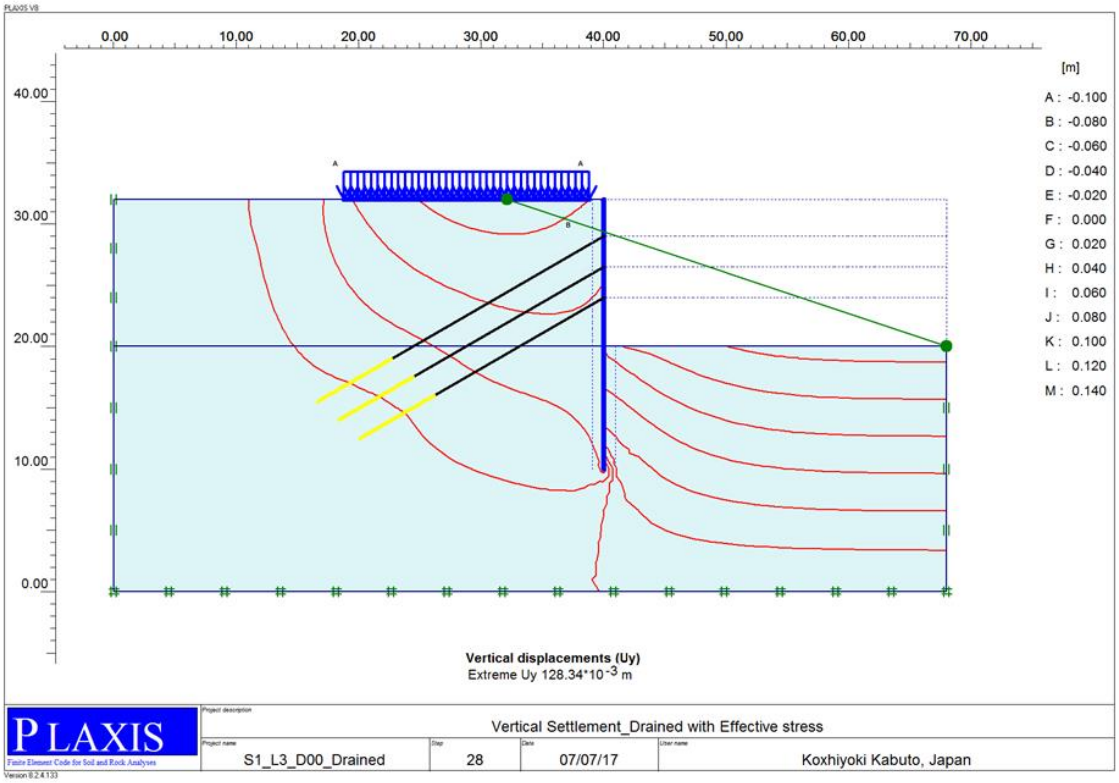

Figure A58: Vertical Settlement of Soil 1_Drained with Effective stress @ **Load 3** & Distance 1

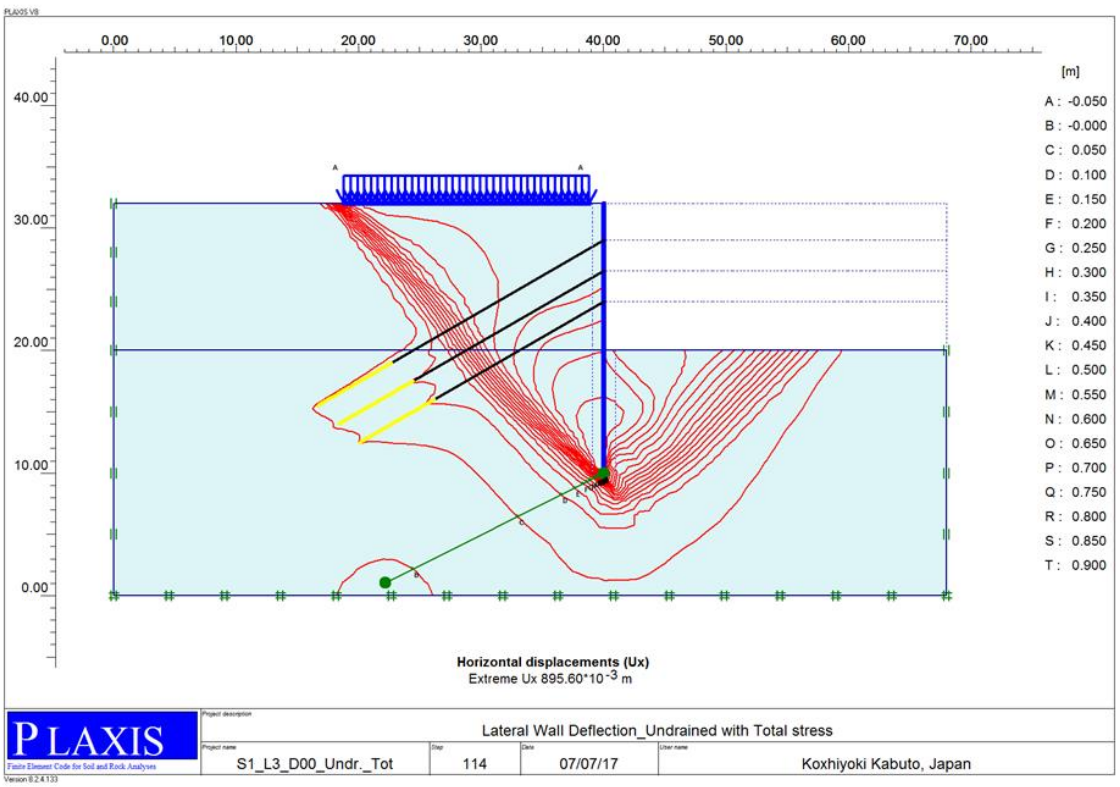

Figure A59: Lateral wall deflection of Soil 1_Undrained with Total stress @ **Load 3** & Distance 1

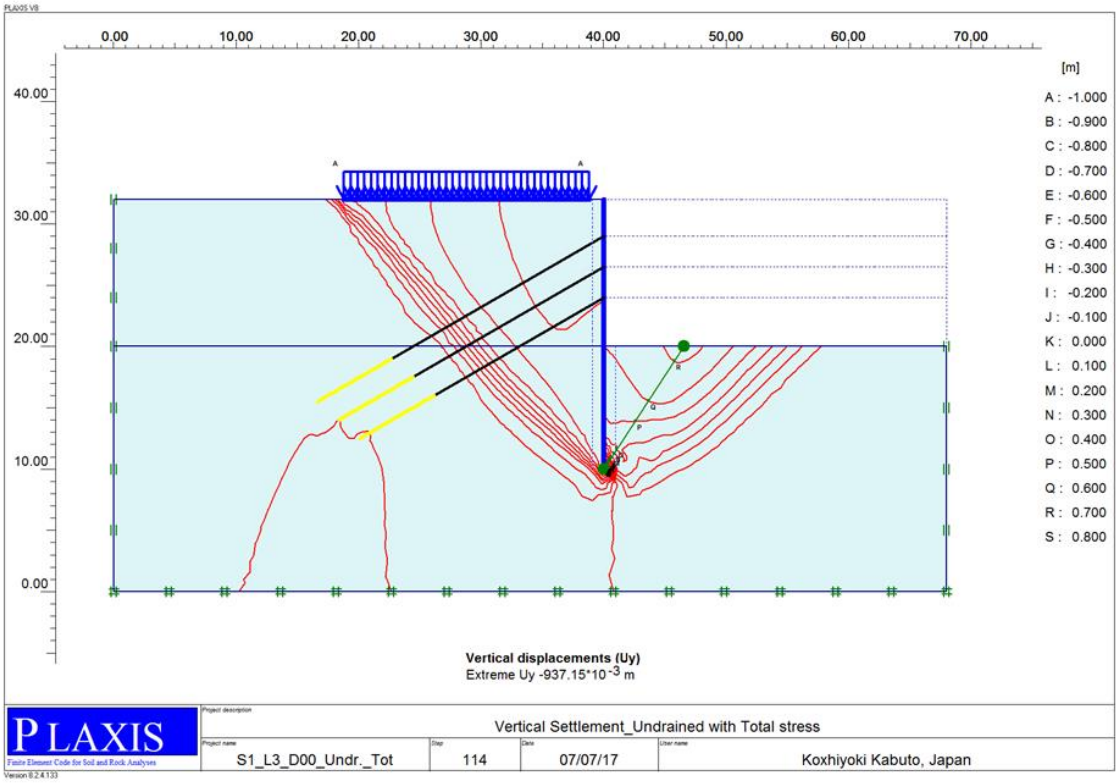

Figure A60: Vertical Settlement of Soil 1_Undrained with Total stress @ **Load 3** & Distance 1

Appendix 3: Different Standard Parameters

Table A.35: Allowable Settlement and Tilt of Structures

Type of Movement	Limiting Factor	Maximum Settlement
Total settlement	Drainage	150 – 300 mm
	Access	300 – 600 mm
	Masonry walled structure Framed structures Smokestacks, silos, mats	25 – 50 mm 50 – 100 mm 75 – 300 mm
Tilting/ Differential movement	Tilting of smokestacks, towers	0.004L
	Stacking of goods, rolling of trucks, or similar	0.01L
	Machine operation-cotton loom	0.003L
	Machine operation – turbogenerator	0.0002L
	Crane rails	0.003L
	Drainage of floors	(0.01 to 0.02)L
	Framed buildings and reinforced load bearing walls: Structural damage Cracking in walls and partitions Open frames In filled frames Framed buildings	 1/150[1] 1/250[2] 1/200[3] 1/300[1] to 1/500[2] 1/300[6] 1/1000[6] 1/300[7]
	High continuous brick walls	(0.0005 to 0.001)L
	One-story brick mill building, wall cracking	(0.001 to 0.002)L
	Plaster cracking (gypsum)	0.001L
	Reinforced-concrete building frame	(0.0025 to 0.004)L
	Reinforced-concrete building curtain walls	0.003L
	Steel frame, continuous	0.002L
	Simple steel frame	0.005L
	Unreinforced load bearing walls: Sagging Hogging	 1/2500[2] L/H < 3; 1/3500 – 1/2500[3] L/H < 5; 1/2000 – 1/1500[3] 1/2500 at L/H = 1[5] 1/1250 at L/H = 5[5] 1/5000 at L/H = 1[5] 1/2500 at L/H = 5[5]

Note: Data from Sowers (1962) unless otherwise indicated [1]Skempton &Macdonald (1956), [2]Meyerhof (1956), [3]Polshin & Tolkar (1957), [4]Bjerrum (1963), [5]Burland & Wroth (1975), [6]Meyerhof (1953), [7]Christian & Vanmarke (1974).

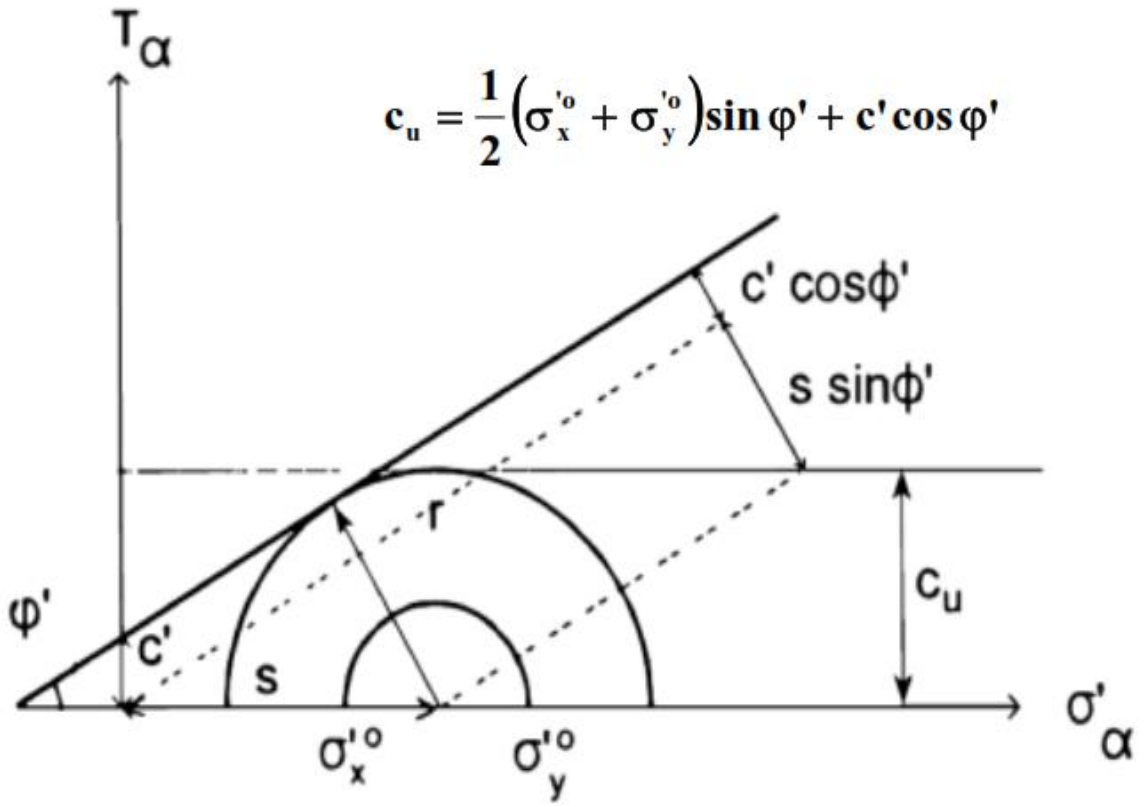

Figure A 61: Mohr circle for evaluating Undrained shear strength (plane strain) (Tan, 2007).